To Sandy and Mairi Davies

GROWTH OF AXONS IN FIBRE TRACTS OF THE ADULT CENTRAL NERVOUS SYSTEM

A thesis presented by

Stephen John Alexander Davies

to the UNIVERSITY OF LONDON

in partial fulfilment of the

requirements for the degree of

Doctor of Philosophy

Division of Neurobiology,

National Institute for Medical Research,

Mill Hill, London, NW7 1AA.

Date: 1st December 1995

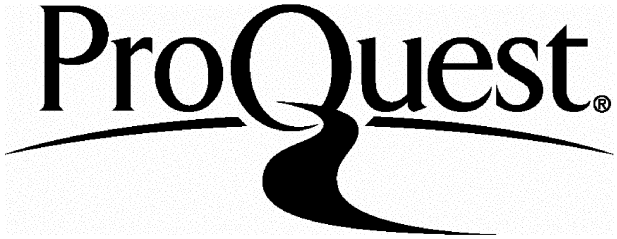

ABSTRACT

A number of experiments have implicated white matter tracts as the site for failure of regeneration in the adult mammalian central nervous system (CNS) (Cajal, 1928; Schwab, 1990). In order to assess the ability of adult white matter tracts to sustain and direct new axonal growth, I have used an air pressure pulse microtransplantation technique, to introduce minute volumes of suspensions of mouse embryonic neurons and glia directly into and completely enclosed within a number of different adult rat CNS tracts. Using mouse specific monoclonal markers (M6 and Thy1.2), I have observed rapid, long interfascicular axon growth from the transplants through the host white matter, aligned with tract glial and axonal elements and invading host terminal fields. These results show that adult white matter tracts are a highly permissive substrate for embryonic axonal growth.

I have demonstrated that the interface between the embryonic neural microtransplants and the adult tract permits the ingrowth of adult tract axons. Injection of biotin dextran tracer into the adult fimbria of rat hosts, labelled host axons within the neuropil of hippocampal intratract microtransplants. Host innervation of the embryonic microtransplants was confirmed by transection of the host fimbrial axons, allowing electron microscopy of their degenerating synapses within the intrafimbrial grafts.

To examine the ability of cut adult central nervous system axons to regenerate through an aligned but reactive adult tract glial pathway, I have designed a microlesion approach, in which a micropipette is used to cut a contingent of p75 immuno-positive adult cingulate axons. No glial scar or necrotic tissue cavity were formed at the lesion site and immunohistochemistry for GFAP (for astrocytes) and OX42 (for microglial) showed that the adult tract glial framework (Suzuki and Raisman, 1992) rapidly regained it's normal alignment. Specific upregulation of p75 immuno-reactivity in the proximal segments of the cut axons showed that regeneration of these axons through the lesion site was totally blocked, even in the absence of a glial scar.

ACKNOWLEDGMENTS

I would like to thank my supervisors, Professor Geoffrey Raisman and Dr. Pauline Field for their superb teaching, support and encouragement during my studies at Mill Hill and for masterminding my transformation from Coral Sea prawn trawler fisherman to neurobiologist.

I would also like to thank Dr. John Skehel, FRS and the Medical Research Council for the use of facilities at the National Institute for Medical Research, and the International Spinal Research Trust (especially Peter Banyard) for funding my scientific endeavours.

Many thanks to Ursula Starega for teaching me histology and Dr. Pauline Field and Yewande Ajayi for their skilled technical assistance. Thanks also to Dr. Carl Lagenaur and Professor Ray Lund for the gift of M6 antibody.

I am very grateful to Melvyn Sherwood and Randa Pember for making sure everything ran smoothly in the Lab and with the MRC, and to my family and Patricia Goggin for their support when the going got tough!

TABLE OF CONTENTS

ABBREVIATIONS

a	anterior commissure
AC	Air cylinder
$AgNO_3$	Silver nitrate
alv	alveus
astro	astrocytes
ax	axons
B	steel block
BV	blood vessel
c	head of caudate nucleus
CA3	hippocampal field CA3
CBF	Cholinergic basal forebrain
CC	corpus callosum
cg	cingulum
CGyr	cingulate cortex
CH	contralateral hippocampus
CM	caudo-medially
CNS	Central Nervous System
COLL	superior collicular transplant
C-6-PG	Chondroitin-6- sulphate containing proteoglycan
CR	corona radiata
CS	corpus striatum
CT	Cytotactin/tenascin

CTX	cerebral cortex
D	degenerating axon terminals
DAB	Diaminobenzidine
dH_2O	Distilled Water
Di-I	1,1'dioctadecyl-3,3,3',3'-tetramethylindocarbocyanine perchlorate
DREZ	Dorsal Root Entry Zone
DRG	Dorsal Root Ganglion
E14,18,19	days of embryonic life (E0 = vaginal plugs)
Fb	fimbria
fx	postcommissural fornix bundles
g	glial cells
GFAP	Glial fibrillary acidic protein
GM-CSF	Granulocyte Macrophage- Colony Stimulating factor
H	Hippocampus
HIPP	Hippocampal transplant
HRP	Horseradish peroxidase
IC	internal capsule
IF	interhemispheric midline fissure
IgG	immunoglobulin G
igr	interfascicular glial rows
IH	ipsilateral hippocampus
IL-1	Interleukin-1
i.p.	intra-peritoneal

LSN	lateral septal nucleus
LIAG	long interfascicular axon growth
LV	lateral ventricle
M	midline
m	microglia
mp	amoeboid macrophage/microglia
mgl	resident tract ramified microglia
N	Neurons
Na_2CO_3	Sodium carbonate
NH_4NH_3	Ammonium nitrate
NV1, NV2	Needle valves 1 and 2
P	micropipette
p	perivascular cell
PB	Phosphate Buffer
PBS	Phosphate Buffered Saline
phago	phagocytosis
PHAL	Phaseolus vulgaris leucoagglutinnin
PNS	Peripheral Nervous System
R	rostral pole of the hippocampus
RGC	Retinal Ganglion Cell
RM	Rostro-medially
S	projection to septal nuclei
SEPT	septum
sg	stratum granulosum

$SiO_2.12WO_3.26H_2O$	Tungstosilicic acid
slm	stratum lacunosum-moleculare
sluc	stratum lucidum
soc	stratum oriens
sp	stratum pyramidale
sr	stratum radiatum
ST	stria terminalis
STIM	Electronic stimulator
SV	solenoid valve
Sy	syringe
T	tip of transplant
TGFß1	Transforming Growth Factor ß1
Th	thalamus
TJ	"T" piece micropipette holder
TR	transplant
TSN	triangular septal nucleus
V	projection to ventral hippocampal commissure
VHC	ventral hippocampal commissure

CHAPTER I

General Introduction

GENERAL INTRODUCTION

The adult mammalian brain and spinal cord have a very limited ability to repair themselves after injury. Adult neurons are not replaced when they die and central nervous system (CNS) axons do not regenerate back to their original targets after axotomy. It is this failure of cut adult axons to regrow after spinal cord injuries in humans that causes the impairment or permanent loss of many sensory and motor functions. The reasons why cut adult mammalian central nervous system axons will not regenerate are as yet not fully understood and there are no clinical treatments to repair human spinal cord injuries.

In contrast to the CNS, cut peripheral nervous system (PNS) axons can regenerate along their former pathways and reinnervate their original terminal fields (Guth, 1956). Immature CNS axons readily grow along immature fibre tracts during development, and if cut at an early stage are also capable of regenerating through the lesion site and on to their original targets (Bates and Stelzner, 1993; Kalil and Reh, 1979, 1982; MacClaren and Taylor, 1995; Schmidt and Bhatnagar, 1979; Schmidt *et al.,* 1980; Varga *et al.*, 1995; Xiao and Martin, 1991). In a brilliant series of studies, Cajal (1928) clearly demonstrated that adult CNS axons cut in white matter tracts similarly produce regenerative sprouts, but these sprouts are transient and abortive, and are unable to cross the lesion site.

However in situations where cut adult CNS axons are not required to elongate back along their original white matter pathways, it can be demonstrated that they do retain the ability to grow and even form synapses. This is indicated by a number of observations:

(1) they will readily grow new synaptic connections in partially denervated central neuropil (for a review see Cotman *et al.,* 1981) as first demonstrated by Raisman (1969) in the septum,

(2) they will regenerate into and form specific patterns of innervation within transplants of embryonic neural tissue grafted into adult grey matter (Campbell *et al.,* 1993; Clarke *et al.,* 1988b; Clinton and Ebner, 1988; Field *et al.,* 1991; Labandeira-Garcia *et al.,* 1991; Pritzel *et al.,* 1987; Raisman and Ebner, 1983; Tønder *et al.,* 1989; Wictorin and Björklund, 1989; Zhou *et al.,* 1985),

(3) they will extend for long distances along peripheral nerve grafts (Benfey and Aguayo, 1982; Berry *et al.,* 1988b; Campbell *et al.,* 1991, 1992; David and Aguayo, 1981, 1985; Richardson *et al.,* 1980; Vidal-Sanz *et al.,* 1987), and

(4) they will sprout in response to transplanted suspensions of Schwann cells (Brook *et al.,* 1994; Li and Raisman, 1994; Montero-Menei *et al.,* 1992; Neuberger *et al.,* 1992; Paíno and Bunge, 1991).

Interestingly, axons of dorsal root ganglion (DRG) cells, cut in the peripheral nerve will regenerate back through the nerve until they reach the dorsal root entry zone (DREZ) where contact with CNS tissue prevents them from growing further and reinnervating their appropriate targets in the dorsal horn of the spinal cord (Bignami *et al.,* 1984; Cajal, 1928; Liuzzi and Lasek, 1987; Perkins *et al.,* 1980; Pindzola *et al.,* 1993; Stensaas *et al.,* 1979, 1987). However, cut DRG axons will regenerate through the dorsal root entry zone in neonates prior to postnatal day 3 (Carlstedt *et al.,* 1987, 1988), and in adults, if the end of the cut spinal root nerve is placed directly into spinal cord grey matter (Siegal *et al.,* 1990) or bridges, coated with immature astroglial cells, used as a pathway across the DREZ (Kliot *et al.,* 1990). Taken together, these observations place the onus for the failure of CNS regeneration on the interaction of cut axons with the tissues of adult central fibre pathways.

Many theories have been put forward to explain the inability of cut adult axons to regenerate in adult white matter tracts.

(1) Axon growth is physically blocked at the lesion site by the formation of a reactive astroglial scar (Berry *et al.,* 1983; Kruger *et al.,* 1986; Reier *et al.,* 1983a,b, 1986; Reier and Houle, 1988; Stensaas et al., 1987) and subsequent loss of aligned glial pathways (Li and Raisman, 1995).

(2) The failure of regeneration is due to the maturation of axons not their pathways or target tissues (Chen *et al.,* 1995; Li *et al.,* 1995).

(3) Adult tracts lack appropriate growth promoting substrate molecules (Kuhn *et al.,* 1995; Liesi, 1985).

(4) Reactive glia express axon growth inhibitory molecules at the lesion site (Bovolenta *et al.,* 1991; Liuzzi and Lasek, 1987; Mansour *et al.,* 1990; McKeon *et al.,* 1991; Pindzola *et al.,* 1993; Stensaas *et al.,* 1987).

(5) There is an inadequate supply of growth factors in the adult CNS to support regeneration (Berry, 1985; Hagg *et al.,* 1991; Lindsay *et al.,* 1982).

(6) Adult astrocytes block axonal regeneration by activating axonal physiological synaptic stop mechanisms (Liuzzi and Lasek, 1987).

(7) Other theories postulate that the normal adult tract environment will no longer support axon growth as it did during development, due to inhibition by mature CNS astrocytes (Fawcett *et al.,* 1989; Rudge and Silver, 1990; Smith *et al.,* 1986; Tiveron *et al.,* 1992; Wang *et al.,* 1994) or axon-growth-inhibitory molecules associated with mature myelinating tract oligodendrocytes (Bandtlow *et al.,* 1990; Schnell and Schwab, 1990; Schwab, 1990).

The purpose of the first part of this thesis was to determine to what extent adult white matter tracts have the ability to support new axon growth and what might be the general rules governing the patterns of any growth observed.

Chapter III describes experiments which tested the axon growth promoting ability of adult white matter tracts by transplanting embryonic neurons directly into the mature tract environment using a microtransplantation technique (Emmett *et al.,* 1989; Suzuki *et al.*, 1989) pioneered and developed in our laboratory. This micro surgical approach has the advantage of causing minimal damage to the local anatomy and new axon growth can be studied against the background of a relatively undamaged adult tract. Mouse donor material was used with an adult rat host so that mouse specific axonal markers could be employed to clearly identify any new axon growth.

The question of whether the embryonic axonal growth would be restricted to a correct matching of donor neuron to host tract type is also addressed in *Chapter III.* In an attempt to answer this question, I carried out a further series of embryonic neuronal microtransplants of donor tissue taken from three different areas of the brain, and placed them in adult tracts in which their axons never normally grow during development. Any resulting new axonal growth was visualized with the mouse specific markers and the patterns of growth and morphology of the mismatched axons compared with that seen for correctly matched tissue.

A recent series of studies from our laboratory (Suzuki and Raisman 1992, 1994) shows that the glial environment through which embryonic axons first grow during development is very different from that which is finally present in adult tracts. This can be illustrated by reference to the development of the fimbria

(See Fig. 11 in Suzuki and Raisman, 1994). In the embryonic tract the newly extending axons grow orthogonally to the parallel array of radial glial processes derived from cell bodies along the ventricular surface. During the early postnatal period, when the tract is already well populated with axons, the radial glial tract skeleton is converted to the adult pattern, where astrocytic cell bodies are scattered throughout the width of the tract (Cf Takahashi *et al.,* 1990; Voigt, 1989; Wu *et al.,* 1995), and the radial processes are reduced to short, tapering structures which no longer span the full width of the fimbria. The tract astrocytes now generate numerous, untapering longitudinal processes which form an array which clearly delineates the longitudinal axis of the tract, and runs parallel to the axons and to the rows of postnatally formed oligodendrocytes which later come to flank the astrocytes. Different tracts of the central nervous system are formed at different times during development, and some mature later than others. In the rat fimbria, the overall glial framework has not finished developing until postnatal day 60 and probably continues to be refined well into adulthood. When the structures of different CNS tracts are compared, the overall pattern of glial cytoarchitecture remains remarkably constant with differences found only in the cross sectional packing density of the tracts and the size of astrocytes (Ying Li, personal communication).

If embryonic axons can grow through adult fibre tracts, how would the patterns of growth relate to the underlying adult tract structure, and what possible glial or axonal cues might be acting to guide this growth? Does the new axonal growth respect intertract boundaries as seen in development (Faissner and

Kruse, 1990; Faissner and Steindler, 1995; Snow *et al.,* 1990; Silver *et al.,* 1993) and what is the glial arrangement at the transplant/host tract interface?

In the final part of *Chapter III,* I have addressed these questions by comparing the orientation of the embryonic axonal growth with that of the surrounding adult tract infrastructure, using 10μm serial section analysis with particular reference to the possible involvement of the tract astrocytes in axon guidance .

If the interface between an embryonic microtransplant and the adult tract permits the outgrowth of embryonic axons, can adult tract axons similarly grow into the graft? This question is answered in *Chapter IV,* which documents experiments where host tract axons have been labelled with a dextran amine tracer and intra-tract embryonic neuronal microtransplants examined for the presence of host axons. In order to confirm the tracer findings I also carried out lesions of host axons most likely to have innervated the transplants and looked using electron microscopy for their degenerating synapses within the neuronal grafts.

Of the possible reasons put forward to explain why cut adult mammalian axons do not regenerate, the formation of a glial scar at the site of injury which physically blocks axons crossing the lesion seems the most attractive. Indeed it is difficult to imagine regenerating axons negotiating the large areas of necrotic and astroglial scar tissue often seen in spinal cord injuries (Kakulas, 1985). If it were possible to cut adult CNS tract axons without forming a glial

scar, would the regenerative sprouts first observed by Cajal (1928) in larger lesions continue to grow through the lesion site and into the distal tract?

In *Chapter V*, I describe an experiment where I have carried out "microlesions" of an adult white matter tract in order to try and create a situation where cut adult axons are presented with a normally "aligned" glial pathway at the lesion site. Unless an adult fibre tract is completely transected, experimental partial lesions invariably present the problem of distinguishing regenerating cut axons from new collateral branches stimulated to grow from adjacent unlesioned axons (Li and Raisman, 1995). In an attempt to solve this problem a system of fibres was chosen which greatly upregulates the expression of a growth factor receptor antigen after axotomy and therefore immunohistochemistry of the antigen selectively stained only cut axons at the lesion site. Familiarity with the normal glial cytoarchitecture of the tract made it possible to study the invasion of any new cell types and/or changes in glial morphology at diferent survival times post lesion.

CHAPTER II

General Materials and Methods

GENERAL MATERIALS AND METHODS

2.1 Microtransplantation procedure

Adult female rats of body weights ranging from 180 to 220 g of a locally maintained AS strain, were placed under tribromoethanol anaesthesia (see below; 20mg/100g body weight, i.p.). The deeply anaesthetised rats were placed into a rat stereotaxic surgery apparatus (N.I.M.R. Engineering, Mill Hill, UK), their heads held firmly in the flat skull position ie. incisor bar 3.3mm below the interaural line. Using the bregma as a reference point, a small burr hole was drilled in the bone of the skull at the required stereotaxic coordinates, and the underlying dura retracted.

Fig. 1 shows a schematic of the "T" piece micropipette valve system (N.I.M.R Engineering, Mill Hill, UK) used for the microtransplantation studies (and microlesion experiment), which was held in a steel block attached to the stereotaxic apparatus. By closing needle Valve 1 and opening needle Valve 2, cell suspension could be drawn into the micropipette by using the syringe attached to valve 2 by an air line. After filling the micropipette, Valve 2 was closed and the end of the micropipette slowly lowered into the brain to the required stereotaxic coordinates. Valve 1 was then opened, thereby allowing pulses of compressed air, generated by an air tank connected to an electronic stimulator (N.I.M.R. Electronics, Mill Hill, UK) controlled solenoid valve (Kuhnke Elektrotechnik und Pneumatik GmbH & Co., Malente, Germany,), to be applied to the cell suspension in the micropipette.

Figure 1

A schematic diagram of the microtransplantation apparatus. An electronic stimulator (STIM) controls the duration and frequency of opening of a solenoid air valve (SV) connecting a compressed air cylinder (AC) via air lines (black lines and arrows) to the "T" piece micropipette holder (TJ). The "T" piece micropipette holder is fixed to the stereotaxic apparatus by a steel block and screw (B). Air flow into the micropipette (P) can be regulated by needle valves 1 and 2 (NV1, NV2) connected by air lines to the solenoid valve and syringe (SY) respectively.

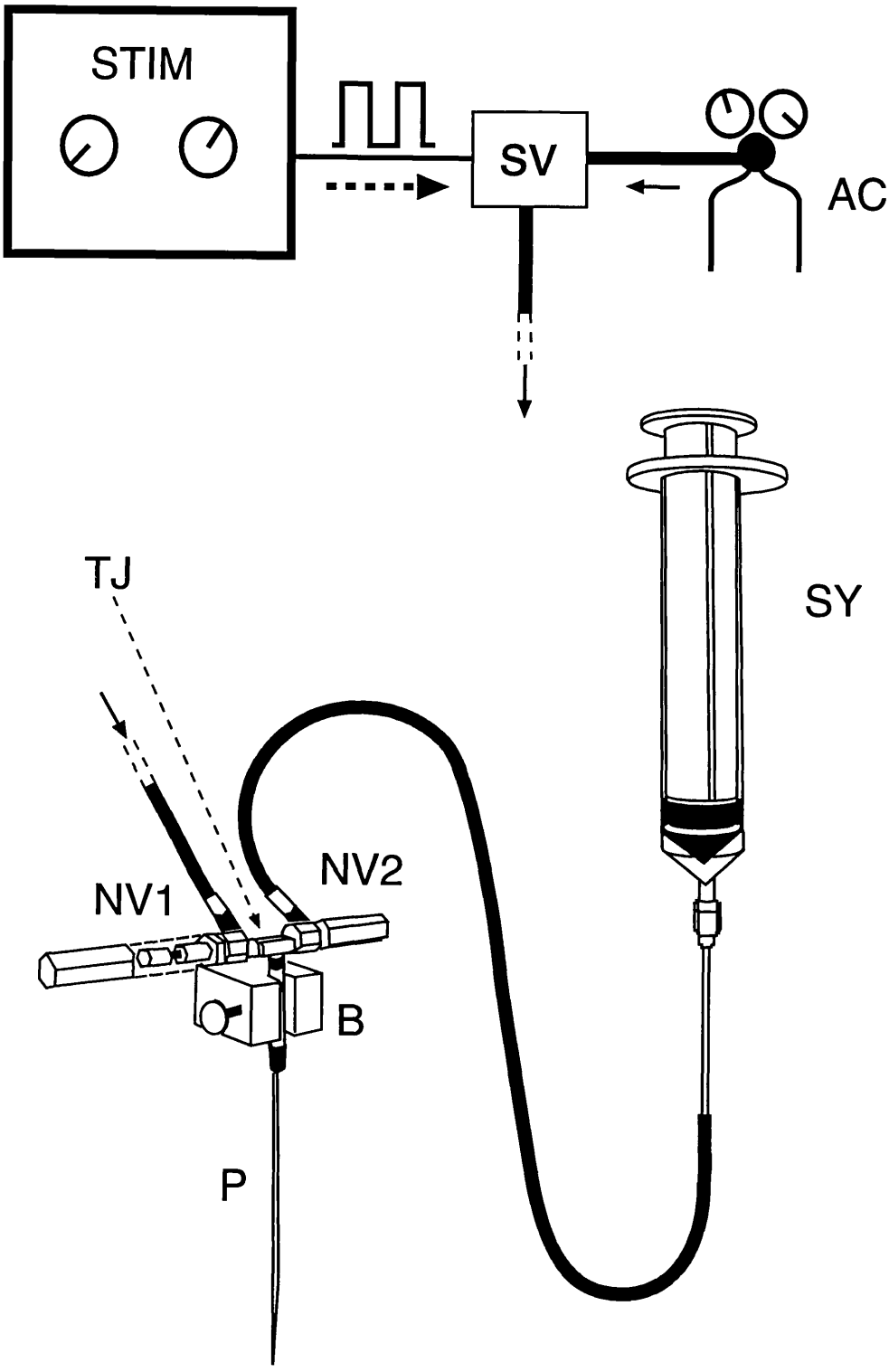
STIM
SV
AC
SY
TJ
NV1
NV2
B
P

Air pressure was set at 10 psi, the air pressure pulses generated at 1Hz, and the duration of the pulses varied to control the rate of microinjection. The micropipettes were graduated in 1mm divisions (see below), and therefore the volume of cell suspension expelled could be ascertained by monitoring the position of the meniscus as it moved down the micropipette. Once a 500nl microtransplant had been injected, the micropipette was left in position for 1 minute and slowly withdrawn over a period of about 30 seconds. The incision in the rat's scalp was then sutured closed, and the transplanted animals maintained on cyclosporin A (Sandimmun, Sandoz, UK) at a concentration of 10 mg/100 ml in their drinking water to prevent xenograft rejection.

2.1.1 Tribromoethanol Anaesthetic

2gm of 2,2,2-Tribromoethanol (Aldrich Chem Co, USA.) to 2ml of 2-Methylbutan-2-ol (B.D.H. Chemicals, UK) were added to 8ml of absolute ethanol and stirred vigorously until dissolved. 100ml of distilled water was then added and the anaesthetic stored in a refrigerator when not in use. The anaesthetic was allowed to warm up to room temperature before use.

2.2 Preparation of micropipettes

Uniform diameter 20 µl glass tubes (Baxter Healthcare Corporation, IL, USA) used for making micropipettes, were given a coating of silicone by brief immersion in Repelcote (BDH, Poole, UK), rinsed with distilled water and thoroughly dried in an oven at 40 °C overnight. Micropipettes with an internal tip diameter of 50 µm were then pulled on a Palmer Bioscience Microelectrode

Puller (heating coil at 100%, solenoid at 0%) whose action was modified with an oil damper (NIMR Engineering). Suitable micropipettes were then held at an angle of 45° to the vertical and their tips bevelled by contact with a horizontal rotating disk (NIMR Engineering) covered with fine glass paper (P400C, English Abrasives, UK) while distilled water was passed continuously through the pipette to prevent blockage with débris. The distilled water was flushed out and the micropipettes thoroughly dried. The micropipettes were then graduated in 1mm divisions with a permanent marker, after having determined that 1mm corresponds to 250nl internal volume along the unpulled section of the micropipettes.

2.3 Transcardiac perfusion

All microtransplanted and microlesioned experimental animals were sacrificed under deep terminal pentobarbitone anaesthesia (Sagatal or Expiral, RMB Dagenham, UK) by intraperitoneal injection (i.p.). The thorax of each animal was opened to expose the heart, the descending aorta clamped (to restrict perfusion to the upper body only), and an incision made to the right atrium. A metal canula was then inserted through the left ventricle and left atrium and clamped in the aorta. The experimental animals were then given a transcardiac perfusion of either 200ml of phosphate buffered saline (PBS) alone or 100ml of PBS followed by 500ml of fixative at 4°C (see below).

2.4 Fixatives

2.4.1 *4% Paraformaldehyde* (for 500ml)

20gm of paraformaldehyde (Sigma) were added to 200ml of distilled water, plus 1ml 1M NaOH. The soution was mixed and heated to 60°C until all the paraformaldehyde had depolymerised. The flask was then cooled in ice at 4°C and the solution filtered into a 500ml measuring cylinder. The volume was made up to 250ml with distilled water and 250ml of 0.2M EM Phosphate buffer then added to make up a final total volume of 500ml. The fixative was then cooled to 4°C.

2.4.2 ***EM Fixative*** - 1% Paraformaldehyde / 1% Glutaraldehyde (For 500ml)

5gm of paraformaldehyde (Sigma) and 1 ml 1M NaOH were added to 200ml of distilled water in a conical flask. The solution was mixed and heated at 60°C until the paraformaldehyde had depolymerised. The flask was cooled in ice to 4°C, 20ml of 25% glutaraldehyde added and the solution filtered into a 500ml measuring cylinder. The volume was made up to 250ml with distilled water and 250ml of 0.2M EM Phosphate buffer then added to make up a final total volume of 500ml. The fixative was then cooled to 4°C.

2.4.3 ***Tracer fixative***- 4% Paraformaldehyde, 0.5% Glutaraldehyde, 0.2% Picric acid (For 500ml)

The same procedure was used as for EM fixative, but 20gm of paraformaldehyde, 10 ml of 25% glutaraldehyde were used and 1ml of picric acid was added.

2.5 Vibratome sectioning

All Vibratome sections were cut on a Vibratome supplied by General Scientific, UK, set at a speed setting of 2 and a blade vibration setting of 10. In the case of sections required for electron microscopy or biotin dextran tracing of fimbrial microtransplants, the ventral surface of the fixed brains were trimmed so that the dorsal surface of the cerebral cortex was parallel to plane of sectioning. Brains to be used for electron microscopy or p75 immunohistochemistry of microlesions were trimmed to remove the right hemisphere allowing sections of the left hemisphere to be taken in the sagittal plane parallel to the midline. All trimmed brains were fixed to the Vibratome chuck with super glue (Loctite, Herts, UK) and immersed in PBS at 4°C prior to sectioning. Sections were cut at 200µm for EM sections and 100µm for all other sections.

2.6 Cryostat sectioning

All frozen sections were cut at 10µm with a Reichert-Jung 2800 Frigocut-E cryostat (Leica, UK) with an object temperature of 12°C and a cabinet temperature of 28°C. Frozen brains were trimmed in an identical fashion to that described above for Vibratome sectioning, and mounted in a thin layer of cryostat embedding compound (Cryo-M-Bed, Jencons Scientific Ltd.). All sections were collected on to gelatin coated slides at room temperature and air dried.

2.7 Palmgren's Silver Stain for axons

Cryostat sections were fixed by immersion in Carnoy's fixative (see below) for 30mins and then given two 5mins washes in absolute ethanol. Polyester wax sections were dewaxed with absolute ethanol. All sections were then immersed in celloidin, and the resulting coat of celloidin hardened by dipping the slides in 70% ethanol. The sections were then rehydrated through a series of ethanols to distilled water. Sections were then treated with acid formalin for 10 mins, given several washes in distilled water, and immersed in silver solution for 15mins. Slides were individually drained and immersed in reducer at 40-45°C, gently rocked from side to side, fresh reducer added, and the slides left for 1 minute. Slides were then rinsed in 50% ethanol for 5-10 seconds, given several washes in distilled water and treated with toner until their brown colour faded. Sections were given 2 washes in distilled water, 5 mins in 5% hypo, washed again in distilled water and dehydrated through a series of ethanols to absolute ethanol. The sections were left in absolute ethanol until all the celloidin had been dissolved. Sections were cleared in Histoclear (National Diagnostics, Aylesbury, UK), mounted with a mixture of dibutyl phthalate with polystyrene and Histoclear and coverslipped.

2.7.1 *Reagents for Palmgren's Silver Stain*

1. **1% celloidin**: 1gm of celloidin was dissolved in 50ml ether overnight and 50ml of absolute alcohol added.

2. **Acid formalin:** Made up on day of use.

	100ml	250ml
40% formaldehyde	25ml	63ml
dist H_2O	75ml	187ml
1% nitric acid	0.2ml	0.5ml

3. **Silver solution:** Made up on day of use

Silver nitrate	15g	37.5g
Potassium nitrate	10ml	25ml
dist H_2O	100ml	250ml
5% glycine	1ml	2.5ml

4. **Reducer:** Allowed to stand for 24hrs before use.

Pyrogallol	10gm
dist H_2O	450ml
Abs. ethanol	550ml
1% nitric acid	2ml

5. **Toner:**

Gold chloride	1gm
dist H_2O	200ml
glacial acetic acid	0.2ml

6. **Hypo:**

5% sodium thiosulphate

2.8 Carnoy's fixative (For 100ml)

Absolute ethanol	60ml
Chloroform	30ml
Glacial acetic acid	10ml

2.9 Gelatin coating of glass slides

Glass slides were placed in metal racks and immersed in a solution of 5% Decon 75 in distilled water and sonicated for 20 min. The slides were then given several washes of distilled water and incubated in a solution of 0.5% gelatin, 0.05% chromic potassium sulphate for 1 min. The coated glass slides were finally dried at room temperature and sealed in polythene bags.

CHAPTER III

Embryonic axon growth in adult white matter tracts

INTRODUCTION

Recently, several observations have challenged the idea that the adult central nervous system is non-permissive to the long growth of axons (Tønder *et al.*, 1990) showed that late embryonic hippocampal cells transplanted into a previously lesioned hippocampus could be labelled by injections of a retrograde tracer in the contralateral hippocampus. Fujii, (1989, 1991) used retrograde and orthograde labelling techniques to show long axon growth from embryonic mouse olfactory bulbs transplanted into adult mouse brain. Wictorin and colleagues (Labandeira-Garcia *et al.*, 1991; Wictorin *et al.*, 1989a; Wictorin *et al.*, 1990a, 1990b; Wictorin *et al.*, 1991) have used a number of different axon labelling techniques to demonstrate that transplanted embryonic neuroblasts are able to grow axons along adult host myelinated fibre tracts to appropriate terminal fields, and Strömberg *et al.*, (1992) have shown that axons from transplanted human neuroblasts can cross the myelinated fibre bundles of the adult rat corpus callosum. Most of these studies have worked with transplants into regions of host neuropil which have been subjected to prior chemotoxic lesions, and used relatively large transplants, which themselves would cause extensive damage at the implantation site.

3.1.1 Microtransplantation

To focus on the factors affecting long axon growth in adult myelinated fibre tracts, I have used a microtransplantation technique developed in our laboratory (Emmett *et al.*, 1989; Suzuki *et al.*, 1989) in which a pulsed air

pressure system (see *Chapter II*) can be used to inject a small volume of a suspension of mid to late embryonic neurons and glia *directly into* an adult myelinated fibre tract. For the initial series of transplants, E14 and E18/19 mouse hippocampal microtransplants were injected into the adult rat fimbria where apart from a few cases with minor contact with the host field CA3, the transplants were completely enclosed within the host tract.

3.1.2 Axonal markers

The cross-species xenografting paradigm (with immuno-suppression) was chosen because it offered the advantage of using the species-specific axonal markers such as anti- M6 and anti- Thy-1.2 antibodies, to identify individual donor axons among the host tract axons.

3.1.2.1 *M6*

M6 antigen is a 35 kD glycoprotein first expressed on the surface of post-mitotic murine CNS neurons at embryonic day 10 (Lagenaur *et al.,* 1992). By embryonic day 11, M6 is expressed extensively throughout the brain and spinal cord and maintained throughout adult life. However, little M6 expression can be detected on myelinated axons and in the optic nerve M6 expression is downregulated with the onset of myelination (Lund *et al.,* 1986). There is little or no expression of M6 on murine glia or their precursors (Lagenaur *et al.,* 1992). The M6 molecule is thought to play an active role in axon growth and antibodies against M6 have been demonstrated to inhibit neurite extension,

without growth cone collapse, in cultures of cerebellar neurons (Lagenaur *et al.*, 1992).

3.1.2.2 *Thy-1*

Thy-1 is a major cell surface glycoprotein expressed on thymocytes and on the majority of neurons and their axons in the mouse and rat CNS from embryonic day 19 onwards (Barclay *et al.*, 1976). At 25 kD molecular weight, it is the smallest known member of the immunoglobulin super family (Williams, 1985). The mature protein contains 111 amino acids and is attached to the cell membrane by a glycosyl-phosphatidylinositol tail. It comes in two allelic forms termed Thy-1.1 and Thy-1.2. I used donor tissue from a Thy-1.2 positive mouse strain and transplanted into a Thy-1.1 positive host rat strain, making it possible to selectively stain mouse axons from the grafts with anti-Thy-1.2 immunohistochemistry. No separate host pre-lesion was carried out, and as far as possible I attempted to minimise local disturbance or damage to the host fibre tract.

3.1.3 Specificity of axonal growth

The microtransplantation approach was then extended to two other adult central tracts - the corpus callosum and the cingulum. Using cell suspensions from three different embryonic areas - the hippocampus, the neocortex and the superior colliculus, I have explored the need for specificity of matching of donor cells and host pathways.

3.1.4 Relationship of donor axon growth to tract structure

Using serial section analysis I have compared the orientation of the donor axons with that of the surrounding axonal and glial structure of the host fibre tracts, and examined whether the course of the newly growing axons respects the boundaries between adjacent tracts. I have also studied the internal neuronal/glial structure of the microtransplants and how it relates to the surrounding adult tract framework.

3.2.1 Preparation of embryonic cell suspensions

E14 and E18/19 (E0=day of vaginal plugs) CBA(II) mouse embryos, and E18 AS rat embryos (as controls for the species-specific M6 marker used for identifying the mouse axons) were obtained under aseptic conditions from adult pregnant female CBA mice and AS rats respectively, under terminal pentobarbitone anaesthesia (Sagatal, RMB Dagenham UK) by laparotomy without repair. The brains of the embryos, were removed under aseptic conditions and immersed in a defined medium (1:1 mixture of Ham`s F12 medium and Dulbecco-Vogt modification of Eagle`s medium (Life Technologies Ltd, Paisley, UK) supplemented with 5µg/ml insulin, 100µg/ml transferrin, 20µM progesterone, 30µM selenium and 100µM putrescine (all components purchased from Sigma, Poole, UK; Bottenstein and Sato, 1979)). Under sterile conditions the meninges were removed, and for the initial series of transplants, hippocampi dissected out and cut into several pieces (viewed with a dissection microscope).

The hippocampal pieces were then washed in 10ml of 0.1M PBS, incubated in 2ml of 0,1% trypsin (Sigma) in PBS at 37°C for 15 mins and the reaction stopped by the addition of 200µl of fetal calf serum. Excess trypsin was removed by centrifuging the above medium and hippocampal pieces at 1200 rev/min for 5 minutes, replacing the supernatant with 10ml of fresh medium and resuspending the pieces. This was repeated 3 times, after which the

hippocampal pieces were triturated into a cell suspension using a fire polished pasteur pipette in 1ml of the medium. The cell density was then counted with a haemocytometer under an inverted microscope; 2-5µl of 0.5% DNAse (Sigma) was added to prevent cell aggregation, and the final cell density made up to approximately $6x10^6$ cells/ml with fresh medium. The cell suspension was kept on ice ready for transplantation with any suspension remaining after operating plated out onto polyethylenimine coated 35mm dishes and further cultured to check neuron viability.

For the specificity and tract structure experiments a further series of cell suspensions were prepared as above, at a concentration of 8-20 x 10^6 cells/ml from hippocampus, parietal neocortex and superior colliculus dissected from E14 and E18 CBA(II) mouse embryos and also kept in a defined medium (Bottenstein and Sato, 1979) on ice at 4°C.

3.2.2 Transplantation

Adult female AS rats (of a locally maintained strain), body weight 180-200 g, were placed under tribromoethanol anaesthesia (20 mg/100 g body weight, ip) and inserted into stereotaxic surgery apparatus (NIMR Engineering) with their heads in the flat skull position i.e. the incisor bar 3.3mm below the horizontal plane passing through the interaural line. A small burr hole was made at the required coordinates and a pulsed air pressure system (Suzuki *et al.,* 1989; Emmett *et al.*, 1989; see Fig. 1) used to inject 0.5 µl of suspension (containing

0.4 - 1.0 x 10^4 cells, which included neurons, glia and precursors) through a glass micropipette (50 µm internal diameter, with a bevelled tip) into one of 4 sites in the left hemisphere - the medial part of the fimbria, the lateral part of the fimbria, the rostrum of the corpus callosum, and the cingulum. The stereotaxic coordinates, measured from the bregma with the head held in the flat skull position, were medial fimbria: 1.6 mm caudal, 1.3 mm lateral, 4.1 mm ventral; lateral fimbria: 3.0, 3.2, and 4.1; corpus callosum: 1.4, 1.2, and 3.0 mm, and cingulum: 1.4, 0.9, and 3.0 mm. Graft rejection was suppressed by maintaining the animals from the time of operation on cyclosporin A (Sandimmun, Sandoz; 10 mg/100 ml in the drinking water).

For the initial series of hippocampal microtransplants to the fimbria, 22 animals with mouse donor cells (8 from E14 donors, and 14 from E18/19 donors; Table 1), and 4 with E18 rat donor cells (as controls), were sacrificed under deep terminal pentobarbitone anaesthesia (Sagatal, RMB Dagenham UK) by transcardial perfusion of about 200ml of PBS after survivals ranging from 7 to 47 days.

For the specificity and tract structure/transplant integration study, 55 animals with mouse donor cells microtransplants and survivals of 3 to 43 days (Table 2) were similarly sacrificed under deep terminal pentobarbitone anaesthesia (Sagatal, RMB Dagenham UK) by transcardial perfusion of about 200 ml of PBS.

Table 1

Mouse hippocampal microtransplants to rat fimbria. Numbers of cases at the two donor ages with different postoperative survival times.

Donor age (E day)	Survival Days postop	Number of cases
14	7	4
	13	1
	14	1
	37	2
18	6	1
	7	2
	8	1
	9	2
	11	1
	12	2
	14	1
	21	2
	47	2
	Total	**22**

Table 2

Specificity and tract structure study. Mouse hippocampus, neocortex and superior colliculus microtransplants to the different host adult tracts.

Donor tissue	Host tract	No of animals	Survival range (days)
E14/18 neocortex	Fimbria	10	6 - 41
	Corpus callosum / cingulum	6	3 - 36
E14/18 hippocampus	Corpus callosum / cingulum	9	6 - 43
E14 superior colliculus	Fimbria	12	7 - 36
	Corpus callosum / cingulum	6	6 - 31
E18 superior colliculus	Fimbria	8	6 - 10
	Corpus callosum / cingulum	4	3 - 7
Total		**55**	

3.2.3 Histology for microtransplantation studies

After perfusion, the brains were dissected out and rapidly frozen in crushed dry ice. Brains were then mounted in a thin layer of cryostat embedding compound (Cryo-M-Bed, Jencons Scientific Ltd.) and 10µm cryostat sections cut (on a Reichert-Jung 2800 Frigocut-E cryostat, Leica, UK) in a horizontal plane parallel to the dorsal surface of the brain, so as to give the longest possible continuous length of the axons and interfascicular glial rows in all the tracts. Serial sections were taken through areas of interest and collected on to gelatin coated slides and dried.

3.2.3.1 *For M6 immunohistochemistry*

Sections were fixed on the slide in 4% paraformaldehyde in 0.1M PBS at room temperature for 20-30 min, washed in several changes of 0.1M PBS for at least 30 min, incubated for 30 min in 1% dried milk (as a source of non-specific protein) in 0.1M PBS, followed by an overnight incubation with a 1:30 dilution of M6 IgG2a antibody (Lund *et al.,* 1985) in 1% dried milk in PBS at 4°C in a humidified chamber. Sections were then washed thoroughly for 30 min in several changes of 0.1M PBS, and incubated for 2 hr in 1:100 anti-rat HRP conjugated secondary F(ab')2 antibody (Amersham, Bucks UK) in 1% dried milk in 0.1M PBS at room temperature. The sections were washed thoroughly for 30 min in several changes of 0.1M PBS, incubated in 50 mg/100 ml diaminobenzidine (DAB) and 0.006% hydrogen peroxide in phosphate buffer with 10mM imidazole at pH 5.8 for 3 min, washed thoroughly for 10 min in several changes of 0.1M PBS, then distilled water for 30-60 min, and silver

intensified using a physical development (Woodhams *et al.,* 1989, see below). The intensified sections were dehydrated through a series of alcohols, cleared with Histoclear (National Diagnostics, Aylesbury, UK), and mounted in a mixture of dibutyl phthalate with polystyrene and Histoclear. Some sections were counterstained lightly with aqueous thionin.

3.2.3.2 *Silver Intensification*

Having been washed in several changes of distilled water after DAB treatment, sections were immersed in a 0.1% gold chloride solution for 5 min and then washed for 5 min in distilled water. Sections were then incubated for 5 min in a 2.5% solution of sodium sulphide at pH 7.4, then washed for 5 min in distilled water and immersed in developer (see below) for between 2 to 10 min depending on the original DAB signal and background. The reaction was stopped by immersing the sections in 1% acetic acid for 1 min, followed by fixation in a 1% sodium thiosulphate solution for 5 min. Sections were then counterstained, dehydrated and mounted as detailed above.

3.2.3.3 *Silver enhancement developer*

Stock solutions

A:	Na_2CO_3 (anhydrous)	4.17g in 100ml of distilled water.
B:	NH_4NH_3	0.2g
	$AgNO_3$	0.2g
	Tungstosilicic acid	1.0g
	($SiO_2.12WO_3.26H_2O$	

Dissolved in 100ml distilled water in order given.

C: To 50ml of solution B, 365 µ l formalin (stock 35-40%) were added.

The following proportions of B were added to A whilst stirring, then C was added, slowly to make up a final volume of 100ml of developer.

A 50ml

B 25ml

C 25ml

3.2.3.4 *Controls*

The immunhistochemical controls consisted of: (1) a specially prepared series of rat-to-rat transplants in which M6 immunohistochemistry was performed, and (2) representative sections from the mouse-to-rat transplants, where the primary antibody was omitted.

3.2.3.5 *Thy-1.2 immunohistochemistry*

Sections were treated as for M6, but with no pre-incubation with dried milk, using 1:1000 anti-Thy-1.2 antibody (Dupont, Wilmington, Delaware), and 1:100 anti-mouse horseradish peroxidase (HRP) conjugated secondary F(ab')2 antibody (Amersham).

3.2.3.6 *Py immunohistochemistry*

Py is a monoclonal antibody that selectively stains a cytoplasmic neurofibrillar component in hippocampal CA3 pyramids, hilar cells and interneurons, but does not stain CA1 pyramids or dentate granule cells (Woodhams *et al.,* 1989). Our laboratory has confirmed (unpublished) that Py has the same cellular

distribution in the mouse hippocampus. Sections were treated as for M6, except that the initial formaldehyde fixation was for only 10 min, and the 30 min pre-incubation with 1% dried milk was omitted. The primary, Py, monoclonal antibody was used at a 1:200 dilution, and the anti-mouse HRP conjugated secondary F(ab')2 antibody (Amersham) at 1:100.

3.2.3.7 *GFAP and vimentin immunohistochemistry*

Adjacent 10µm cryostat sections were either fixed with 4% paraformaldehyde (as above) for glial fibrillary acidic protein (GFAP), or fixed with 5% acetic acid in 96% ethanol at -20°C, for 15 min for GFAP or vimentin. The primary antibodies were monoclonal anti-GFAP antibody (Amersham) at 1:1000, and monoclonal anti-vimentin IgG (Amersham) at 1:100, respectively. The secondary antibodies and subsequent processing were: for GFAP: 1:100 HRP-conjugated sheep anti-mouse IgG (Amersham) for 2 hrs at room temperature in 1% dried milk in 0.1M PBS, washed, DAB treated; for vimentin: 1:300 horse biotinylated horse anti-mouse IgG (Vector) in 0.1M PBS for 30 min, washed and treated with ABC Vectastain (Vector). All sections were washed, DAB treated, silver intensified, and lightly counterstained with aqueous thionin.

3.2.3.8 *Other antibodies*

Adjacent sections were either fixed with paraformaldehyde (as above) for laminin immuno-histochemistry, or Griffonia lectin staining for microglia (as in Streit, 1990; Suzuki and Raisman, 1992), The primary antibody was rabbit anti-laminin antiserum (Serotec, Oxford) at 1:500, The secondary antibody and

subsequent processing were: 1:200 biotinylated goat anti-rabbit IgG (Vector, Peterborough UK) in 0.1M PBS for 30min, washed, ABC Vectastain (Vector), washed, DAB treated.

3.2.3.9 *Electron microscopy*

Deeply anaesthetised rats were transcardially perfused with a mixture of 1% paraformaldehyde and 1% glutaraldehyde in 0.1M PB at pH 7.3. The brains were removed, blocks taken, postfixed for 1.5 hours in 2% aqueous osmium tetroxide, dehydrated from 30% to absolute alcohol over 3 hours, and embedded in Epon embedding resin (TAAB Laboratory Equipment Ltd, Reading, UK). 2µm semithin and 80nm ultrathin sections were cut on a Reichert-Jung Ultracut E microtome (Leica, UK). Semithin sections were collected on gelatin coated glass slides and ultrathin sections dried on to copper grids. Semithin sections were stained with a mixture of methylene blue and Azur II, and ultrathin sections with uranyl acetate and lead citrate. Electron microscopy was carried out on a Philips EM201C transmission electron microscope.

RESULTS

3.3.1 Hippocampal microtransplants to the fimbria

3.3.1.1 Transplant location

22 transplants (including the rat controls) were located about 1mm from the midline (e.g. Fig. 2), in the part of the fimbria between the rostral edge of the hippocampus and the lateral edge of the septal nuclei. A further 4 transplants were located in the lateral edge of the fimbria immediately adjacent to the alveus of field CA3.

3.3.1.2 Morphology of the transplants

The transplants were readily recognised in the thionin stained sections (Fig. 2) as compact neuronal clusters, around 1mm in length, and elongated along the axis of the fimbria. They were sharply demarcated from the surrounding fibres of the neuron-free host fimbria with its characteristic longitudinal interfascicular rows of much smaller glial nuclei (Fig. 2; Suzuki and Raisman, 1992).

Counts from a series of thionin-stained sections through a representative E14 transplant at 7 days survival, with a volume of about $1.5 \times 10^4 \mu m^3$, showed that there were about 4,000 cells (Abercrombie split nucleus correction method; (Konigsmark, 1970), and semithin sections indicated that about 75% of the cells were neurons. The majority of the transplanted neurons (Fig. 2) had the large, pale nuclei, voluminous cytoplasm, and wide dendrites typical of hippocampal

Figure 2

A transplant (T) in the medial edge of the fimbria. Enlarged boxes indicate (**a**) transplant neurons and (**b**) host pyramidal cells of the rostral hilus. Thionin stain. E14 donor tissue; 37d survival. This and all subsequent sections up to figure 39 are taken in a horizontal plane parallel to the dorsal surface of the brain so as to display the greatest longitudinal extent of axons and interfascicular glial rows of the rostral fimbria. (sg) stratum granulosum. Scale bars, 500μm;(a,b) 50μm.

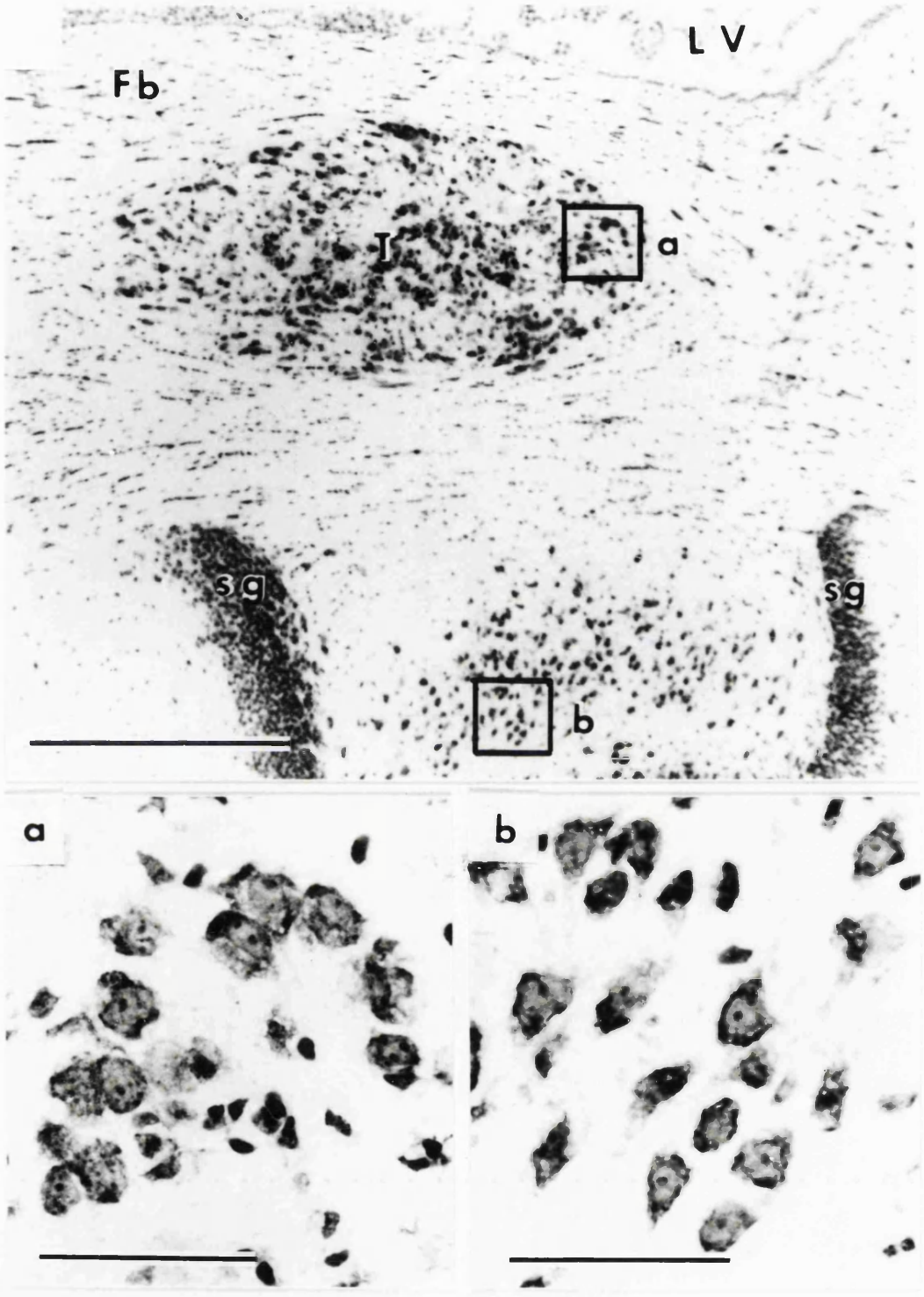
Fb
LV
I
a
sg
sg
b
a
b

pyramidal cells (Fig. 2a, compare with the rostral part of the host field CA3 in Fig. 2b).

In a proportion of the transplanted pyramidal cells (1-10 per section; e.g. arrows in Fig. 3A) the soma and dendrites had a dense fibrillar cytoplasmic component (Fig. 3B) which was strongly immunostained with the Py monoclonal antibody (Woodhams *et al.,* 1989), which is characteristic of hippocampal CA3 pyramidal cells in situ (Fig. 3A). The transplant cells and neuropil as a whole were strongly stained with M6 and Thy-1.2 (e.g. Fig. 4).

The transplants were well vascularised, with normal, narrow capillaries and a few, prominent, large diameter, thin-walled, vessels (Fig. 5A; see also Fig. 3a in (Wictorin *et al.,* 1991)Wictorin et al., 1991) and vascular-associated 'spikes' of basal lamina (Lawrence *et al.,* 1984). There were no histological signs of immune rejection (infiltration of immunocytes or cuffing of blood vessels; (Lawrence *et al.,* 1990).

3.3.1.3 Minimal disturbance to host

The transplants made direct contact with the bundles of host myelinated axons (Figs. 5A,B, 6A). There was little evidence of damage to the host fimbria. Semithin sections and electron microscopy at 6 days after transplantation showed a mass of healthy transplant cells at various stages of maturity, occasional electron dense dying donor cells, healthy neuropil processes, but no synapses, and only occasional degenerating host axons.

Figure 3

A. A hippocampal microtransplant with Py-positive donor cells (e.g. arrows) in the medial edge of the fimbria (Fb). Note strongly Py-positive host CA3 pyramidal cells in the rostral hippocampal pole (R); (LV) Lateral ventricle; (sg) stratum granulosum . **B.** High power of a Py-positive donor pyramidal cell in the transplant (T). Py immunohistochemistry. E18 donor; 47d survival. Scale bars, 500, 50µm.

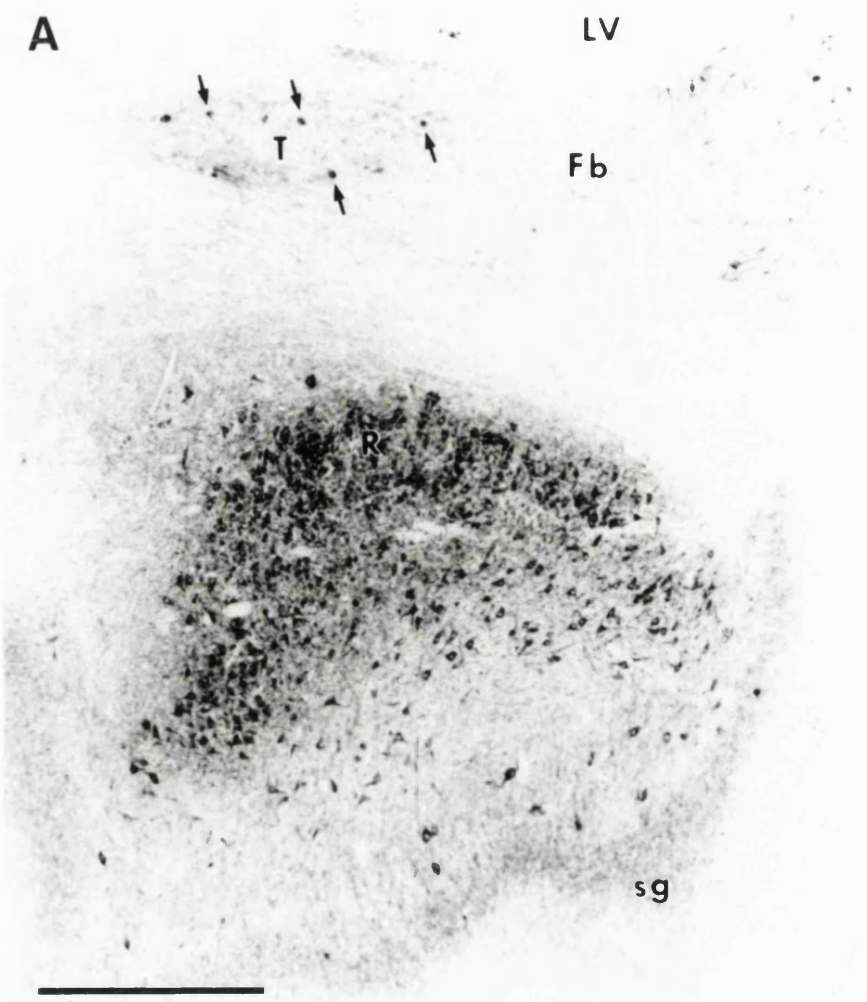
A
LV
T
Fb
R
sg

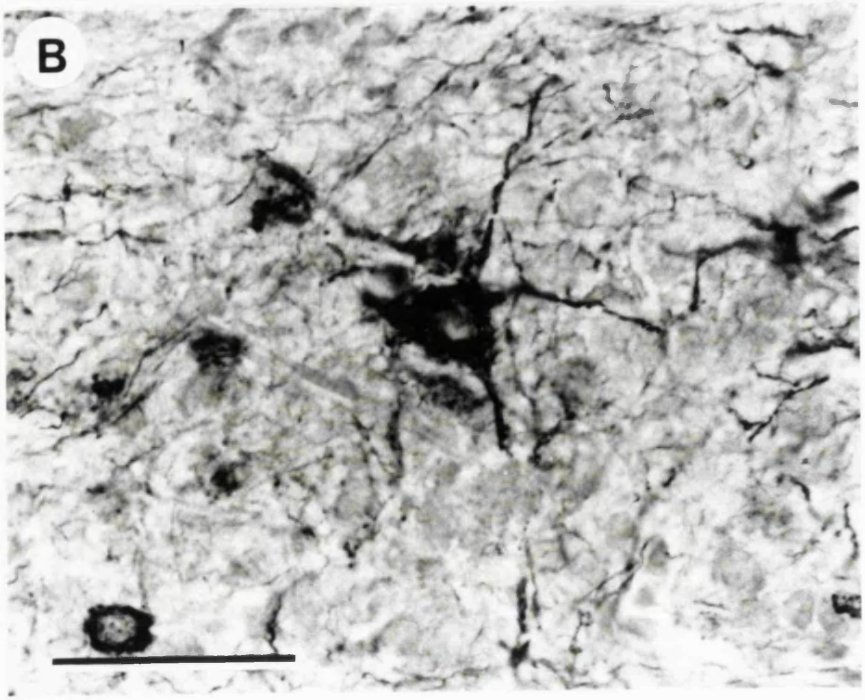
B

Figure 4

A transplant (T) in the medial edge of the fimbria (Fb); (LV) Lateral ventricle . Thy-1.2 immunohistochemistry. E14 donor; 37d survival. Scale bar, 250µm.

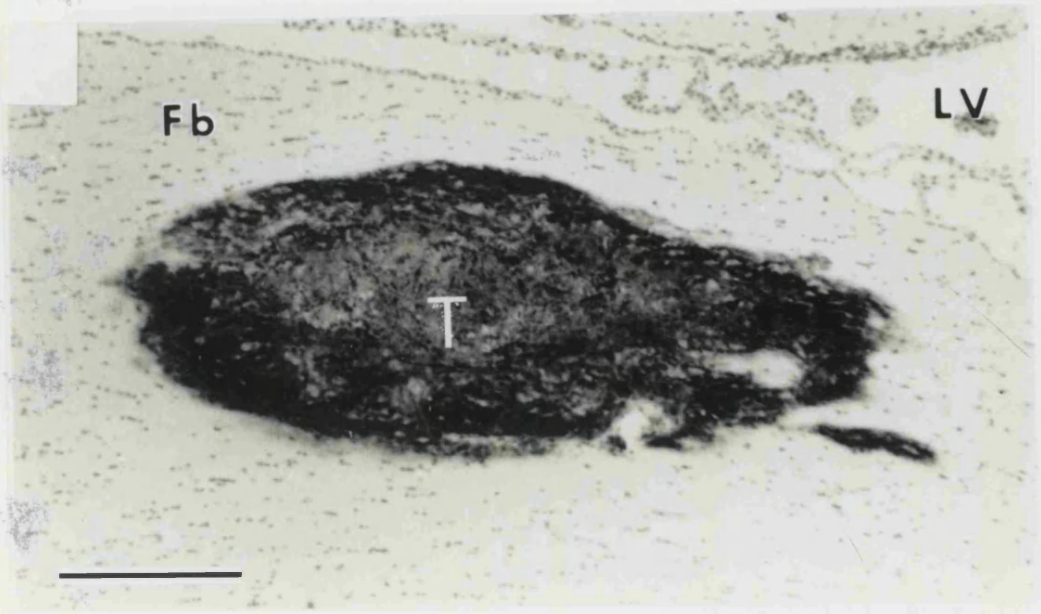
Fb
LV
T

Figure 5

A. Small, dorsal tip of a transplant (T) in the medial edge of the fimbria (Fb). Semithin section, methylene blue and Azur II stain. (BV), prominent, thin-walled, wide-diameter blood vessels. **B.** Enlargement of part of Fig. 5A to show myelinated axons (arrow heads) traversing the transplant, and a neuron (asterisk keys to Fig. 5A) with 2 small dark satellitic glia (g). E18 donor tissue, 47d survival, Scale bars, 100µm (A), 10µm (B).

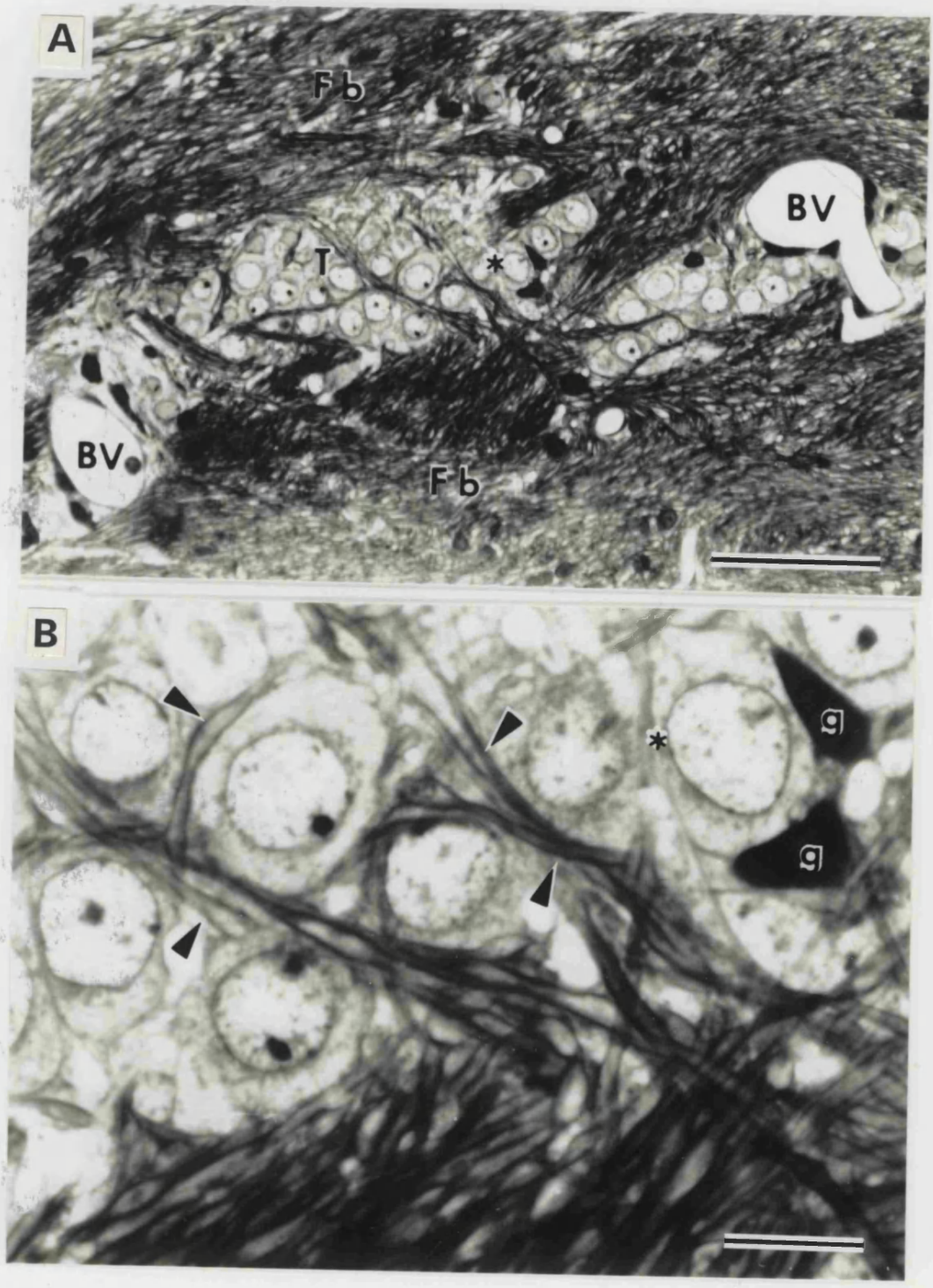
A
Fb
BV
T
*
BV
Fb
B
g
*
g

Figure 6

Electron micrographs. **A.** Mature transplant neurons (N) in close contact with myelinated fibres (e.g. arrow heads). **B.** Neuropil showing many synapses (e.g. arrow heads). E18 donor; 47d survival. Scale bars, 5µm (A), 1µm (B).

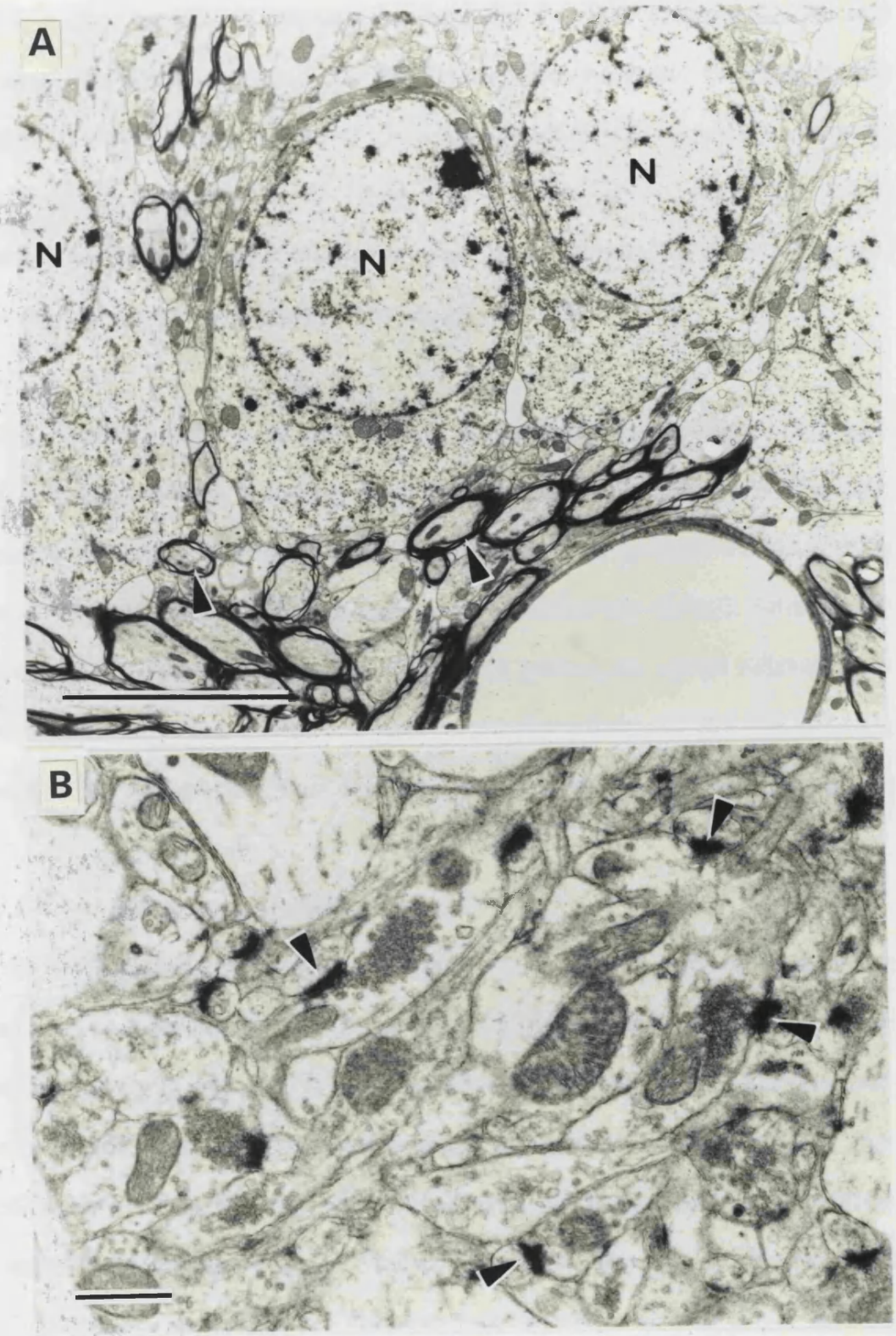
A
N
N
N
B

The rows of interfascicular host glial nuclei (Fig. 2) and the host fibres (stained with methylene blue in the semithin sections; Fig. 5A,B) swept around and through the transplants as if they had been opened out and infiltrated by the injected suspension. At longer survivals the transplants tended to become organised with an outer shell of fibres (Fig. 4) and semithin sections (Fig. 5A,B) and electron microscopy showed mature donor neurons (Fig. 6A) and well developed areas of synapse-rich neuropil (Fig. 6B).

GFAP immunostaining showed that the astrocytes in the transplant were more heavily stained than in the surrounding host tract. Vimentin immunostaining gave a complementary pattern: the graft was practically unstained (as was the host neuropil), but the host tract astrocytes were strongly stained. Neither stain showed any major hypertrophy of the host astrocytes, which retained their normal organisation. The host tract astrocytic processes did not form any recognisable barrier structure at the interface with the transplants (see below).

3.3.1.4 Identification of donor axons

The transplant-to-host projection fibres were well stained with the mouse species-specific markers M6 ((Lund *et al.*, 1985)Lund et al., 1985) and Thy-1.2, neither of which stained the rat host axons. M6 continued to stain transplant axons satisfactorily in this material at 47 days post transplantation (e.g. Figs. 8D,E, and 13A,B), the longest time studied. From the lateral end of the dorsal part of the transplant (Fig. 7A; Thy-1), and the medial end of the ventral part (Fig. 7B; M6), axons extended into the host fimbria either singly or in fascicles (Fig. 8A,B,C).

Figure 7

Projections from intrafimbrial transplants. **A.** Dorsal part of a transplant (T) showing fascicles of fibres (arrow) emerging at its lateral pole. E14 donor tissue, 37d survival, Thy-1.2 immunohistochemistry; (LV) Lateral ventricle. **B.** Ventral part of a transplant showing projections (arrows) leaving the medial pole. S, rostro-medial projection to the septal nuclei; (V) projection into the ventral hippocampal commissure. E18 donor tissue, 12d survival, M6 immunohistochemistry, Scale bar 500µm (A), 100µm (B).

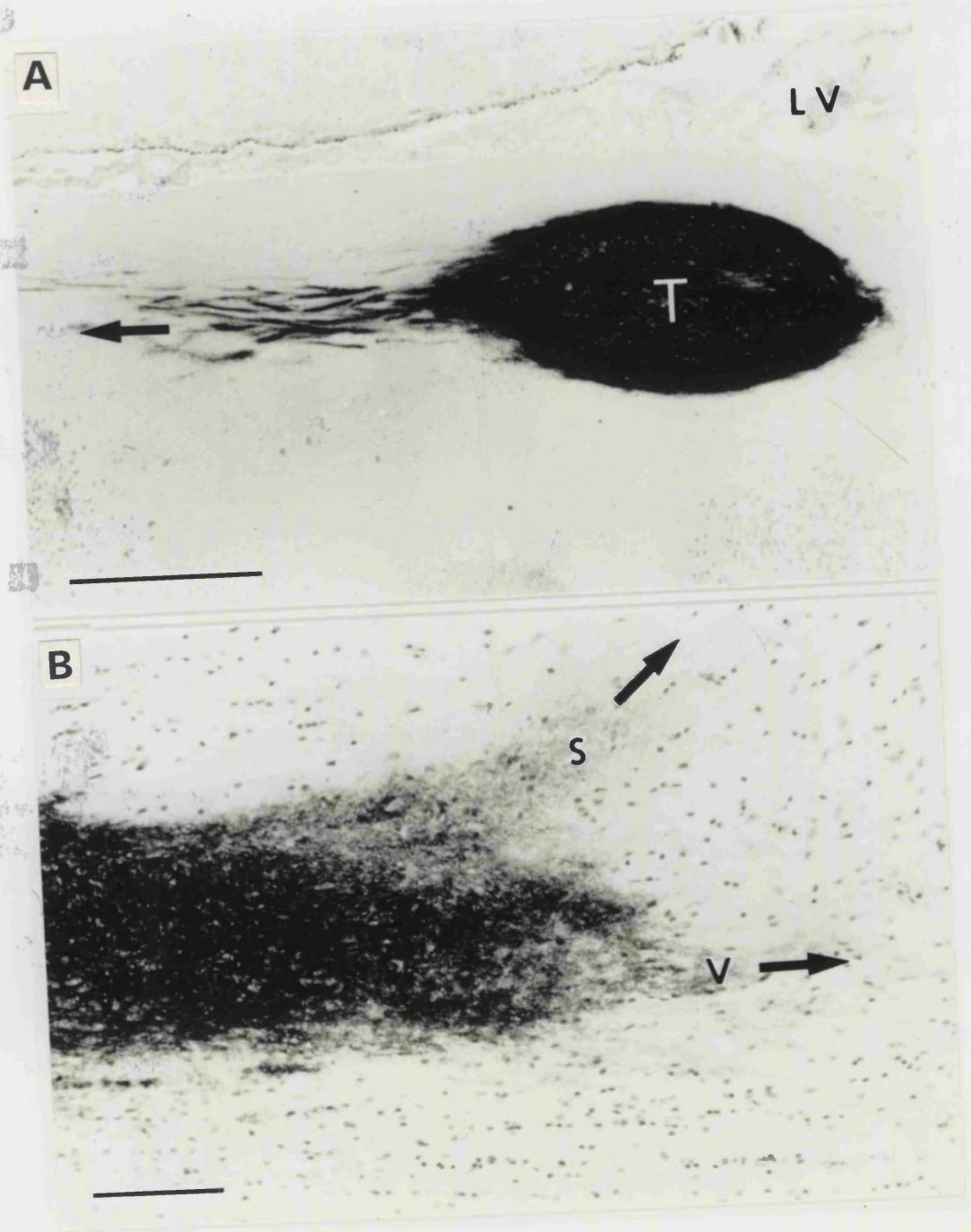
A
LV
T
B
S
V

Figure 8

Transplant fibres in the host fimbria. **A.** Masses of laterally directed fibres (arrow heads) leaving the extreme dorso-lateral tip of an intrafimbrial transplant (T), and running in the dorsal alveus (alv); (sr) stratum oriens; (sp) stratum pyramidale; (sr) stratun radiatum; (LV) lateral ventricle; (CS) corpus striatum . E14 donor tissue, 7d survival. **B.** Three fascicles of medially directed fimbrial fibres arising from a laterally placed intrafimbrial transplant. E18 donor tissue, 7d survival. **C.** Intrafimbrial fibres in fascicles (downward arrows) and singly (upward arrow heads) running parallel to the host fimbrial interfascicular glial rows (igr). E14 donor tissue, 7d survival. **D, E.** Interference contrast pictures showing individual transplant axons (dense black silver deposit) intimately integrated among the parallel host axons (faint lines), and also parallel (in E) to the rows of nuclei of the host fimbrial interfascicular glia (arrow heads). E18 donor tissue, 47d survival, M6 immunohistochemistry, Scale bars 250µm (A), 100µm (B,C), 5µm (D,E).

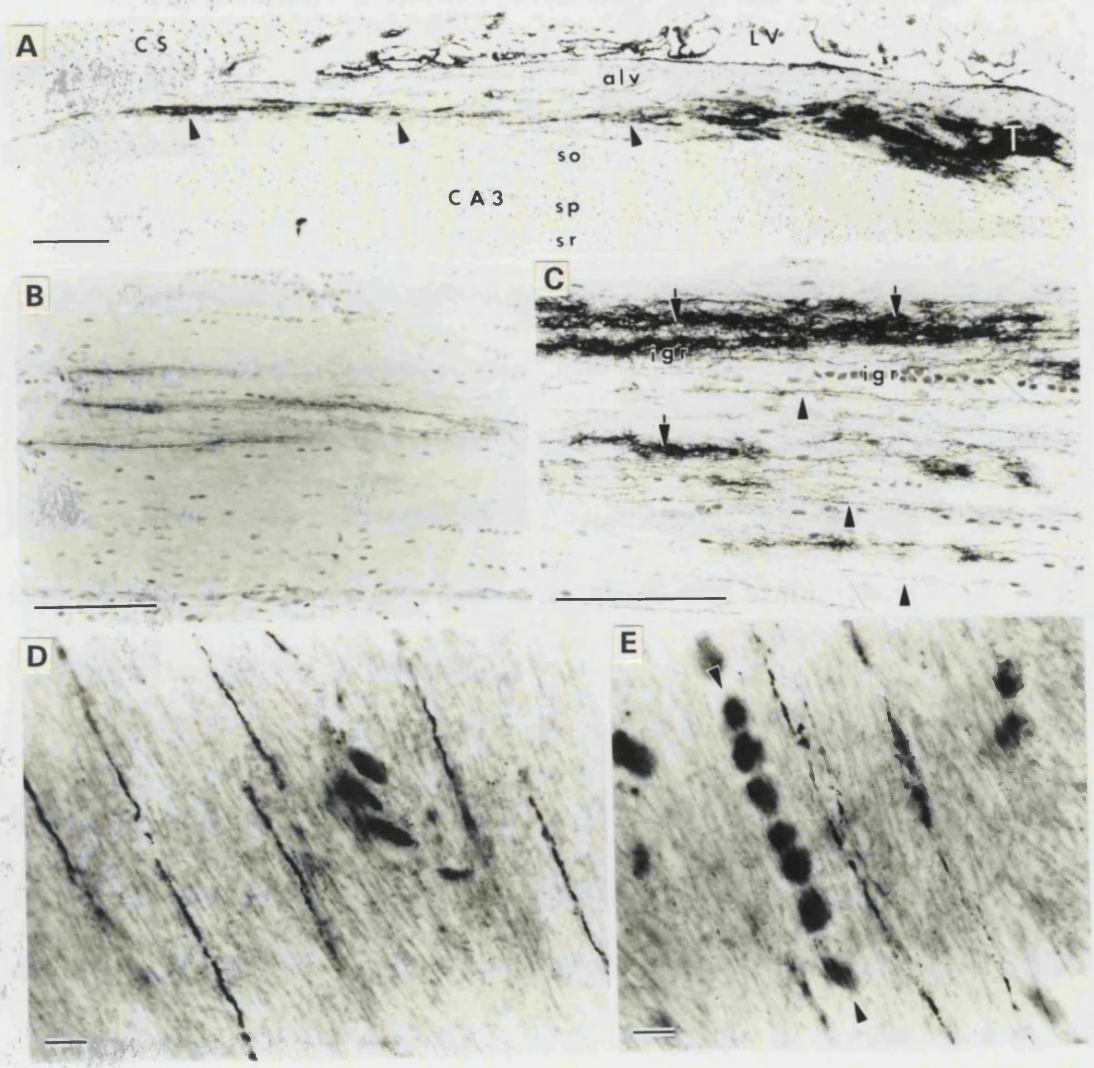
A
CS
LV
aly
T
so
CA3
sp
sr
B
C
igr
igr
D
E

The individual transplant projection fibres were very fine (of less than 0.5µm diameter) and untapering. I was not able to identify the leading edge of the growing axons.

As described in Material and Methods, sections were cut in a horizontal plane which approximates to the longitudinal axis of the host rostral fimbrial axons and interfascicular rows of glial nuclei (e.g. Fig. 8C,E). This plane of section showed clearly that the transplant axons were intimately integrated among the host fimbrial axons, parallel to them (Fig. 8D,E) and to the rows of host tract interfascicular glial nuclei (Fig. 8C,E).

3.3.1.5 Controls

In alternate sections from animals with M6 positive axonal projections, omission of the primary antibody prevented all immunostaining of the transplant neuropil or its axons or terminal fields (Cf Lund *et al.*, 1985). In sections from the 4 control experiments in which E18 rat hippocampal cells were used as the donor material, no M6 immunoreactivity was detected (Fig. 9). M6 primary antibody is raised in rat and therefore needs an anti rat secondary antibody for its detection. Use of the anti rat secondary on rat host sections produced an immune response associated background stain that was present even when the primary was omitted. The background varied from animal to animal and decreased with the longer survival times.

Figure 9

Control rat-to-rat transplant stained for M6 with silver intensification; (Fb) fimbria; (T) transplant; (R) rostral; (sg) stratum granulosum. E18 donor tissue, 7d survival, Scale bar 250µm.

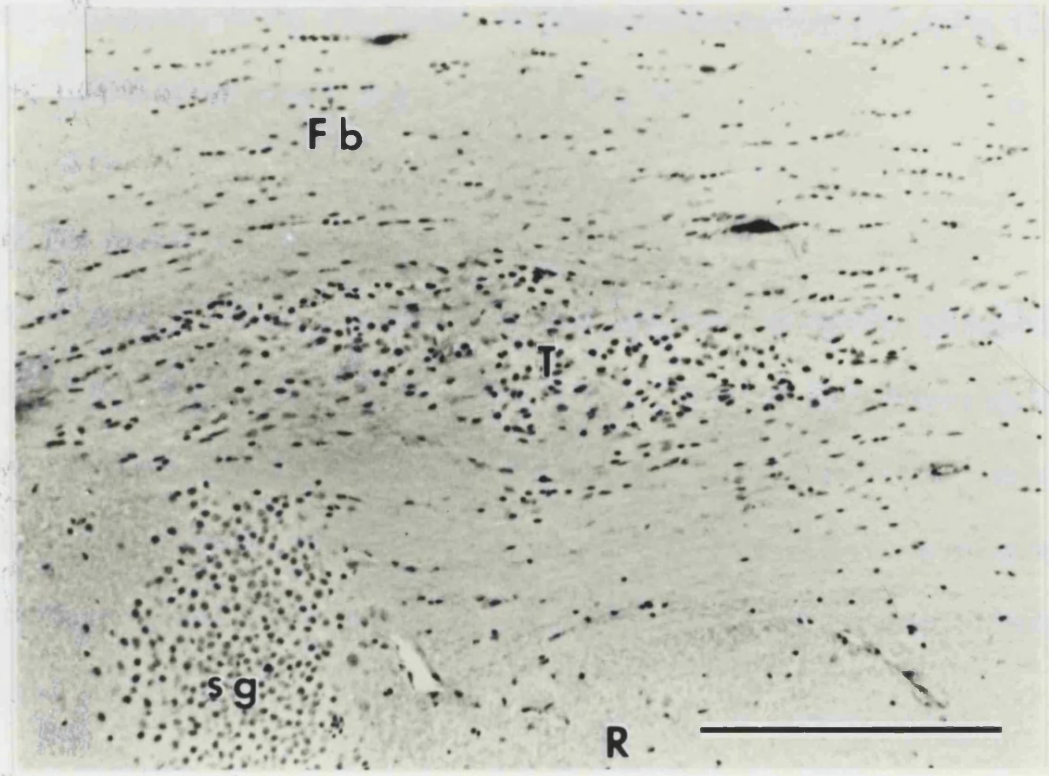
Fb
T
sg
R

3.3.1.6 Distribution of transplant projections

The medially placed intrafimbrial transplants projected to (1) *the ipsilateral hippocampus* (IH in Fig. 10), (2) *the contralateral hippocampus* (CH in Fig. 10), and (3) *the septal nuclei* (LSN and TSN in Fig. 10).

(A) *The ipsilateral hippocampus*

In the lateral direction, the series of horizontal sections showed that transplant axons (e.g. Figs.11A, and 16C) ascend to progressively more dorsal levels of the fimbria as they run back towards the rostral pole of the hippocampus, where fibres fan out into the alveus dorsal to the hippocampus, while other labelled bundles turn ventrally in the fimbria parallel to the border with the adjacent field CA3.

In the M6 material, the zone where the parent axons leave the alveus and enter the stratum oriens of field CA3 was marked by branching and the appearance of horse-tail like masses of extremely fine axonal profiles (Fig. 11B,C). The terminal regions had an amorphous overall staining of a browner colour than the transplant itself (Fig. 16C; seen also in the septal projection in Fig. 16D).

Compared with adjacent M6 stained sections, Thy-1.2 immunostaining (in 3 cases with survivals of 37 (2) and 47 days) gave a more distinct impression of a network suggesting terminal axonal arborization (Figs. 12, 15A,B, and 16A,B).

Figure 10

A schematic representation of the distribution of projections (arrows) from an intrafimbrial transplant. (CH) contralateral hippocampus; fx, fornix column; IH, ipsilateral hippocampus; LSN, lateral septal nucleus; TSN, triangular septal nucleus; VHC, ventral hippocampal commissure.

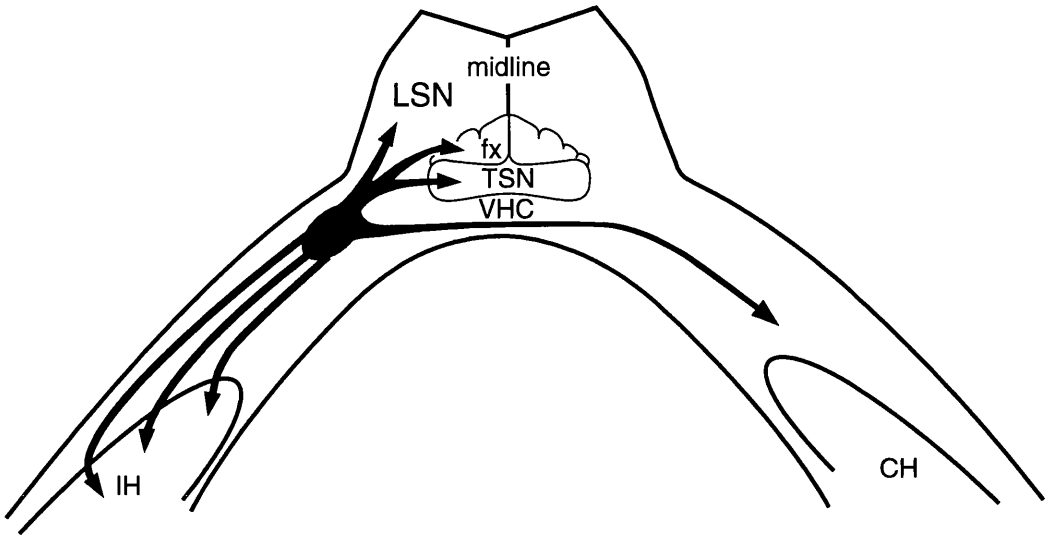
midline
LSN
fx
TSN
VHC
IH
CH

Figure 11

A. Intrafimbrial transplant (T) with laterally directed projection (downward arrow heads) entering the terminal field (upward arrows, see Fig. 11C) in the stratum oriens (so) of the hippocampus; (Fb) fimbria; (CS) corpus striatum; (alv) alveus; (sp) stratum pyramidale; (sluc) stratum lucidum; (slm) stratum lacunosum-moleculare. **B.** A pre-terminal axon (arrow head) entering the stratum oriens (so). **C.** Enlargement of the axons (arrows) entering the terminal field in Fig. 11A. E14 donor tissue, 7d survival, M6 immunohistochemistry, Scale bars 500μm (A), 50μm (B,C).

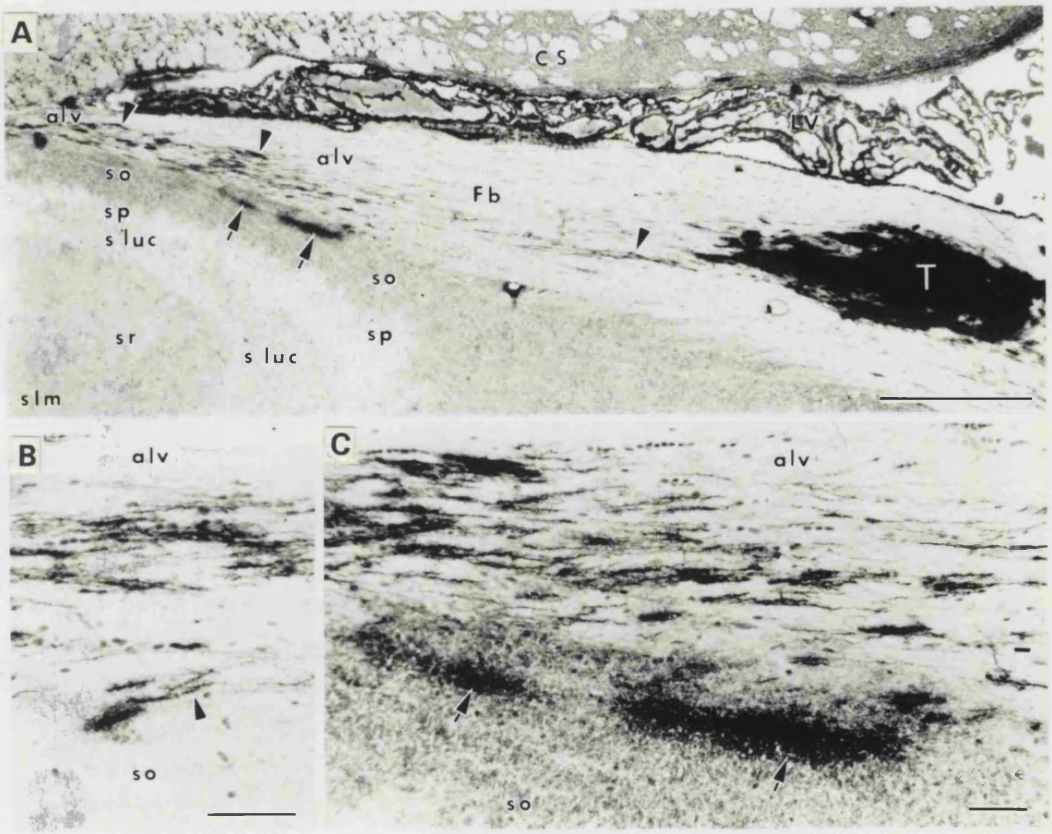
A
C S
alv
LV
alv
so
Fb
sp
s luc
so
T
sr
sp
s luc
slm
B
alv
so
C
alv
so

Figure 12

Lamination of terminal fields (arrow heads) in the stratum oriens (so) and stratum radiatum (sr) of field CA3 (dorso-rostral pole of the hippocampus). Staining absent in the alveus, stratum pyramidale (sp), stratum lucidum (sluc) and stratum lacunosum-moleculare (slm). Below: camera lucida drawing to show laminar boundaries; (LV) lateral ventricle; (IC) internal capsule . E18 donor tissue, 47d survival, Thy-1.2 immunohistochemistry, Scale bar 250μm.

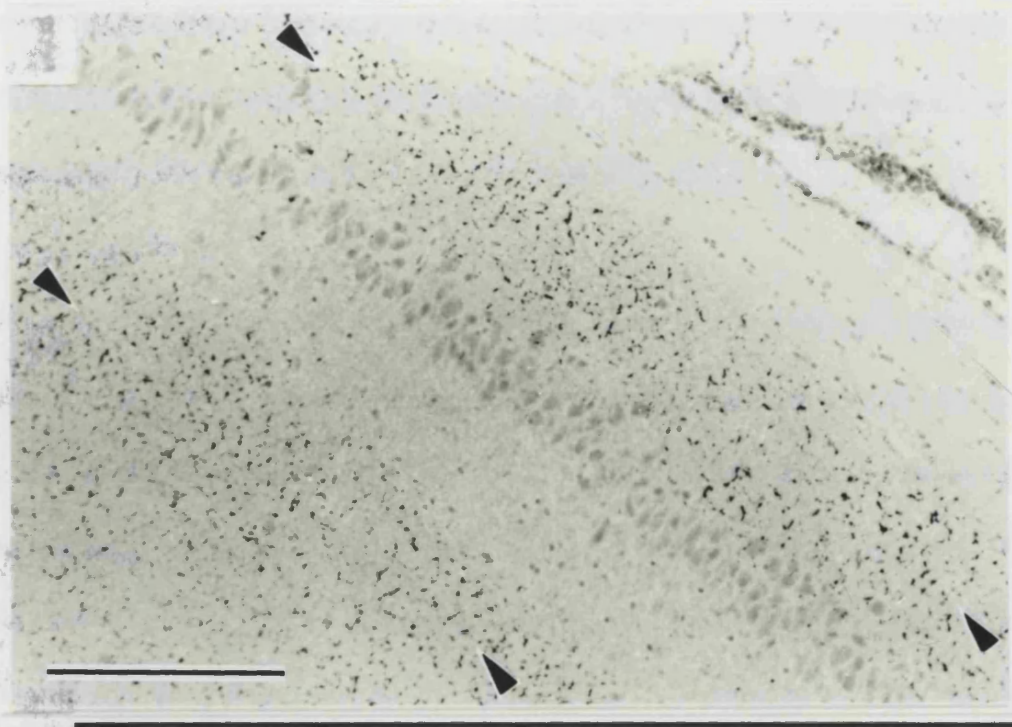

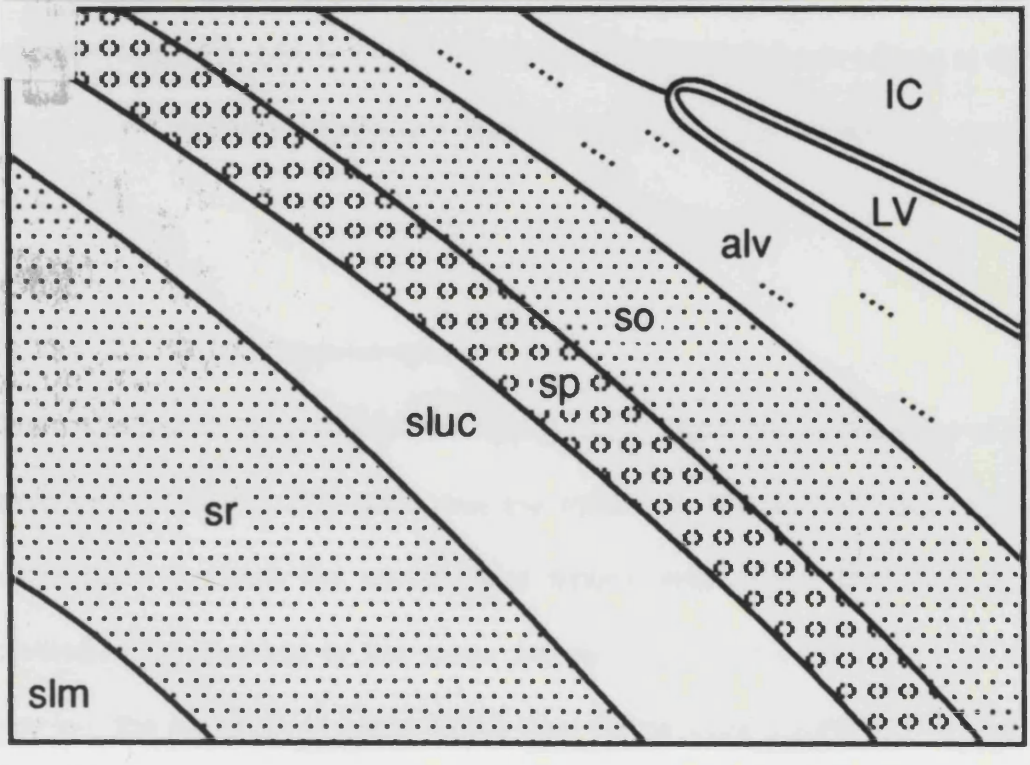
IC
LV
alv
so
sp
sluc
sr
slm

In an E18 donor case at 47 days, where the invasion of field CA3 of the host rostral hippocampal pole was more extensive, the entire width of the stratum oriens and stratum radiatum, but not the stratum pyramidale or stratum lucidum, were evenly filled for considerable distances (Fig. 12).

The majority of the transplant axons ran longitudinally along the axis of the host fimbria. However, as early as 7 days after operation, and increasingly at longer survivals, sections through the region where the dorsal tip of the transplant lay immediately in front of the rostral pole of the host hippocampal field CA3, showed M6-positive transplant fibres taking a direct route to the terminal field by running transversely across the fimbria (Fig. 10, arrow to R; Figs. 16A,B). In some cases (Fig. 13A,B) these could be seen to be collaterals arising at right angles to the course of the parent fibres running along the longitudinal axis of the fimbria.

(B) ***The contralateral hippocampus***

Fibres destined for the contralateral hippocampus leave the medial edge of the transplants (V in Fig. 7B) and cross the midline in the ventral hippocampal commissure to reach the contralateral fimbria and alveus (Fig. 14), in a distribution symmetrical to the much heavier ipsilateral projections. In my samples, the numbers of contralateral tract axons were insufficient to give a clear indication of terminal fields.

Figure 13

A. Dorso-lateral pole of a transplant emitting long, laterally directed projections (upward arrow head) parallel to the axons and interfascicular glial rows of the host fimbria (Fb), and caudally directed collaterals (horizontal arrows) running directly to the rostral pole (R) of the host hippocampal field CA3 in a direction at right angles (transverse) to the host fimbrial axis. **B.** Enlargement of the caudally directed transverse collateral (arrow on the left in A) to show its origin at right angles from a longitudinally directed parent axon. E18 donor tissue, 47d survival, M6 immunohistochemistry, Scale bars 100µm (A), 50µm (B)

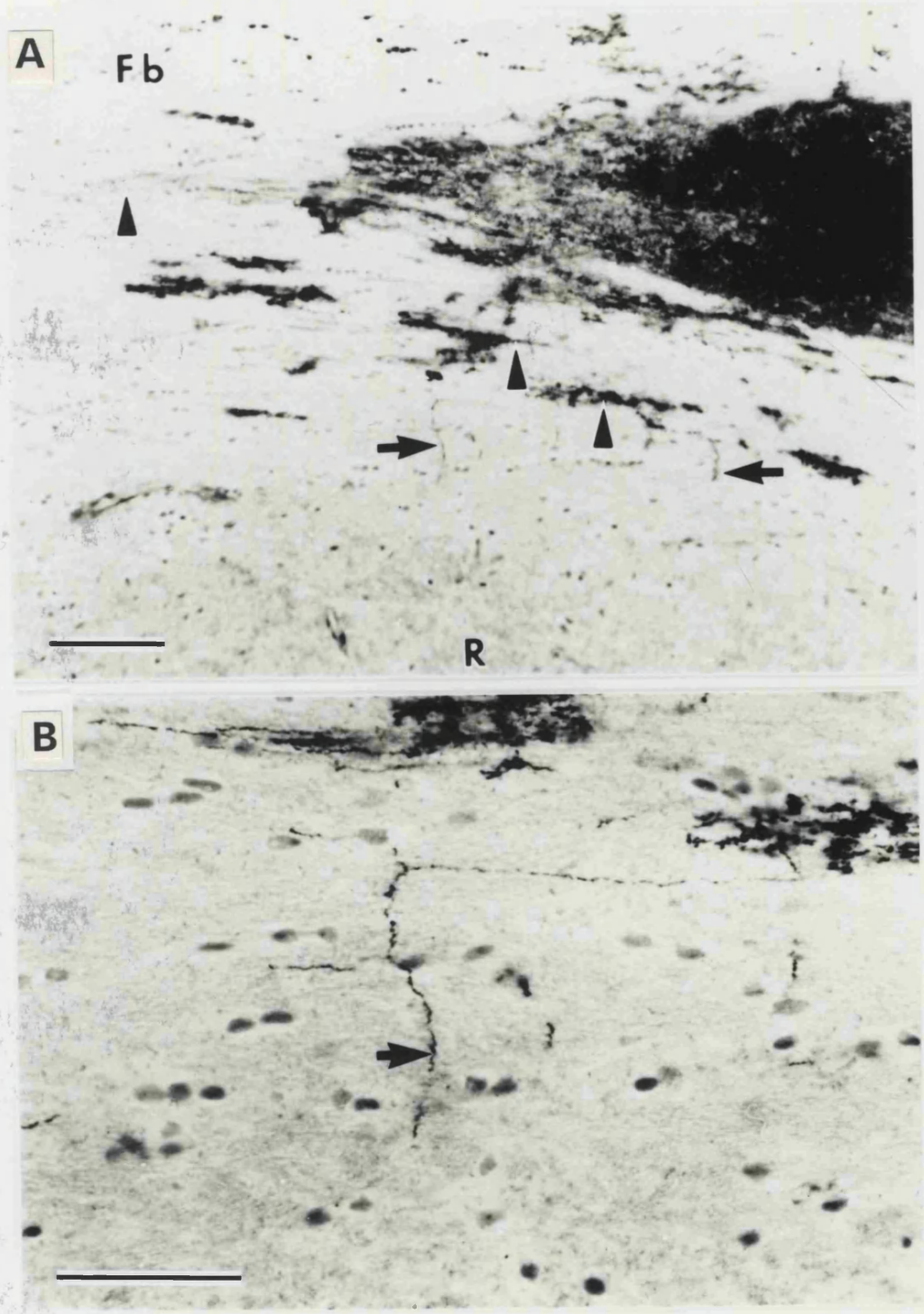
A
Fb
R
B

Figure 14

A single donor axon, about 8mm from the transplant, in the contralateral fimbria/alveus (alvc). (soc) stratum oriens of contralateral host hippocampal field CA3. E18 donor tissue, 12d survival, M6 immunohistochemistry, Scale bar 50µm.

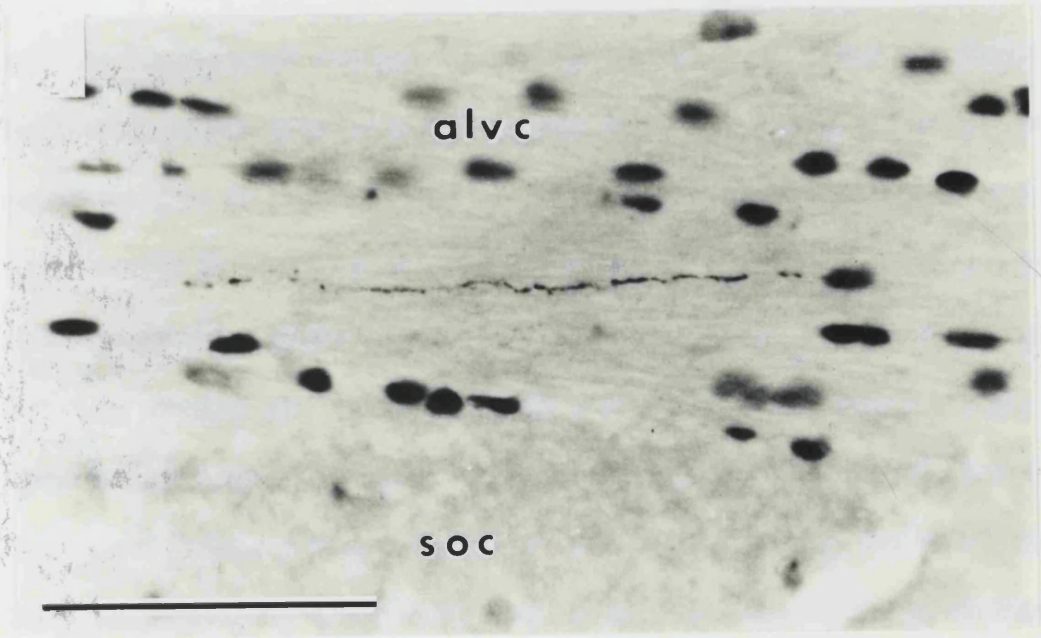
alvc
soc

(C) ***The septal nuclei***

Fibres destined for the septal nuclei leave the medial edge of the transplants (S in Fig. 7B) and generate amorphous (M6) or reticular (Thy-1.2) immunostaining which spreads out into the adjacent parts of the host terminal fields of the ipsilateral lateral septal nucleus (Fig. 16D). Caudally, the triangular septal nucleus (Fig. 15A,B), is a prominent target for the transplant axons, which are distributed mainly, but not exclusively to the triangular septal nucleus of the same side. Within this nucleus, the transplant axons form pericellular networks around the triangular septal nuclear neurons, which occupy a characteristic position, wrapped around, and partly inserted among the bundles of axons of the host postcommissural fornix (see also Fig. 10). I have not seen immunostained donor axons in the host dorsal fornix, and only few in the lateral bundles of the post commissural fornix at septal levels.

In the 4 cases with transplants in the lateral part of the fimbria, the transplant axons extended both medially (Fig. 8B), and also ventro-laterally in the host fimbria.

3.3.1.7 <u>Extent of axonal outgrowth</u>

By 7 days, fibres from the medially placed transplants had extended 5mm laterally from the transplant, the furthest point which they reach on the ipsilateral hippocampal circumference. At the same time the donor axons were observed about 4mm medial from the transplant, which took them through the ventral hippocampal commissure, across the midline, and into the contralateral fimbria/alveus. Beyond this time there was no appreciable further extension on

Figure 15

A. Terminal field in the triangular septal nucleus (arrow). (CC) corpus callosum; (fx) postcommissural fornix bundles; (LSN), lateral septal nucleus;(CS) corpus striatum; (LV) lateral ventricle; (VHC) ventral hippocampal commissure. **B.** Enlargement of the terminal field (arrow) from A. E14 donor tissue, 37d survival, Thy-1.2 immunohistochemistry, Scale bars 500μm (A), 100μm (B).

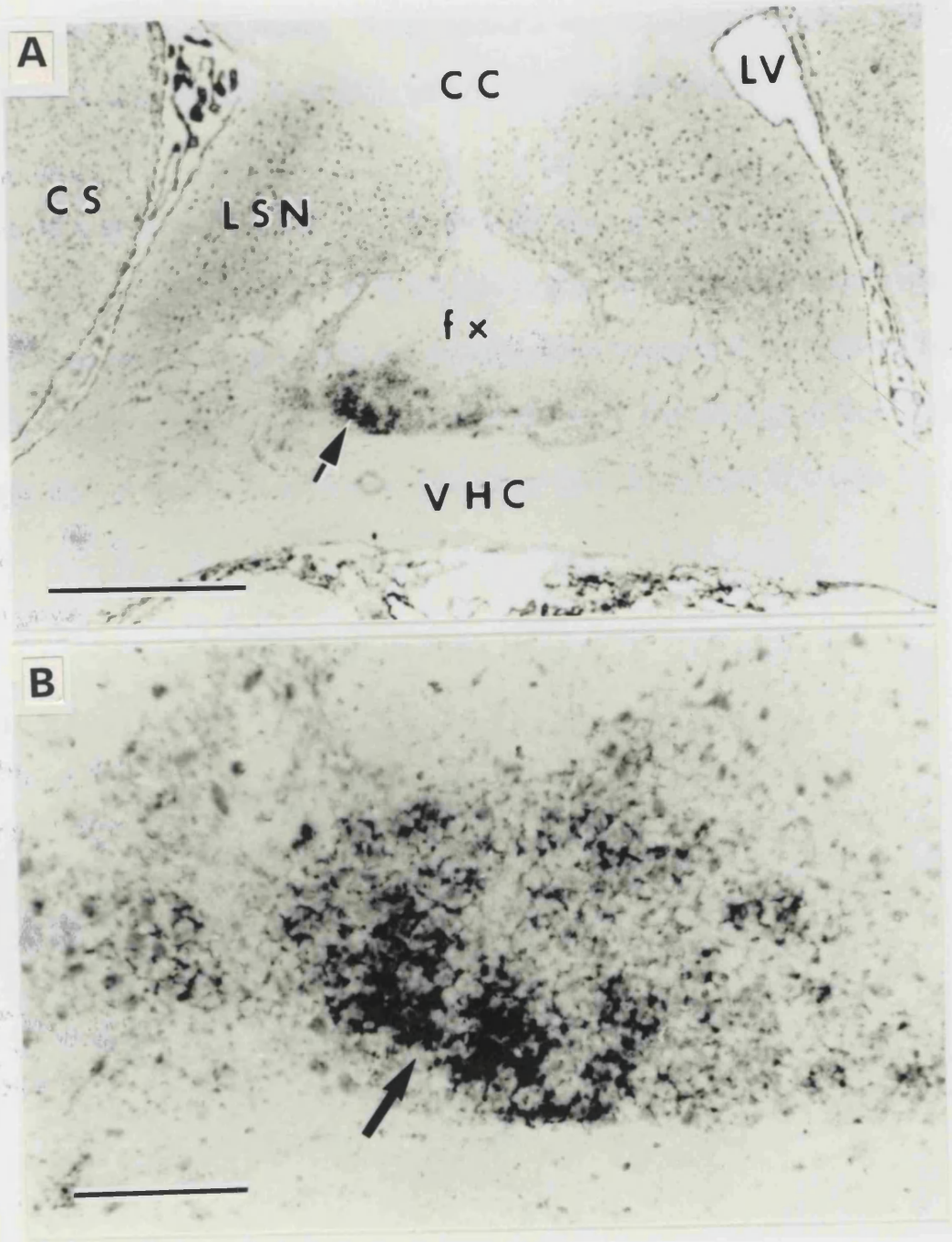
A
CC
LV
CS
LSN
fx
VHC
B

the ipsilateral side. On the contralateral side, fibres had extended 8mm by 12 days, and 10mm by 5 weeks. The projections were stable for at least 7 weeks (the longest time point available), with no indication of retraction.

Transplants of E14 hippocampal donor cells gave a denser pattern of axon growth. It is not clear whether this is due to a greater growth capacity of the donor axons, or to larger grafts (i.e. a higher yield of neurons due to precursor division, better survival, or higher neuron/glia ratio). The projections from E14 cells did not extend more rapidly, nor further than those from E18 cells.

Figure 16

Sections at 4 successive dorsal-to-ventral horizontal levels (**A**, **B**, **C**, **D** are 3.5, 3.7, 4.0, and 4.2 mm ventral to the bregma, respectively) in representative camera lucida (on the left) and microphotographs (on the right). Arrows, transplant (TR) intrafimbrial projections; asterisks, terminal fields of transplant projection fibres in the rostral pole of host hippocampal field CA3 (**A,B**), the main part of ipsilateral hippocampal field CA3 (**C**), and the host lateral septal nucleus (**D**); (so) stratum oriens; (FIM) fimbria; (alv) alveus; (sp) stratum pyramidale; (sluc) stratum lucidum; (sg) stratum granulosum; (LV) lateral ventricle; (VHC) ventral hippocampal commissure. E14 donor tissue, 37d survival, Thy-1.2 immunohistochemistry (A,B); M6 immunohistochemistry (C,D), Scale bars 1mm.

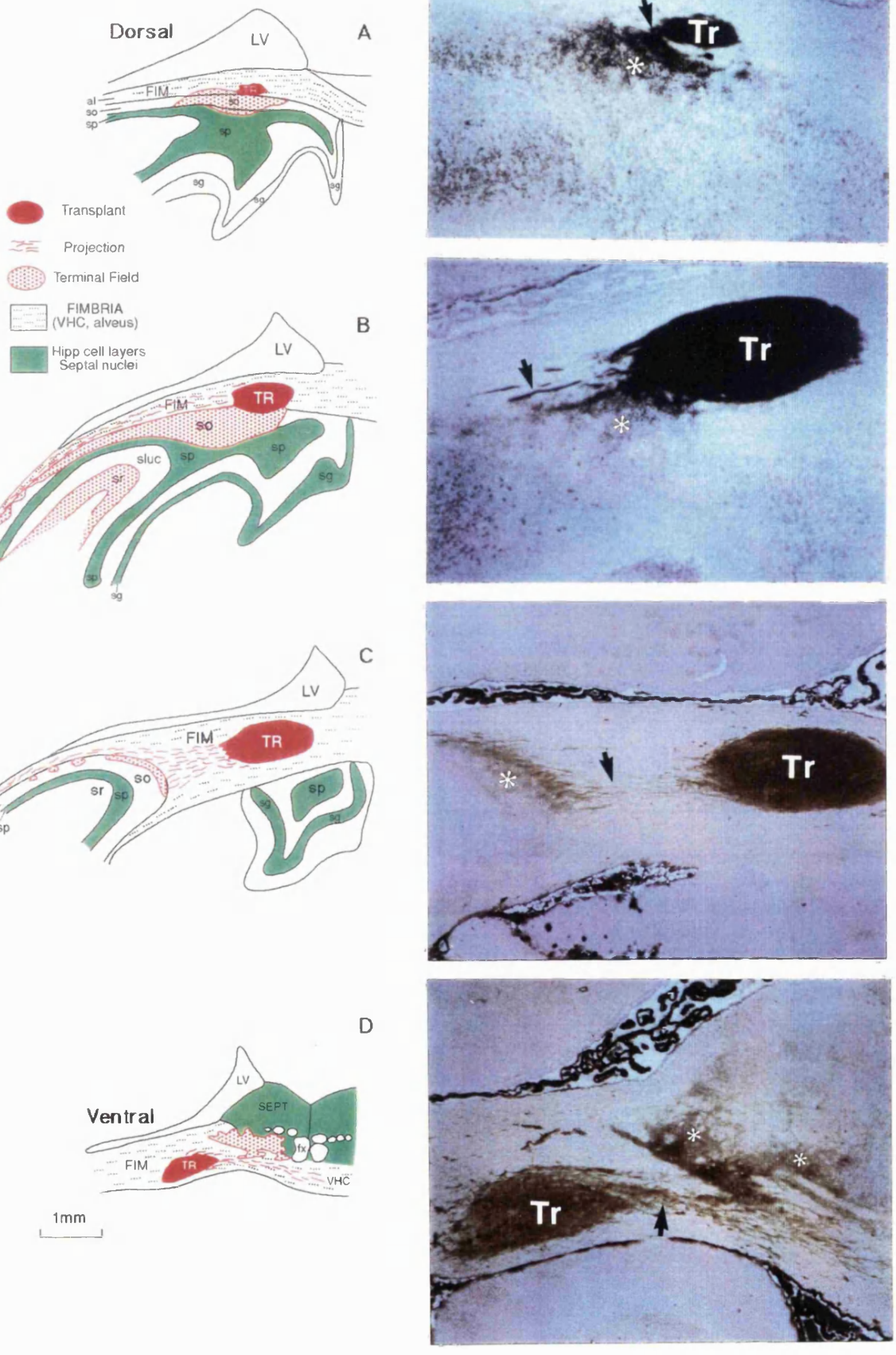
Dorsal
A
LV
FIM
al
so
sp
sg
Transplant
Projection
Terminal Field
FIMBRIA
(VHC, alveus)
Hipp cell layers
Septal nuclei
B
TR
sluc
sr
alv
C
D
Ventral
SEPT
fx
VHC
1mm
Tr

Specificity of axon growth

3.3.2.1 M6 immunohistochemistry

(A) *Time course*

At 3 days after operation (the earliest time examined), hippocampal, neocortical and superior collicular transplants and their projection fibres were all M6 positive. The intensity of M6 immunoreactivity increased to a maximum by about 6 days. The hippocampal and neocortical transplants remained M6 positive for about 6-7 weeks, after which time the intensity of M6 immunoreactivity was decreased, eventually becoming virtually undetectable. In the case of the E14 superior collicular transplants, M6 immunoreactivity was downregulated by 3 weeks - i.e. 3-4 weeks earlier than with the other donor tissue types.

(B) *Morphology of transplant-to-host axonal projections*

The M6 immunoreactive axons from all three types of donor tissue were of a uniform diameter of less than 1 μm, and emerged from the transplants singly or in fascicles which gradually separated into individual axons. The donor axons followed the axis of the host tracts and, as observed for hippocampal microtransplants in the fimbria, gave rise to collaterals at right angles running towards neuropil areas.

There were two patterns of staining whose distribution indicated the formation of terminal fields. These consisted of (a) branched 'pre-terminal' axons

surrounded by an area of fine staining (especially seen in the stratum oriens of the hippocampus), and (b) amorphous finely granular deposits (e.g. in the septal nuclei or the cingulate cortex).

3.3.2.2 Projections from transplants in the fimbria

Cortical and superior collicular donor cells

Both E14 and E18 neocortical cells (n = 10 cases; table 2) and E14 superior collicular cells (n = 12 cases; table 2) generated patterns of axon growth indistinguishable from those produced by the hippocampal donor cells (n = 22 cases; table 1) transplanted into the host fimbria in the earlier study.

The serial horizontal sections demonstrated the topographical course of the projections from transplants of E14 or E18 cortical tissue (Fig. 17). In sections dorsal to the transplant (Fig. 17A), the fibres were cut in their lateral course as they arched upwards from the transplant, running towards the ipsilateral host hippocampus. At progressively more ventral levels (Fig. 17B-D), the fibres fanned out into alveus (Fig. 17E,F) over the lateral pole of the hippocampal field CA3, becoming progressively more vertical as they followed the curve of the hippocampus. Along the whole of this interface, the donor projection fibres turned into the underlying stratum oriens (Fig. 18), giving rise to prominent collaterals (Fig. 18C,D) and diffuse staining suggesting the formation of terminal fields (Fig. 18B,D). The same pattern, extent and density of projections was produced by transplants of E14 superior collicular tissue (Fig. 19).

Figure 17

A-F, A series of 6 horizontal sections (from dorsal to ventral) showing an E18 cortical transplant (T) generating a major laterally directed projection (arrows) through the fimbria (Fb) to the alveus (alv) over the lateral pole of the hippocampal field CA3. Asterisk, staining beneath the ventricular ependyma of the lateral ventricle is non-specific (appears with secondary anti-rat IgG alone), probably due to a regional inflammatory response. The numbers in the bottom left corners of each panel are the vertical distances in μm from the dorsal-most section. Survival, 6 days. Scale bar, 500 μm.

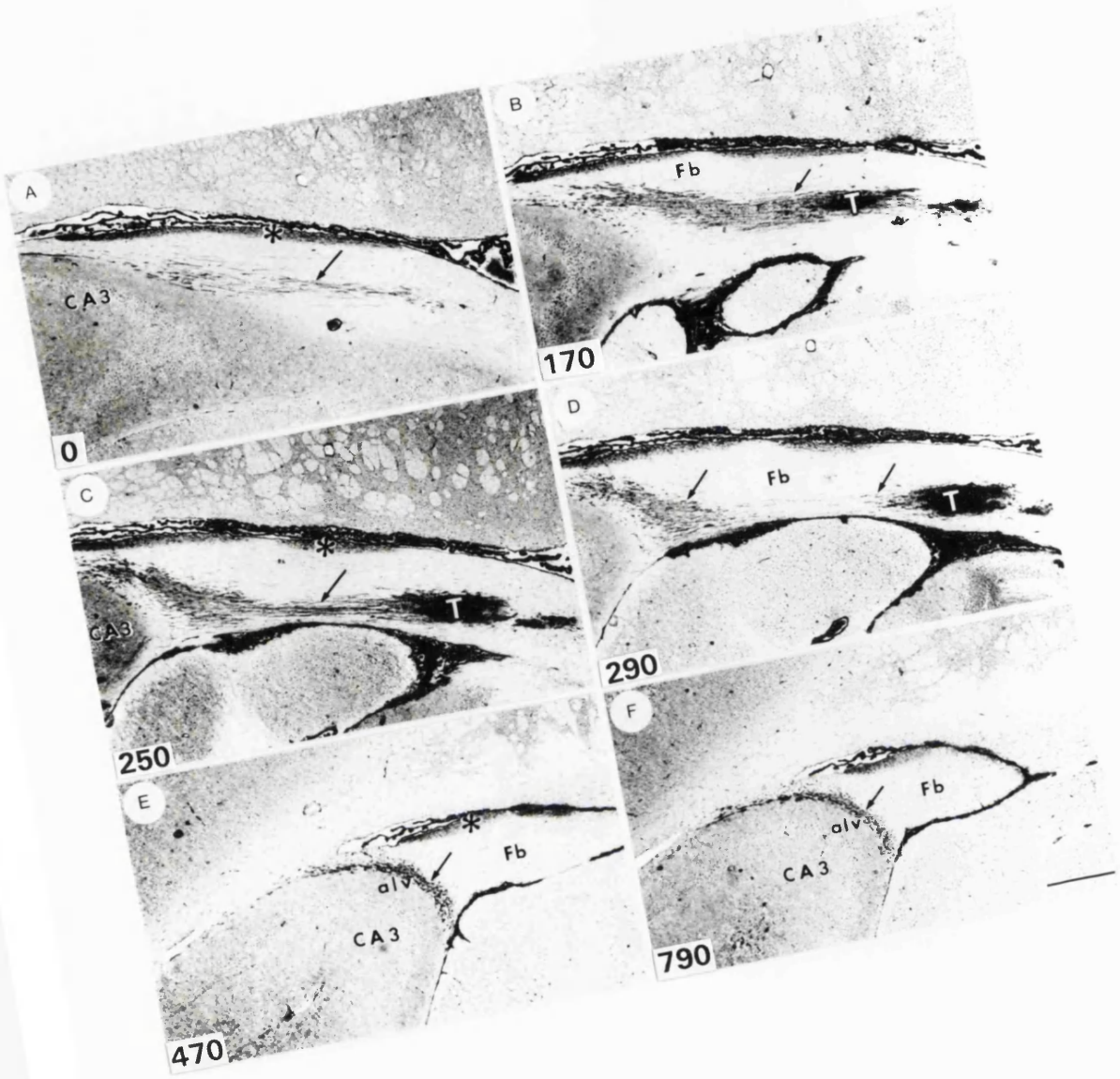
A
CA3
0
B
Fb
T
170
C
CA3
T
250
D
Fb
T
290
E
Fb
alv
CA3
470
F
Fb
alv
CA3
790

Figure 18

A, Enlarged view at the level of *Fig. 17A* to show a horizontally orientated, loose fascicle of M6-positive E18 cortical axons (ax) in the fimbria (Fb). **B**, Horizontal section through the lateral end of a horizontally running intrafimbrial bundle of axons (ax) at the level (shown in *Fig.17C*) where they are beginning to turn ventrally into the alveus (alv); arrowheads, terminal fields in the stratum oriens. **C**, A prominent collateral (arrows) in a fascicle of axons (ax) such as illustrated in panel *A*. **D**, Section from a level ventral to *B* (Cf *Fig. 17E,F*), showing ventrally directed axons in the alveus (alv) cut end-on, and a prominent collateral (arrows) leading to the upper of the two terminal fields in the stratum oriens (arrowheads). E18 cortical tissue. Survival, 6 days. Scale bars, 100 µm (*A,B*), 25 µm (*C,D*).

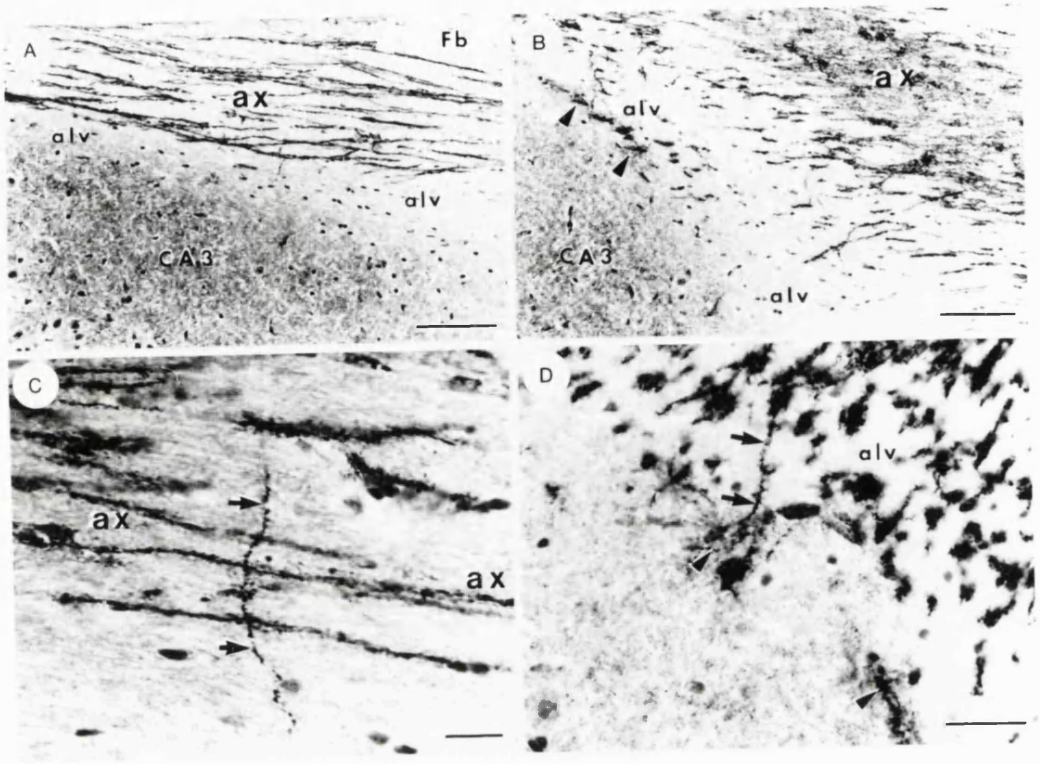
A
Fb
ax
alv
alv
CA3
B
ax
alv
CA3
alv
C
ax
ax
D
alv

Figure 19

A, An E14 superior collicular transplant (T) generating a laterally directed intrafimbrial projection (arrow) which reaches the alveus of the hippocampal field CA3 (asterisk, region enlarged in *B*). **B**, Preterminal M6 positive projection fibres traverse the alveus (asterisks) to produce terminal field type staining in the stratum oriens (so). Survival, 16 days. Scale bars, 500 µm (*A*), 100 µm (*B*).

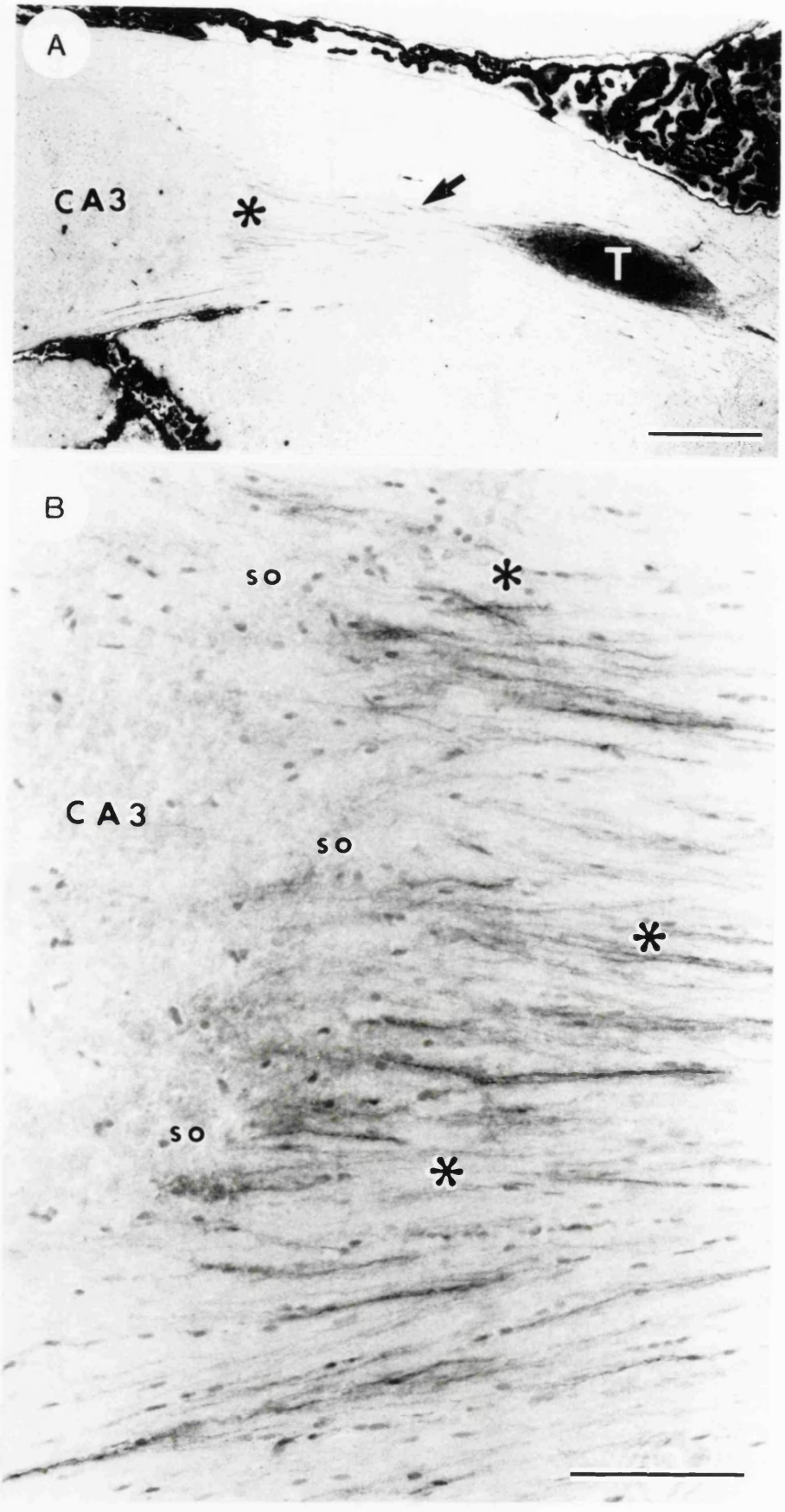
A
CA3
T
B
so
CA3
so
so

Rostro-medially from both cortical and collicular transplants, the emerging fibres (RM in Fig. 20; Cf Fig. 7B) entered the septal nuclei, and produced a diffuse, terminal field type of staining (Fig. 21), which was no less dense or extensive than that produced by transplants of the appropriate, hippocampal cells. In the more ventral sections isolated individual M6 positive donor fibres entered the host postcommissural fornix columns where they were cut, like the host fornix fibres, end on (solid arrow in Fig. 21B). Caudal to this a contingent of fibres (CM in Fig. 20) left the transplant to enter the ventral hippocampal commissure and cross the midline into the contralateral fimbria (Fig. 22).

3.3.2.3 Projections from transplants in the corpus callosum and cingulum

Embryonic donor cells injected into the corpus callosum and/or cingulum generated long interfascicular axon projections. The patterns of distribution of the donor projections were the same for E14 or E18 hippocampal (n = 9 cases), or cortical (n = 6 cases) cells, or for E14 superior collicular cells (n = 6 cases), but as in the fimbria, the M6 immunoreactivity consistently disappeared from the superior collicular axons much earlier than from the hippocampal or neocortical axons.

(A) ***Intracallosal transplants***

The transplants were placed in the rostrum of the corpus callosum, about 1.0-1.2 mm lateral to the midline. The overall pattern of the projections is shown at 9 representative horizontal levels in Fig. 23. Fibres emerging from the dorsal

Figure 20

Medial edge of an intrafimbrial E18 cortical transplant (T) generating rostro-medially (RM) and caudo-medially (CM) directed streams of axons (arrows) towards the septal neuropil and ventral hippocampal commissure respectively. Survival, 34 days. Scale bar, 100 µm.

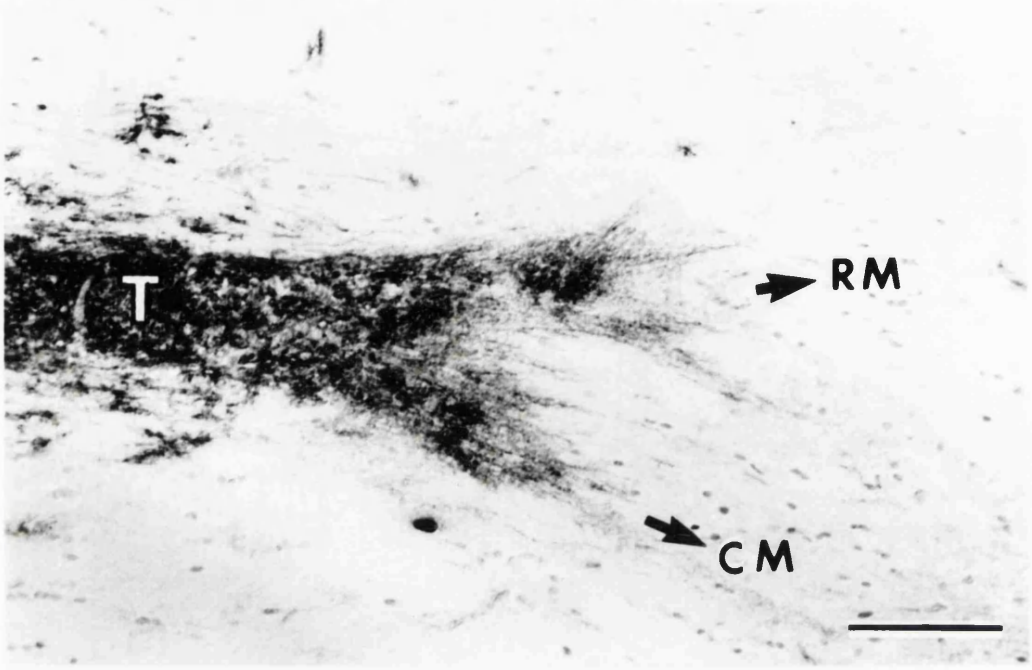
T
RM
CM

Figure 21

A, Diffuse terminal field like staining (arrows) in the caudal part of the lateral septal nucleus (LSN); CC, corpus callosum; VHC, ventral hippocampal commissure; IIIV, third ventricle. **B**, Enlarged view of part of the terminal field in A, showing adjacent clear areas occupied by the host fornix bundles (open arrows). Solid arrow shows a fornix bundle containing scattered M6-positive transplant axons cut end on. E14 superior collicular transplant. Survival, 14 days. Scale bars, 500 μm (*A*), 100 μm (*B*).

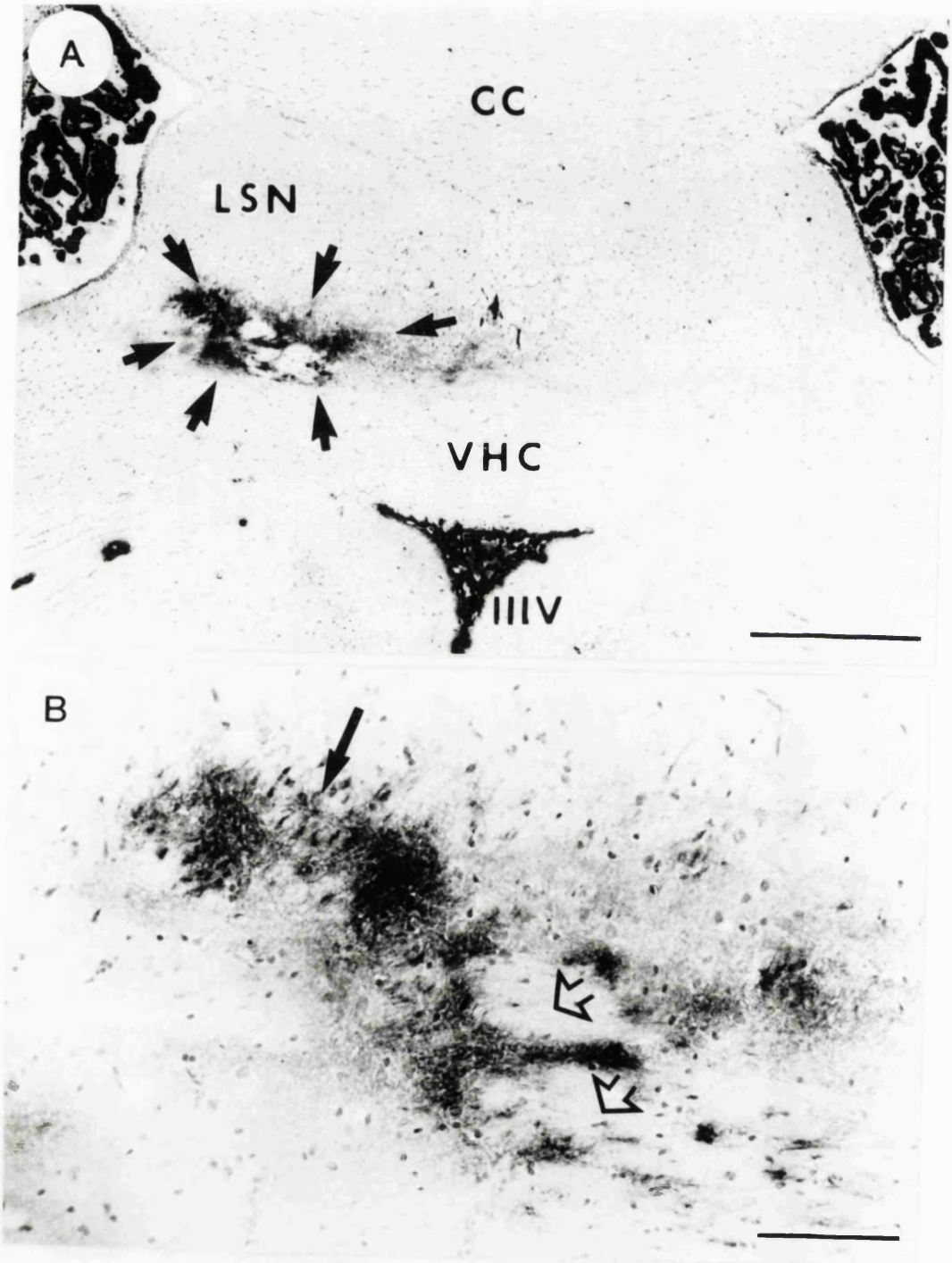
A
CC
LSN
VHC
IIIV
B

Figure 22

Scattered M6 positive axons in the contralateral fimbria; generated by an E18 cortical transplant in the ipsilateral fimbria. Survival, 6 days. Scale bar, 100 µm.

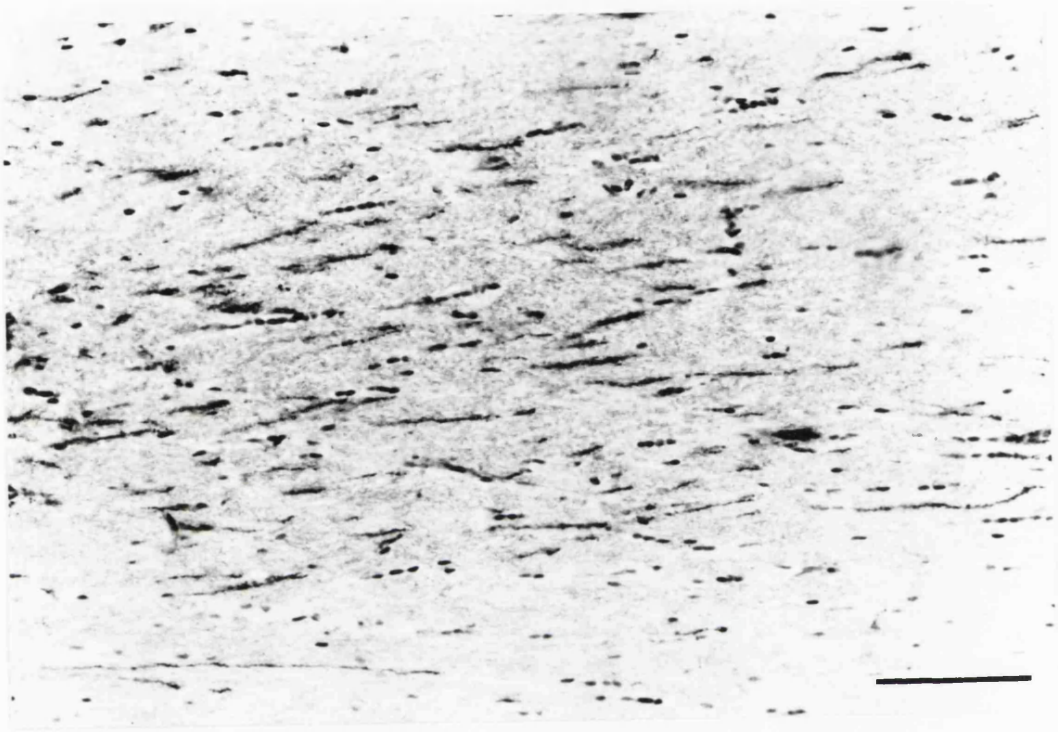

Figure 23

A-I, Series of horizontal sections from dorsal to ventral through an E14 superior collicular transplant (T) in the rostrum of the corpus callosum. **A,B**, levels with M6 positive axons (ax) radiating from the rostro-lateral aspect of the transplant. Arrows show projection into the cingulum. **C,D**, intermediate part of the transplant with no projection fibres leaving the transplant in the plane of the section. **E-H**, Ventral levels, showing medially directed projection fibres (arrows) running across the midline (M) in the corpus callosum. Asterisk (in *F*), fibres which have crossed the midline and are ascending on the opposite side in a position symmetrical to the transplant. IF, interhemispheric midline fissure. The numbers in the bottom left corners of each panel are the vertical distances in µm from the dorsal-most section. Survival, 21 days. Scale bar, 500 µm.

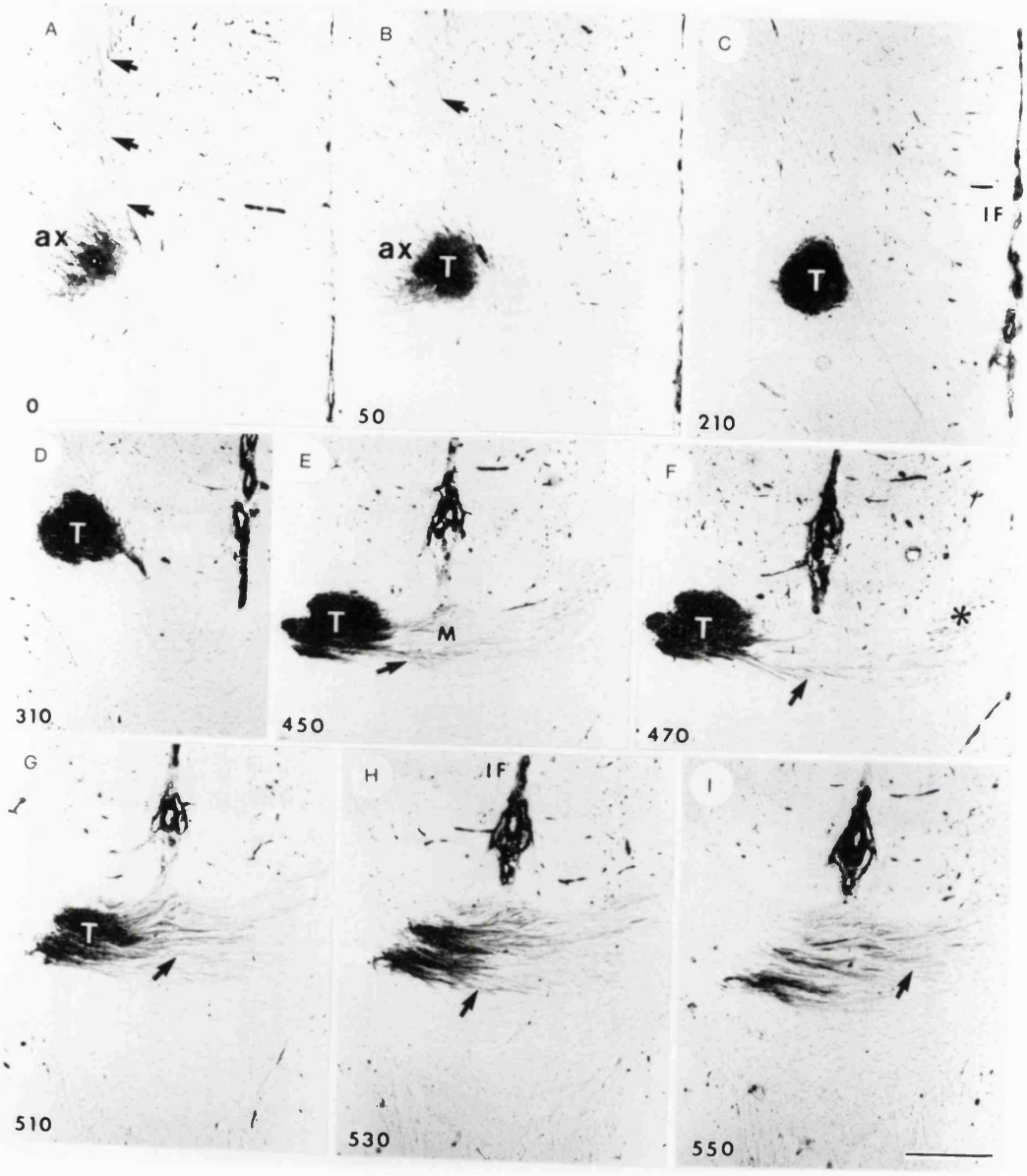
A
ax
0
B
ax
T
50
C
T
IF
210
D
T
310
E
T
M
450
F
T
*
470
G
T
510
H
IF
530
I
550

part of the transplants radiated out through the callosum dorsally, laterally and rostrally into the cortex (Figs. 23A,B, 24). In the horizontal plane of section, these radiating fibres were cut in short segments, with numerous collaterals arising from the main axonal stems, and many bifurcations as the fibres formed an increasingly complex plexus at the entry to grey matter of the overlying cortex.

Throughout the approximately 300 μm of horizontal distance represented by levels *C,D* of Fig. 23 no projections emerged from the transplants in the horizontal plane of section. (As will be seen below, this correlates with the orientation pattern of the host tract astrocytic processes).

At more ventral levels (Fig. 23E-I) major projections arose from the medial surface of the transplant. The most dorsal of these projection fibres ran medially into the grey matter of the cingulate cortex and generated a diffuse-type terminal field (asterisks in Fig. 25). The majority of the medially directed fibres took a downward course to mingle with the midline-crossing fibres of the callosum (Fig. 26), where they formed characteristic, rather coarse, interweaving fascicles, exactly matching the pattern of the host callosal axons (Fig. 27). Once they had crossed the midline, the fibres took a course (ascending laterally and rostrally in the contralateral hemisphere) which was a mirror image of their previous trajectory through the ipsilateral hemisphere (asterisk in Fig. 23F). Collaterals arising from these axons were directed radially into the contralateral cerebral cortex.

Figure 24

A, Fascicles of M6 positive axons (ax) radiating rostrally from an E14 hippocampal transplant in the rostrum of the corpus callosum. **B**, Enlarged view. Survival, 43 days. Scale bars, 100 μm (*A*), 50 μm (*B*).

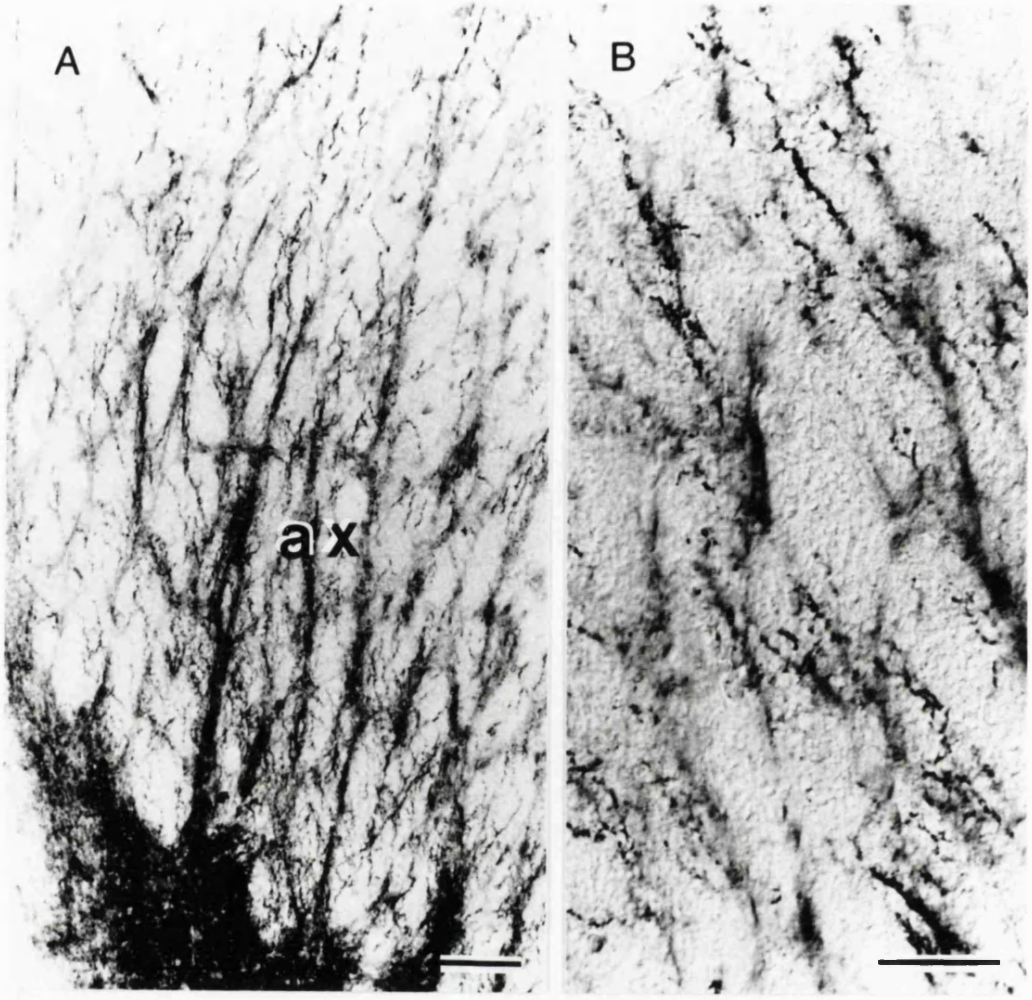
A
ax
B

Figure 25

A, Caudal edge of an E14 hippocampal transplant (T) with a short bundle of M6 positive fibres (arrow) forming a terminal field (asterisk) in the grey matter of the cingulate cortex (CGyr). **B**, A section from a more ventral level, where the projection (arrow) to the cingulate cortex is still present, but on its lateral surface there is now a contingent of callosal fibres (arrowheads) running ventrally on their way to cross the midline. Survival, 43 days. Scale bar, 100 µm.

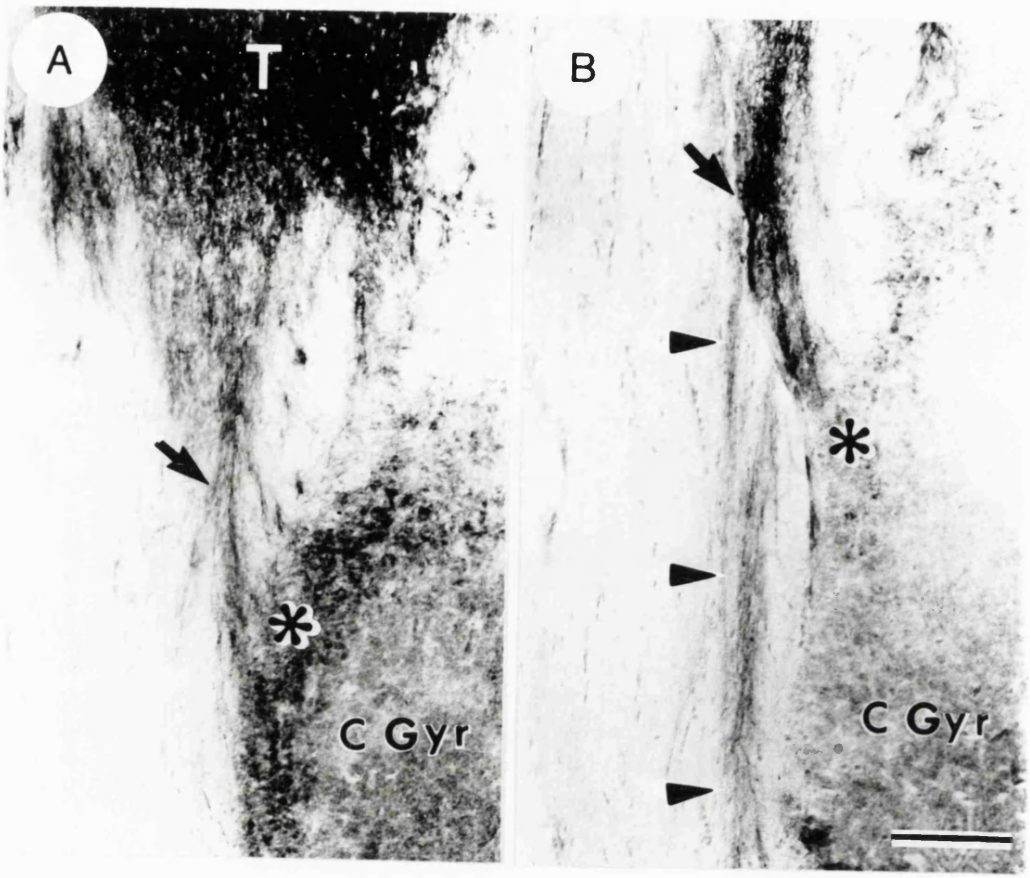
A
T
C Gyr
B
C Gyr

Figure 26

.

Midline-crossing M6-positive axonal projections (arrows) from intracallosal transplants (T) of E 14 cortical (CTX, in **A**), E14 superior collicular (COLL in **B**), and E14 hippocampal (HIPP in **C**) cells. CC, corpus callosum; CGyr, cingulate gyrus; H, hippocampus, M, midline. Survivals, 7,21,43 days (*A,B,C*). Scale bar, 500 µm.

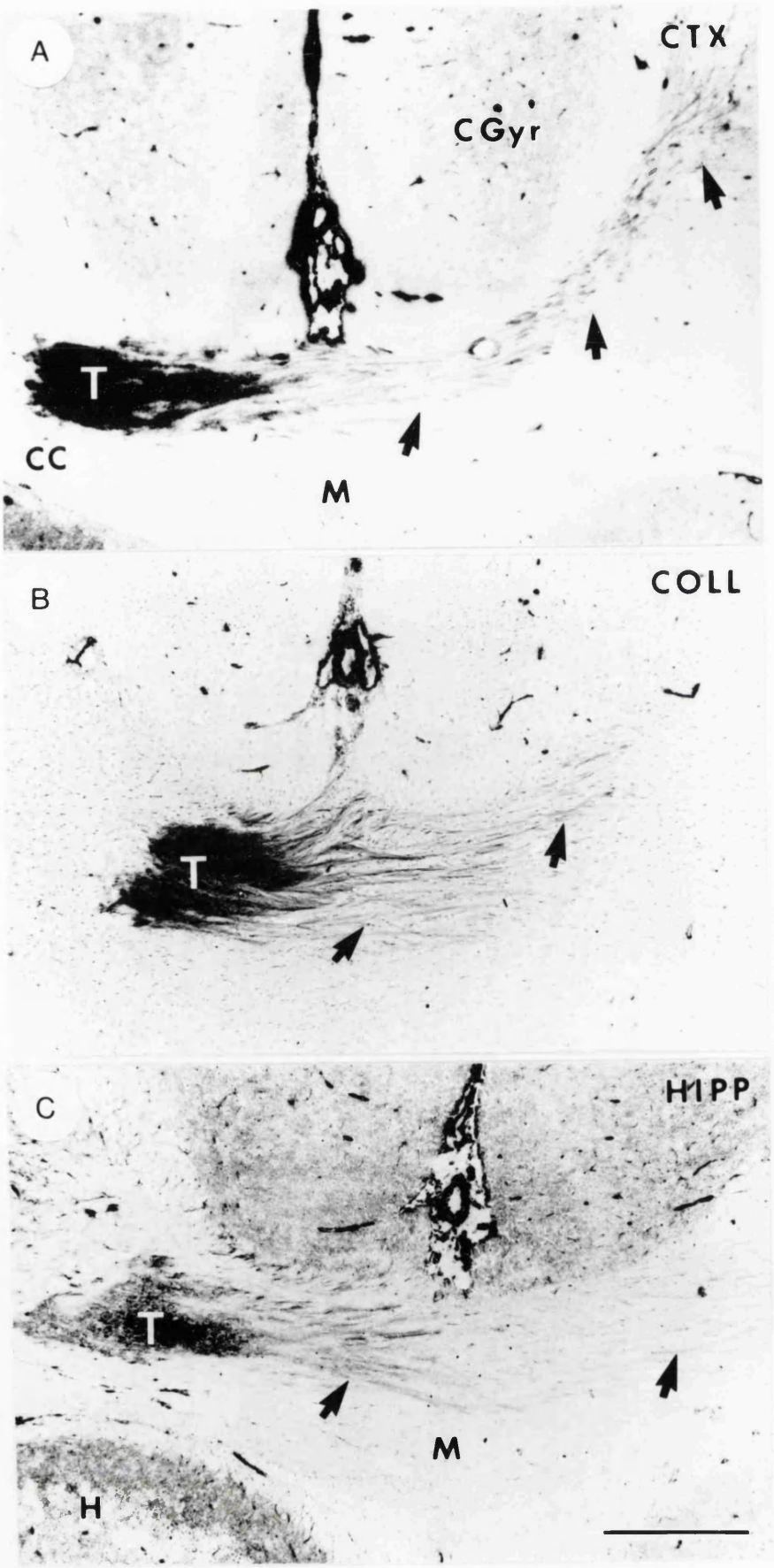
A
CTX
CGyr
T
CC
M
B
COLL
T
C
HIPP
T
M
H

Figure 27

Interweaving of interhemispheric crossing fibres at the midline of the corpus callosum. **A**, Host fibres (Palmgren stain) from a normal animal. **B**, Donor axons (M6 stain) from the E14 cortical transplant shown in *Fig.26A*. Survival, 7 days. Scale bars, 100 µm (*A*), 50 µm (*B*).

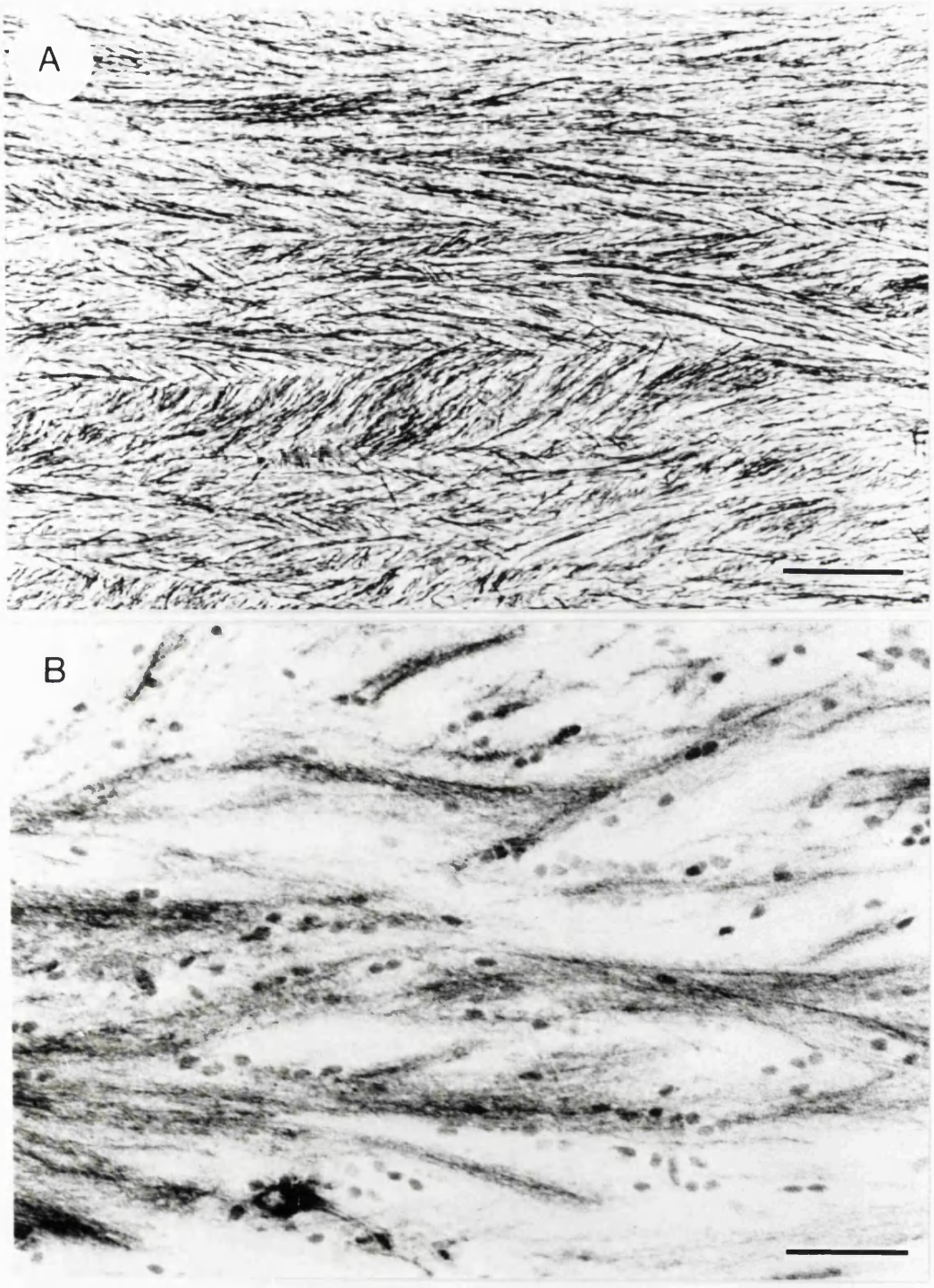
A
B

(B) ***Intracingulate transplants***

Cell suspensions from each of the 3 types of donor tissue, were injected into the cingulum in a position slightly medial to the intracallosal transplants. The difference from the intracallosal transplants was striking: Whereas the intracallosal transplants generated transversely orientated fibres, in conformity with the transverse orientation of the host callosal axons, in contrast, the intracingulate transplants generated longitudinally orientated fibres, in conformity with the longitudinal orientation of the host cingulate fibres (Fig. 28 illustrates a transplant making both types of projection).

Long fibre projections arising from the intracingulate transplants ran in a rostro-caudal orientation within the bundles of host cingulate fibres (Fig. 28), and gave rise to diffuse type terminal field staining in the grey matter of the cingulate gyrus (Fig. 29).

With all 3 donor cell types, a consistent peculiarity of the intracingulate grafts was a characteristic, narrow M6-positive column, about 50 - 100 μm wide (Fig. 38), which passed radially for 1 mm or more through the grey matter of the cingulate gyrus, in a direction rostrally and dorsally at an angle to the injection track.

(C) ***Distance and speed of axon growth***

In the present material I found a comparable speed and distance of axonal growth from each of the different viable donor tissue types in each of the host tracts examined. Thus, the axons from neocortical and superior collicular cell

Figure 28

A, M6 positive projections from an E14 superior collicular transplant (part of which is visible at T), which straddles the corpus callosum (CC) and cingulum (cg), and gives rise to axons radiating rostro-laterally in the corpus callosum (arrow), and rostrally (boxed area shown in *B*) in the cingulum. **B**, Enlarged view of intracingulate fascicles boxed in A. Survival, 21 days. Scale bars, 500 µm (*A*), 50 µm (*B*).

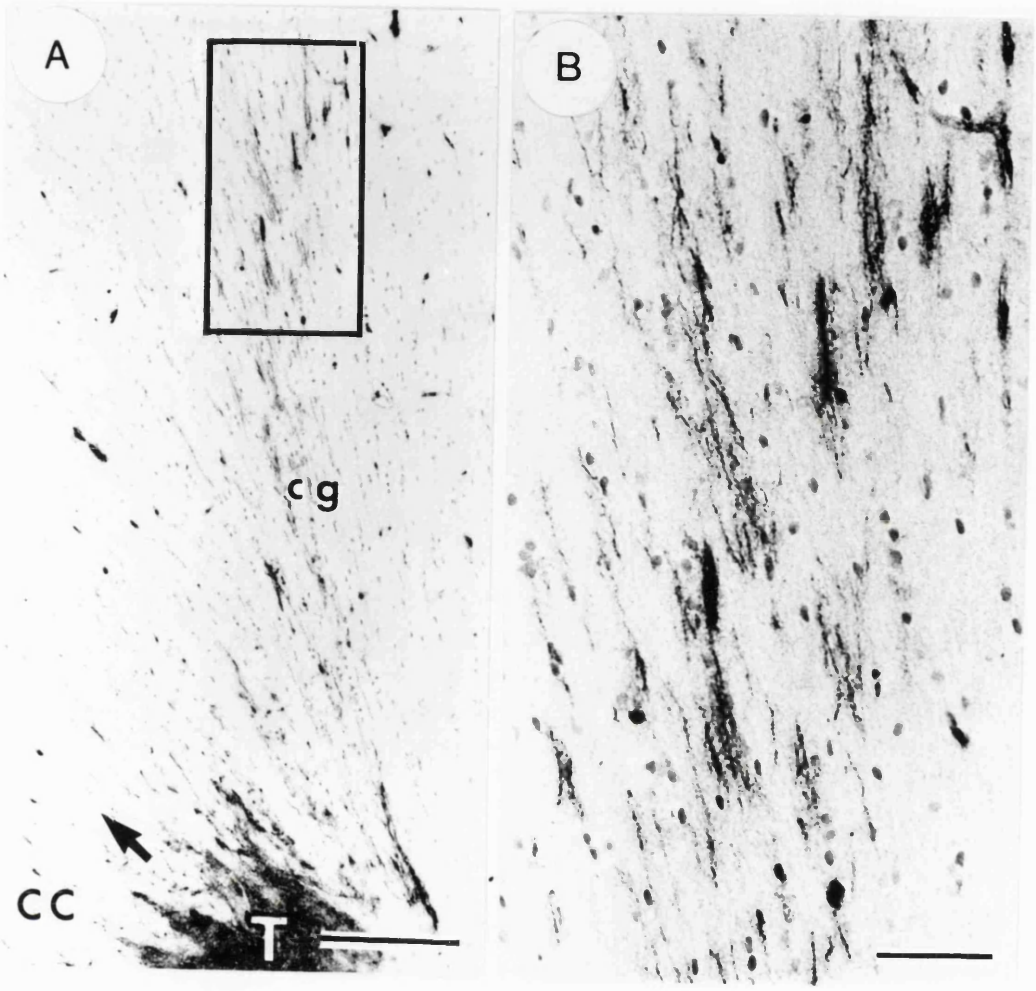
A
B
cg
CC
T

Figure 29

Distribution of projections formed by an E18 cortical transplant (the main part of which lies out of the plane of section) straddling the boundary of the corpus callosum (CC) and cingulum. *Small arrows*, densely M6 positive, diffuse type terminal projection in the grey matter of the cingulate cortex (CGyr); large arrows, fascicles crossing the midline (M) in the corpus callosum; arrowhead, small fascicle in the cingulum bundle. Survival, 19 days. Scale bar, 500 µm.

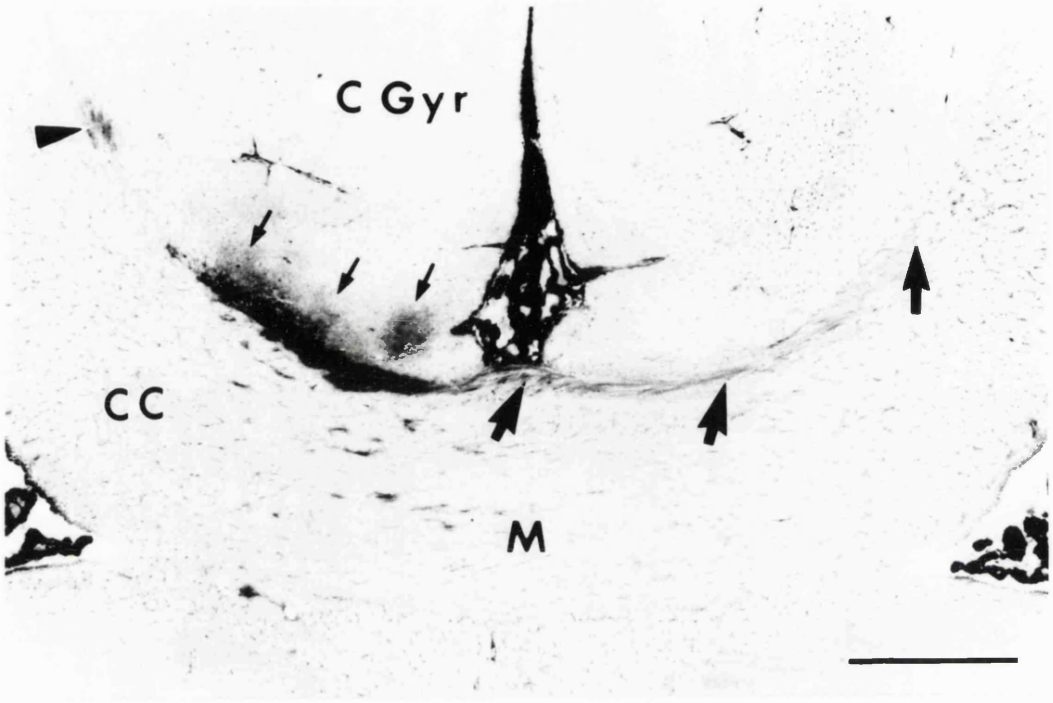
C Gyr
CC
M

grafts traversed the host fimbria at the same rate as the axons from donor hippocampal cells, reaching the ipsilateral hippocampus and contralateral fimbria by 6 days. At the same survival time, projection fibres from intracallosal transplants of all 3 types of donor cells had already traversed the midline and started to ramify in the contralateral cortex.

Relationship of axonal growth to tract structure and inter-tract boundaries

3.3.3.1 Fimbria

As previously described, sections were cut in a horizontal plane which approximates to the longitudinal axis of the host rostral fimbrial axons and gives the longest lengths of interfascicular rows of glial nuclei and the host axons in one section. This plane of section clearly showed that the transplant axons were intimately integrated among the host fimbrial axons, parallel to them and to the rows of host tract interfascicular glial nuclei (Fig. 8C,D,E).

Effect of location in the fimbria

Smaller intrafimbrial transplants produced less extensive projections, which varied according to the location of the transplants in the fimbria. Three individual cases exemplify these 'partial' patterns:

1. A transplant in the caudal part of the fimbria at the level of the ventral hippocampal commissure gave rise to a 'beam' of fibres which remained confined to the caudal fimbria and ran directly into the alveus over the medial part of field CA3 (Fig. 30A).

2. A small transplant of hippocampal cells lay further back, and laterally at the level of the hippocampal flexure. This transplant straddled the boundary between the fimbria and *stria terminalis*, with some donor cells in both tracts.

Figure 30

A, A small E14 superior collicular transplant (T) in the caudal edge of the fimbria (Fb) generates an M6 positive projection (arrow) which remains confined to the caudal margin of the fimbria (Cf *Fig.* 17) and runs directly into the alveus of the adjacent part of field CA3 (arrowhead). **B**, Narrow, aligned beam of axons (arrows) in the stria terminalis (ST) and fimbria (Fb), derived from a E18 hippocampal transplant (out of the plane of section) which straddles the junction of the tracts. **C**, An E14 superior collicular transplant (T) partially surrounding the host fornix columns (asterisk; into which the transplant contributes M6 positive fibres at a more ventral level (as at solid arrow in *Fig. 21B*). This transplant generates terminal field type diffuse staining in the adjacent part of the host lateral septal nucleus (arrow), but does not project laterally into the host fimbria (Fb). Survival, 7 days. Scale bars, 500 μm (*A*), 200 μm (*B*), 100 μm (*C*).

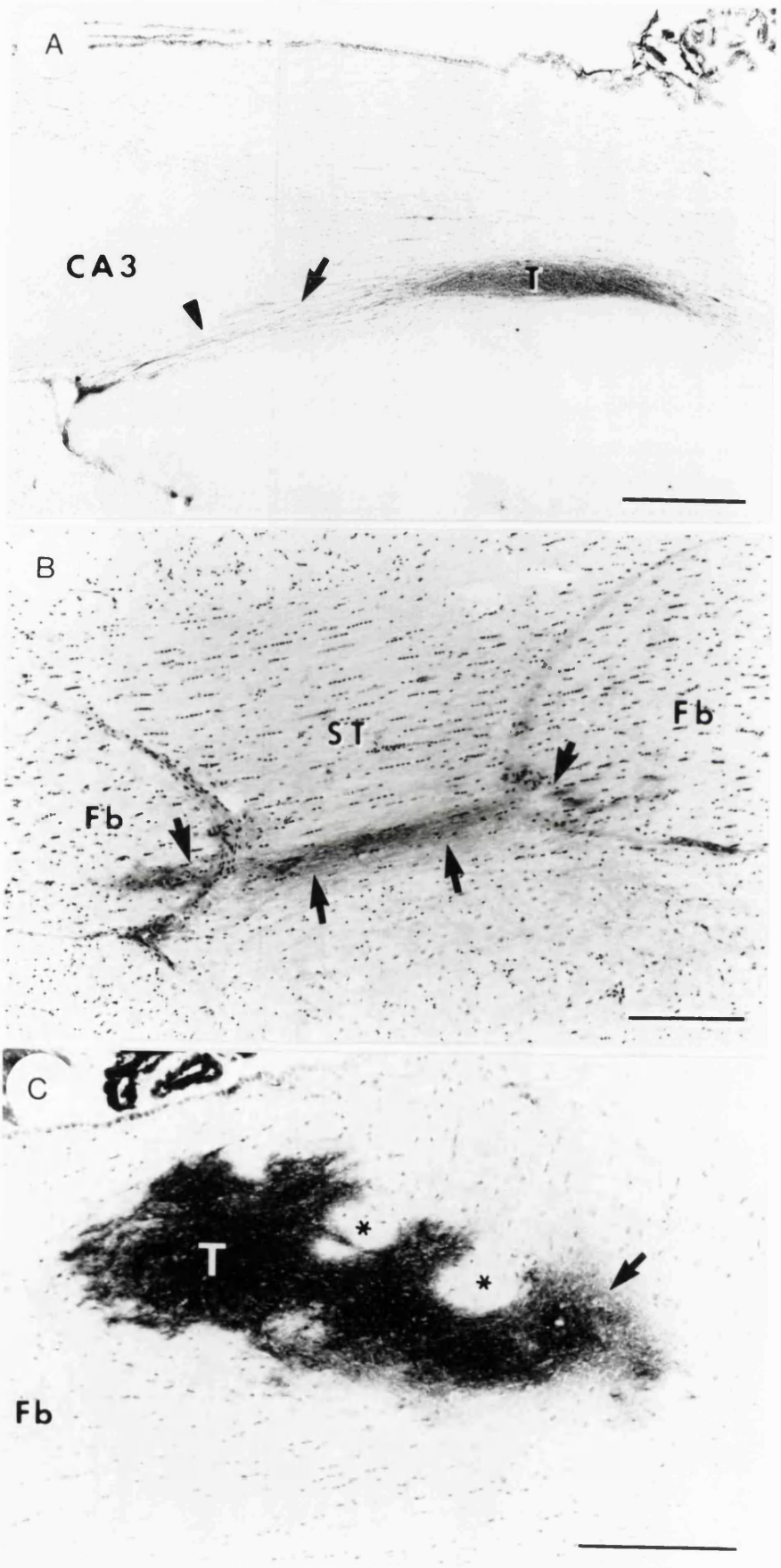
A
CA3
T
B
ST
Fb
Fb
C
T
*
*
Fb

The transplanted cells gave rise to two narrow beams of axons, one in the fimbria, and one in the stria terminalis (Fig. 30B).

3. A transplant lying in the dorso-medial edge of the fimbria did not send any fibres laterally in the fimbria, but did project medially, to produce a large area of terminal field type staining in the immediately adjacent lateral septal nucleus (Fig. 30C).

3.3.3.2 Astrocytic markers (GFAP and vimentin)

GFAP and vimentin both showed astrocytes, but with different distributions, depending on fixation. With aldehyde fixation, GFAP immunoreactivity was present in astrocytes in the neuropil of both host and transplant, but less in tract astrocytes. Acid alcohol fixation gave a converse pattern: both GFAP and vimentin immunoreactivity were present in the host tract astrocytes, and absent in the neuropil astrocytes.

Acid alcohol fixed material (Fig. 31) showed the radial and longitudinal processes of the host tract astrocytes as described by Suzuki and Raisman, (1992). The most striking feature was the regular array of fine parallel longitudinal astrocytic processes which became visible when the plane of section passed through the longitudinal axis of the host tract.

Figure 31

A, A single vimentin-positive fimbrial astrocyte (through focus double exposure), with radial process (arrowhead) and many uniform, untapering, fine longitudinal processes (e.g. p); arrows, rows of interfascicular glial nuclei. **B**, Lower power view (GFAP staining, acid alcohol fixation, interference contrast) to show the parallel arrays of longitudinal, fimbrial astrocytic processes and interfascicular glial rows. Scale bars, 20 μm (*A*), 50 μm (*B*).

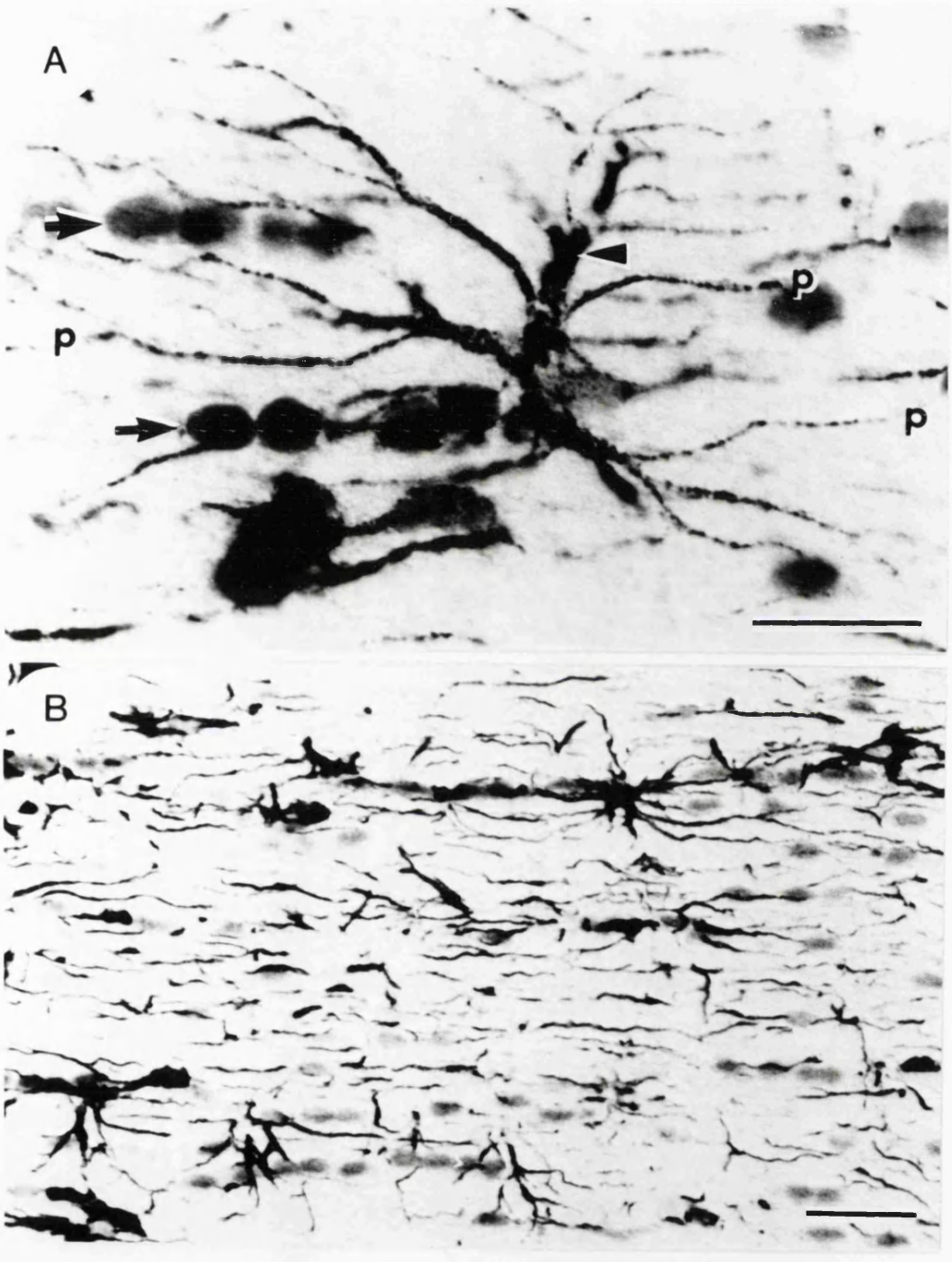
A
p
p
p
B

3.3.3.3 Correlation of donor axon projections and the orientation of the host tract structures

The present material consistently confirmed that the orientation of the M6-positive donor axons (e.g. arrows in Fig. 32A) is parallel to that of the host fimbrial axons (arrowheads in Fig. 32A), and to the interfascicular rows of glial cell bodies (igr in Fig. 32A). Where the longitudinal structures of the host tract were cut end-on (e.g. arrows in Fig. 32B), the donor axons were also cut end-on (ax in Fig. 32B).

A prominent element in the fimbrial architecture is the parallel array of longitudinal astrocytic processes along the axonal axis of the tract (Fig. 31; Suzuki and Raisman, 1992). Using the vimentin immunoreactivity of these processes in the fimbria, it can be seen that the pathway taken by the donor axons strictly follows the orientation of the host longitudinal astrocytic tract processes (Figs. 33,34).

In contrast, the astrocytes of the transplant neuropil are vimentin negative (Fig. 33B), but they can be stained with GFAP, which shows that along the transplant/host interface, the processes of the astrocytes in the transplant neuropil are orientated so that they flow out smoothly and merge with the plane of orientation of the surrounding host tract longitudinal astrocytic processes (illustrated for an intracallosal transplant Fig. 36).

Figure 32

A, A long M6-positive donor axon (arrows) lying parallel to the host fimbrial axons (e.g. arrowheads) in the contralateral fimbria. igr, row of interfascicular glial nuclei lying in the plane of section. **B**, alvear region where the M6-positive bundles of fasciculating donor axons (ax) are cut end-on, and the interfascicular glial rows are also cut end on, and are therefore represented by single nuclei (e.g. arrows). E 18 cortical transplants. Survivals, 36 days (*A*), 6 days (*B*). Scale bars, 20 μm (*A*), 50 μm (*B*).

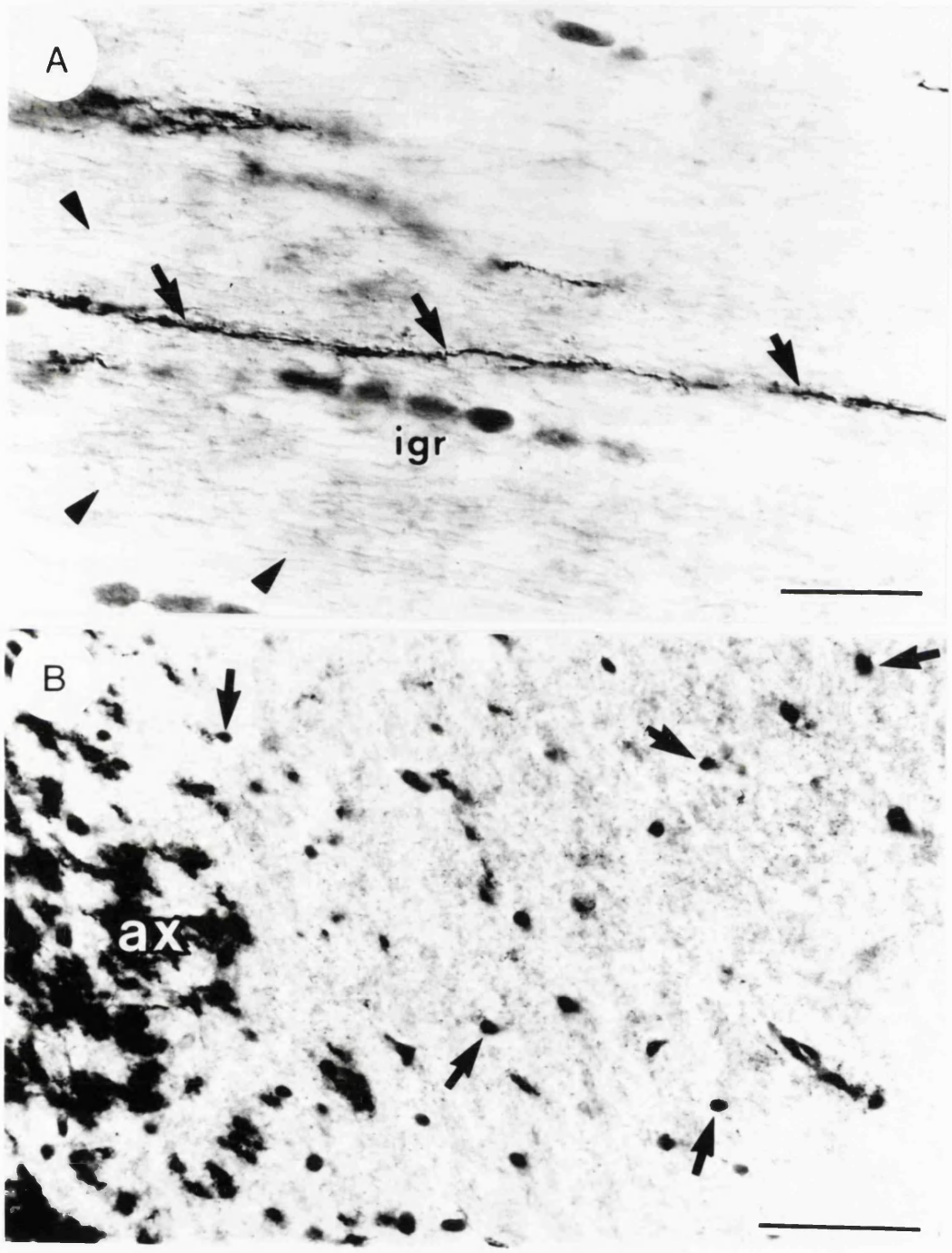
A
igr
B
ax

Figure 33

A, Lateral edge of an E18 cortical transplant (T) generating a long M6-positive fibre projection (arrow) into the fimbria (Fb). **B**, The same area (located by the position of the large blood vessel, asterisk) from an adjacent section to show vimentin positive longitudinal astrocytic processes (e.g. at arrow) orientated in parallel with the transplant axons. Note that the astrocytes in the transplant neuropil (T) are vimentin negative. Survival, 34 days. Scale bars, 100 μm.

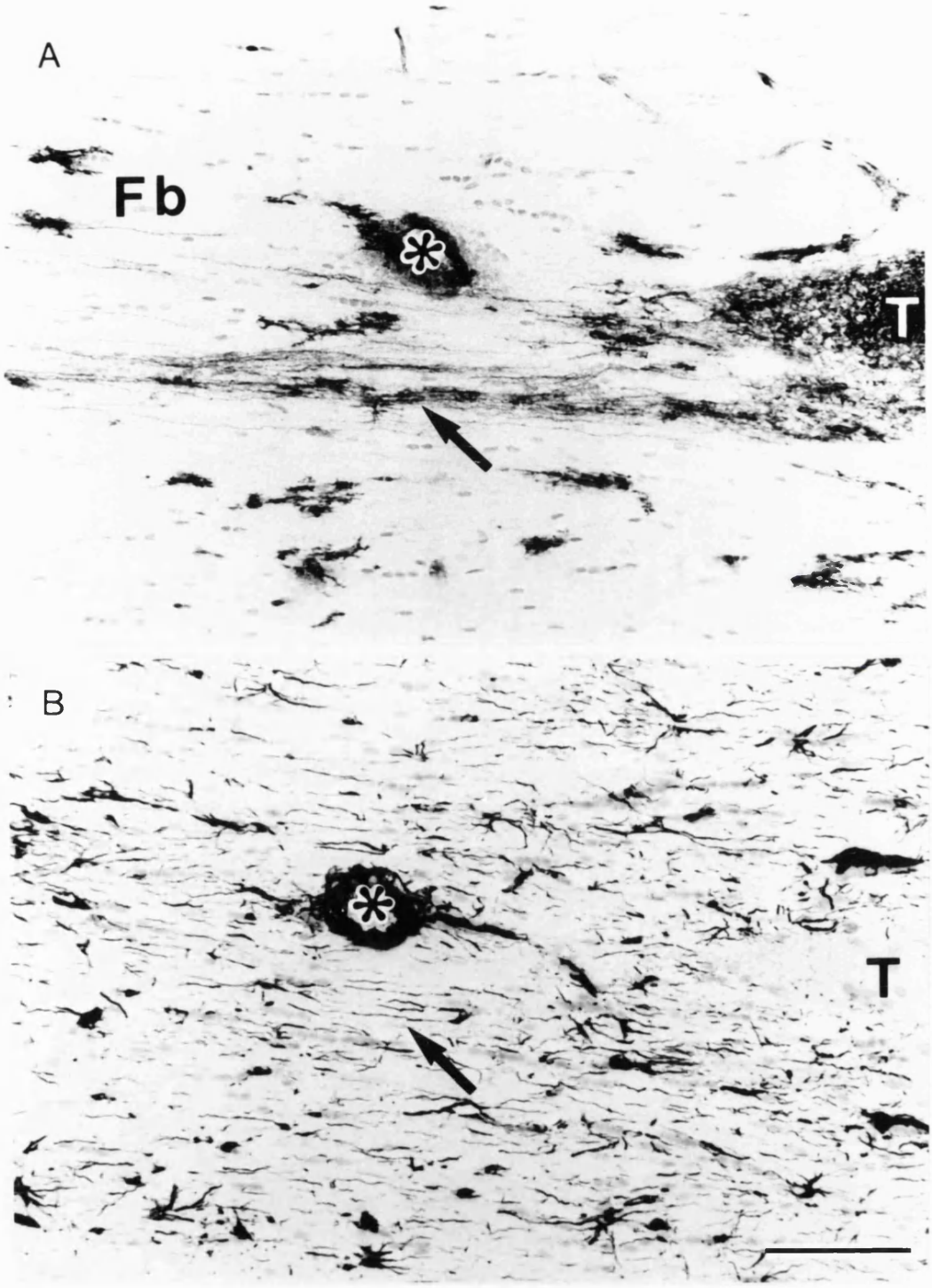
A
Fb
T
B
T

Figure 34

A, Crescent shaped area of M6 positive axons (ax) in the alveus over the medial pole of the hippocampal field CA3 at the levels shown in *Fig. 17C,D*. These axons are seen in an almost end-on view as they run vertically through the horizontal plane of the section (as in Fig. *32B*). Arrow, collateral; arrowhead, terminal field in the stratum oriens; Fb, fimbria; Th, thalamus. **B**, Adjacent section stained for vimentin to show the predominantly end-on views (Cf *Fig. 32B*) of the fimbrial longitudinal astrocytic processes which are parallel to the M6 positive axons. E18 cortical transplant. Survival, 6 days. Scale bars, 100 μm.

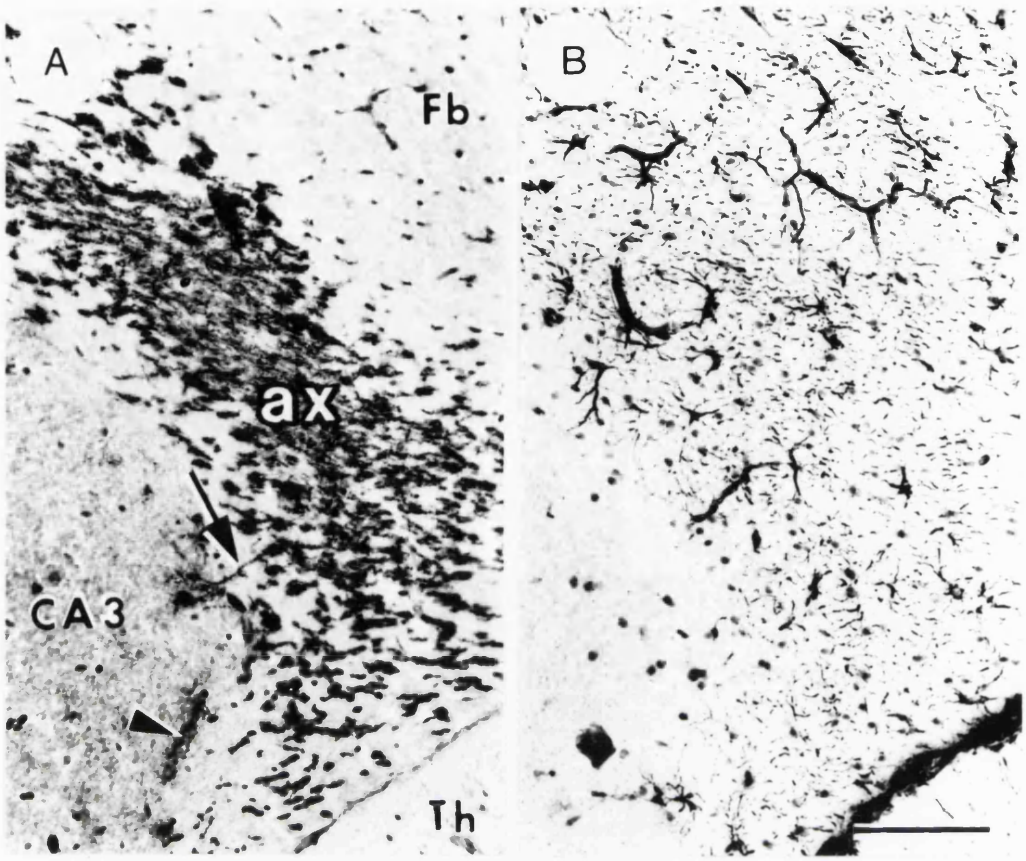
A
Fb
ax
CA 3
Th
B

In the positions where the M6-positive axons ran laterally in the fimbria, there was a matching parallel stretch of longitudinal astrocytic processes (Fig. 34). Further laterally, where the transplant axons (Figs. 32B,34A) turned ventrally through the plane of the section (and were therefore cut end on), the inclination of the vimentin-positive host longitudinal astrocytic processes (Fig. 34B) and the rows of host interfascicular glial nuclei (Fig. *32*B) changed exactly in parallel, so that the M6-positive donor axons, the host interfascicular glial nuclei, and the host astrocytic longitudinal processes were all cut end-on.

3.3.3.4 Corpus callosum and cingulum

As with the intrafimbrial transplants, the donor axons in the corpus callosum and cingulum were parallel to the host axons, to the rows of interfascicular glial cell bodies, and to the vimentin-positive longitudinal processes of the host tract astrocytes (e.g. Cf Fig. 36 with Fig. 33).

Thus:

1. From the dorsal parts of the transplants the host callosal astrocytic longitudinal processes lay in line with the M6-positive cortico-petal projection fibres leaving the transplant.

2. In sections through the intermediate dorso-ventral course of the transplants at levels (Fig. 23C,D) where no fibres emerged in the plane of section, the longitudinal astrocytic processes of the host tract were cut end-on (Fig. 35).

3. From the ventral parts of the transplants, the longitudinal astrocytic processes paralleled the donor axons on their way to cross the midline (Fig. 36).

4. The M6-positive column (Fig. 37A,C) through the grey matter of the cingulate gyrus was intensely vimentin-positive (Fig. 37B,D), and stood out against the adjacent vimentin-negative host grey matter of the cortex. This was the only situation in which I observed vimentin induction in grey matter. The column was cut transverse to its long axis, and both the M6-positive transplant projection fibres and the host vimentin-positive longitudinal astrocytic processes were also orientated end-on to the plane of section.

GFAP

As with the intrafimbrial transplants, the GFAP-stained astrocytic processes of the intracallosal and intracingulate transplants ran in continuity from the interior of the transplant to become confluent with the adjacent vimentin-stained longitudinal astroglial processes of the host tract astrocytes (Figs. 35C,38).

Figure 35

A, A densely M6 positive E14 cortical transplant (T) in the medial edge of the corpus callosum. No long projections are emitted in the plane of section (comparable to the intermediate segment in *Fig. 23 C,D*). **B**, Adjacent section showing vimentin positive astrocytic processes in the surrounding host tract, which are here cut end-on, and vimentin negative transplant neuropil. **C**, Adjacent section showing the intense GFAP reactivity of the astrocytic processes in the transplant and at the interface, and much weaker GFAP in the host tract; aldehyde fixation. Survival, 6 days. Scale bar, 100 μm.

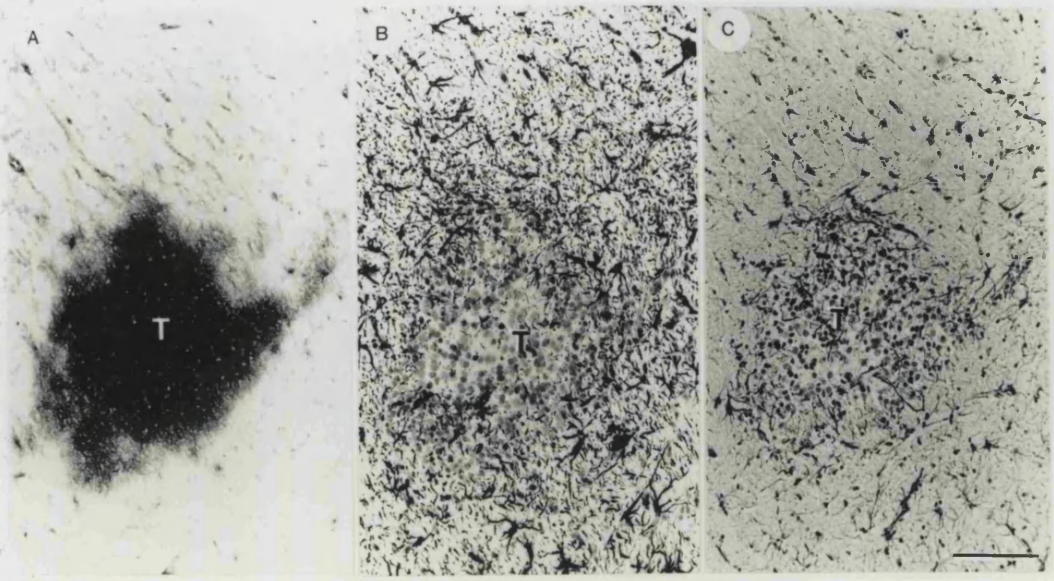
A
T
B
T
C
T

Figure 36

A, Ventral part of a transplant (T) of E14 hippocampal cells which lies in the rostrum of the corpus callosum and shows two groups of ventrally directed M6 positive projections (Cf. *Fig. 25 A,B*): viz. a lateral group (arrowheads) passing ventrally in the corpus callosum, and a medial group (asterisk) passing towards the cortex of the cingulate gyrus (CGyr). **B**, Adjacent section showing vimentin positive longitudinal astroglial processes of the corpus callosum are parallel to the trajectory of the axons. Survival, 7 days. Scale bar, 50 µm.

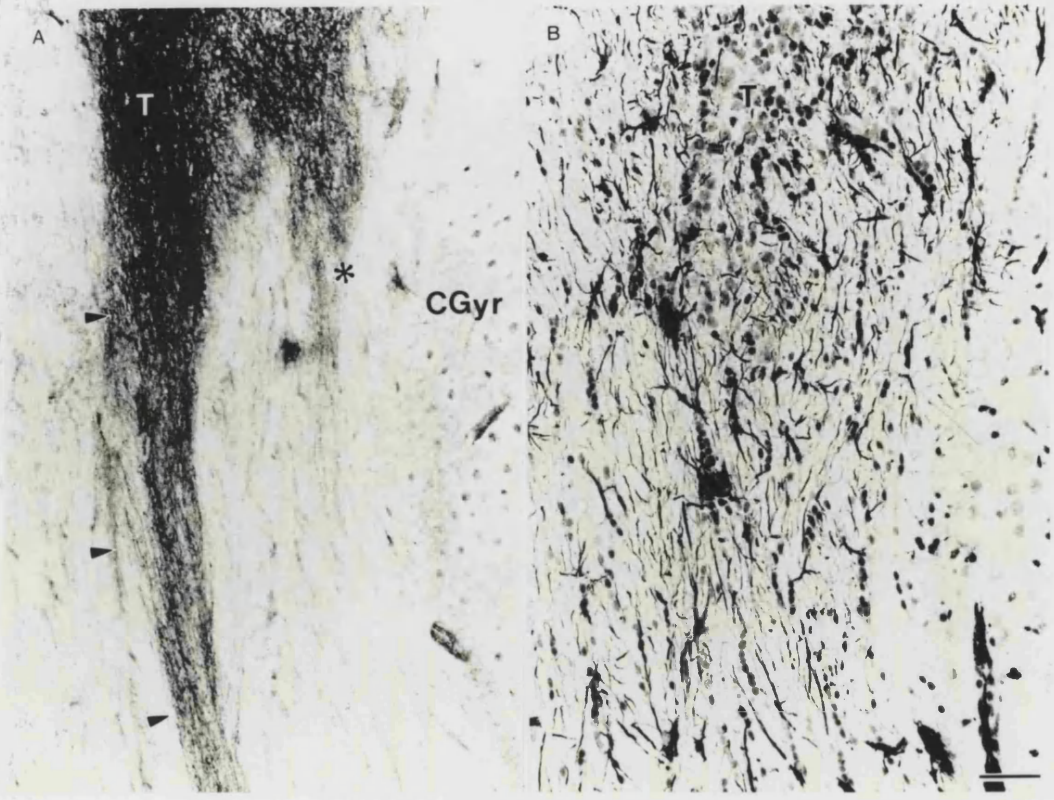
A
T
*
CGyr
B
T

Figure 37

A, Low power view of a column of M6-positive material (arrow), which arises from a transplant of E14 hippocampal cells placed in the cingulum ventral to the plane of this section, and extends radially for about 1 mm through the cingulate cortex (CGyr); arrowheads, fascicles of axons in the cingulum; M, midline. **B**, Adjacent section stained for vimentin. **C**, Enlarged view of the M6-positive column in *A*. **D**, Vimentin stain of adjacent section. E14 hippocampal transplant. Survival, 14 days. Scale bars, 500 µm (*A,B*), 50 µm (*C,D*).

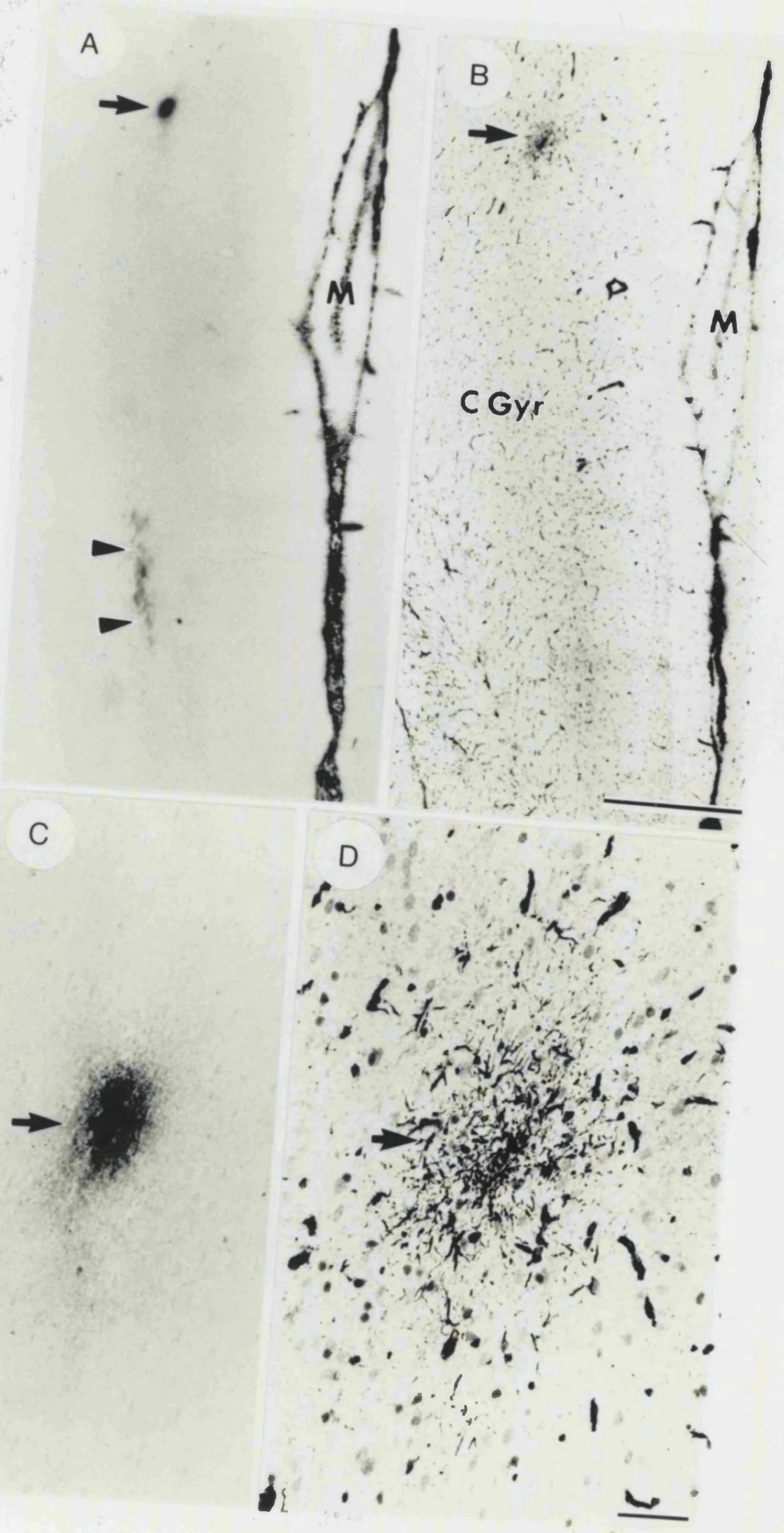
A
M
B
M
C Gyr
C
D

Figure 38

GFAP immunostaining of the neuropil of an E18 cortical transplant (T) in the cingulum to show the swirling pattern of the intra-transplant astrocytic processes running to the graft-host interface. At this level the cingulum, which is GFAP-poor, is cut almost at right angles to its longitudinal axis. Aldehyde fixation. Survival, 36 days. Scale bar, 100 μm.

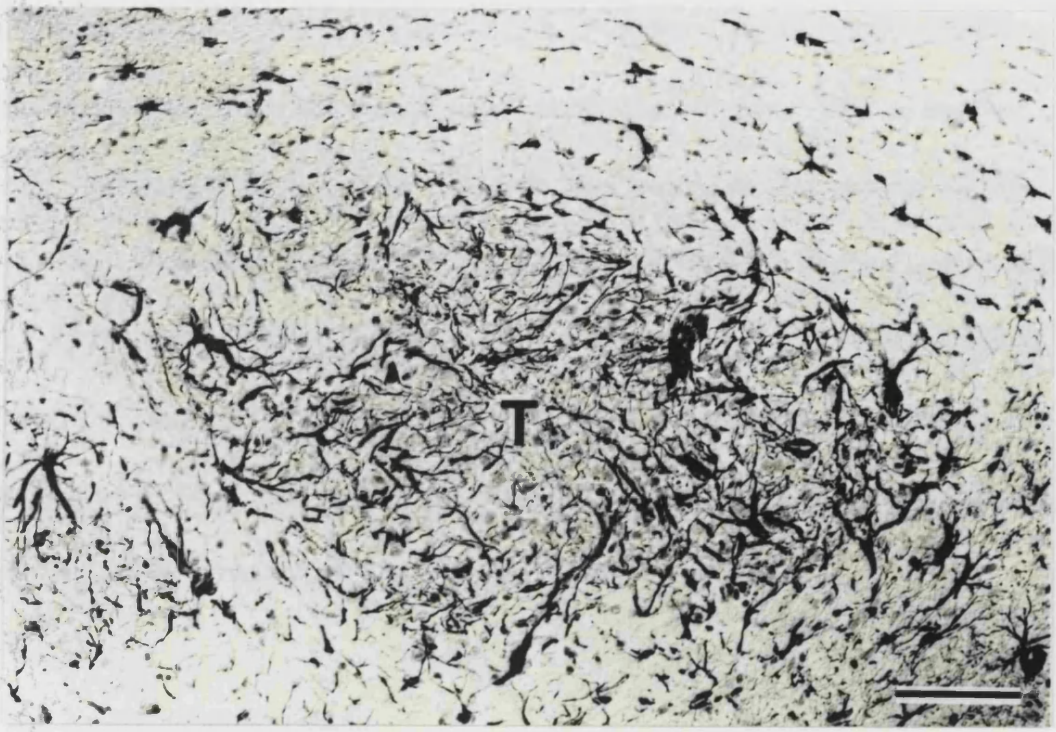
T

DISCUSSION

A striking feature of the intra tract micro-transplants was the speed, efficiency and vigour with which the transplanted embryonic neurons grew axons along adult myelinated fibre tracts. Due to the relatively atraumatic injection procedure, astrocytic scarring is virtually eliminated and the donor neurons and glia come rapidly into contact with, largely undisturbed host tract structures. The axons formed by the microtransplants are not abortive (at least up to 7 weeks), and can successfully grow along a variety of different adult myelinated tracts and invade even distant terminal fields.

3.4.1 Speed of axon growth

In peripheral nerves cut axons have been reported to regenerate with speeds of around 3-4mm/day (Guth, 1956). So and Aguayo, (1985) reported that, after allowing for an initial delay of 4.5 days, cut central (retinal ganglion cell, RGC) axons regenerated along peripheral nerve grafts at speeds of more than 1mm/day. Given that I have made no allowance for any initial delay, the present observations show that microtransplanted mid to late embryonic mouse hippocampal neurons give rise to axons which grow through the adult fimbria at speeds approaching 1mm per day for a maximum observed distance of at least 10 mm.

3.4.2 Donor axon morphology

The initial series of hippocampal microtransplants to the fimbria indicate that the donor neurons form axons which grow along the longitudinal axis of the host fimbria, dispersed singly or in fascicles among the host axons, and following the guidelines associated with the orientation of the host axons and the row pattern of the host interfascicular glia. Suzuki and Raisman, (1992) described the interfascicular rows of the fimbria as consisting of segments of around 8 contiguous oligodendrocytes separated at intervals by solitary astrocytes. Both types of glia generate longitudinal and transverse processes, and the interleaved longitudinal processes of adjacent astrocytes form a continuous carpet along the direction of the axons.

3.4.3 Collateral branches

It is interesting that transplant fibres directed towards the terminal fields can arise as collateral branches at right angles to the main parent projection fibres (see also Fig. 2c in Wictorin *et al.,* 1990a). This form of growth resembles that described by O'Leary and colleagues (O'Leary *et al.,* 1990; O'Leary and Terashima, 1988) in the developing subcortically projecting axons of layer 5 pyramidal neurons, where the growth of the main axon along the fibre pathways is followed by the production of 'interstitial' collaterals directed towards individual terminal target areas.

3.4.4 Terminal field formation

The light microscopic patterns of diffuse M6 immunostaining and the preliminary

Thy 1.2 data (fibre branching, and lattice-like terminal patterns), and the selective distribution to the stratum oriens and radiatum of field CA3 (and absence from the stratum pyramidale and the mossy fibre layer in the stratum lucidum), as well as to the lateral and triangular septal nuclei, suggest that the transplant hippocampal axons are terminating in the host terminal fields appropriate to CA3 pyramidal cell axons (Swanson and Cowan, 1977; Swanson *et al.,* 1980, 1981). I have not confirmed the presence of donor synapses by electron microscopy (Cf Lund *et al.,* 1985), but Wictorin et al., (1990b) used *Phaseolus vulgaris* leucoagglutinnin (PHAL) staining to demonstrate that long interfascicular axons formed by embryonic mouse striatal neurons transplanted into the adult rat striatum are able to traverse the internal capsule for 1.2mm and form synaptic terminals in the globus pallidus.

3.4.5 Microtransplant size

The injections of Wictorin et al., (Wictorin *et al.,* 1989a, 1990a,b, 1991) contained 2 orders of magnitude more cells (2-4 X 10^5) than my present injections (3 x 10^3), in at least 10 times the injection volume (6-9µl compared with 0.5µl; e.g. Cf Fig. 1 in (Wictorin *et al.,* 1989a). I feel that, taken in proportion to the differences in the numbers of grafted cells, the amount and extent of axonal outgrowth from my microtransplants in the fimbria is comparable to that from their larger grafts. Wictorin *et al.,* (1990a) suggested that the length (about 20mm) of their observed axon growth from human neuroblasts transplanted into rat hosts may be an expression of an intrinsically greater growth capacity of the human neuroblasts which in situ would obviously

produce much longer axons than the rat. In my material, however, I observe axonal elongation of at least 10mm, when the donor/host size disparity is in the other direction - i.e. the mouse donor hippocampal neurons would normally produce shorter axons than the rat. It must also be borne in mind that the distance embryonic axons are required to grow to reach their targets during development, is a fraction of that which has been induced by contact with an adult tract environment in the present material.

3.4.6 Degeneration of host axons

It has been a general observation (e.g. Björklund and Stenevi, 1984; Zhou *et al.,* 1985, 1989) that transplants will not project to terminal fields in a host brain unless they have been denervated. The microtransplantation was carried in such a way as to produce the least possible damage to the host tract, and very little degeneration of host axons was detected. The rat fimbria contains about 1 million axons (Suzuki and Raisman, 1992; Wyss *et al.,* 1980). I have not estimated how many axons are produced by my present microtransplants, but if the estimated 3,000 neurons per transplant each produced one axon, the total number of donor axons would still be much less than 1% of the total number of host fimbrial axons. However atraumatic the micro-transplantation procedure, I cannot exclude the possibility that the transplant might have damaged 0.3% of the host fibres. Preliminary experiments with complete transection of the host fimbria indicate that the very much higher level of host axon damage thus produced does not appreciably alter the pattern or increase the quantity of long

interfascicular axon growth from embryonic donor hippocampal neurons. However, this may indicate that the lower level of host axon damage incurred by microtransplantation alone (i.e. without the added fimbrial section) may have been sufficient to induce the maximal donor axon growth possible. For these reasons, I am currently unable to assess the extent to which denervation was a factor in the formation of the projections.

3.4.7 Inhibition of axon growth

3.4.7.1 *Oligodendrocytes*

Much recent work has focused on the idea that a major element in the failure of central regeneration is that mature myelinating oligodendrocytes express surface molecules which cause collapse of growth cones and thus inhibit regenerative axon growth (Bandtlow *et al.,* 1990; Schnell and Schwab, 1990; Schwab *et al.,* 1993). To reconcile the concept of an inhibitory molecule with their observation of long axon growth from embryonic rat (Wictorin *et al.,* 1989b, 1990b), mouse (Wictorin *et al.,* 1991) and human neuroblasts (Wictorin *et al.,* 1990a) along myelinated fibre tracts in the adult central nervous system (see also Fujii, 1989; Strömberg *et al.,* 1992; Tønder *et al.,* 1990), Wictorin and collaborators suggested that immature axons may not have the receptors to respond to the inhibitory influences present in adult myelinated tracts. The immaturity of the early human embryonic donor tissue they used, combined with its slower normal rate of maturation, may have contributed to the extensive growth they reported for this donor tissue.

Shewan *et al.*, (1995) have also proposed that neurons acquire receptors for tract associated axon growth inhibitory molecules late in embryonic development. Using a cryoculture technique in which dissociated embryonic neurons are seeded on to sections of neonate (unmyelinated) or adult (myelinated) optic nerve they have shown that E14-15 embryonic RGC's will extend neurites on neonate tract but not adult tract. Early DRG neurons will however grow extensive neurites on both neonate and adult tract sections but this ability also declines with neuron age. In my material vigorous axon growth occurred in adult myelinated tracts, even when late (E18/19) embryonic mouse donor hippocampal cells were used, although this may be associated with the later generation time of these cells (Schlessinger *et al.,* 1978).

Kobayashi *et al.*, (1995) have demonstrated DRG neuron growth cone collapse and inhibition of neurite extension when in contact with mature oligodendrocytes in culture (in accordance with Bandtlow *et al.,* 1990), but however have also shown that embryonic retinal ganglion cell (RGC) neurons will grow extensive neurites without growth cone collapse in the same environment. In a study in which embryonic retinal explants were co-cultured with myelin basic protein positive oligodendrocytes, no inhibition of neurite extension was noted by Ard *et al.,* (1991). Fawcett *et al.*, (1992) have also shown that dorsal root ganglion axon growth is inhibited when grown on oligodendrocyte monolayers in culture. However, when they cocultured astrocytes with the oligodendrocytes, DRG

axonal growth was not inhibited, and axons were seen to grow in contact with both glial cell types.

It is clear that different neurite growth responses can be elicited from peripheral versus central neurons grown in contact with mature oligodendrocytes in culture and obviously a number of issues regarding the possible action of myelin inhibition of central axon growth remain to be resolved (discussed further in *Chapter V*).

3.4.7.2 *Astrocytes*

Adult reactive astrocytes have also been shown to present molecules inhibitory to axon growth in tissue culture, such as cytotactin/tenascin (CT), chondroitin-6-sulphate containing proteoglycan (C-6-PG) and some as yet not fully characterized inhibitors (Bovolenta *et al.,* 1993; Liuzzi and Lasek, 1987; Mansour *et al.,* 1990; McKeon *et al.,* 1991; Stensaas *et al.,* 1987; discussed further in *Chapter V*). In the present study I have not immuno stained for the expression of putative inhibitory molecules in microtransplanted adult tracts, however if these molecules are present, they can be having little effect on the vigorous embryonic axon growth I have observed.

3.4.8 Do donor astrocytes modify the tract environment?

Is it possible that the embryonic astrocytes and their precursors present within the microtransplants have in some way modified the adult tract environment and

made it more permissive to axonal growth? A number of groups have shown that embryonic astrocytes support axon growth in tissue culture (Fawcett *et al.,* 1989; Geisert and Stewart, 1991; Noble *et al.,* 1984; Rudge *et al.,* 1989; Smith *et al.,* 1990; Wang *et al.,* 1994) and secrete a variety of growth promoting molecules (reviewed in *Chapter IV*).

In invivo experiments, millipore implants coated with embryonic astrocytes have been shown to promote the regeneration of adult axons from experimentally induced neuromas in the adult corpus callosum (Smith *et al.,* 1986) and cut axons at the dorsal root entry zone (Kliot *et al.,* 1990). Wunderlich *et al.*, (1994) have observed increased sprouting of cut adult axons towards transplants of E14-16 cultured astrocytes placed in the lesioned fornix fibre tract. Immature astrocytes transplanted into adult brain (Emmett *et al.,* 1991; Lindsay and Raisman, 1984) migrate extensively within adult white matter tracts and I therefore cannot discount the possibility that they may change the adult tract environment and make it more permissive to axon growth. I have not made a systematic study of the migration patterns of the embryonic astrocytes and their precursors in the present material, however vimentin and GFAP immunostaining failed to show the long distance growth of donor glial processes as reported by Deacon et al., (1994) for porcine foetal lateral ganglionic eminence cells xenografted to rat.

Specificity of axon growth

3.4.9.1 Long interfascicular axon growth does not require correct matching of donor tissue origin to host tract

In the initial series of hippocampal microtransplants, I had observed the formation of axons by embryonic hippocampal neurons transplanted into the adult fimbria. Since this is the tract in which the host hippocampal axons run, it was appropriate that the donor hippocampal axons should have reproduced the normal patterns of axon trajectory through the fimbria, and entered the same terminal fields in the hippocampus and septal nuclei as those innervated by the normal adult host hippocampal axons which make up this tract.

3.4.9.2 Projection patterns

However it was surprising to find in the specificity study that transplanted embryonic neocortical and superior collicular donor neurons, whose axons never normally enter the fimbria, consistently generated exactly the same pattern of intrafimbrial distribution, at no lesser speed or density than hippocampal donor cells, and mimicked hippocampal donor cells even to the point of forming collaterals and entering terminal fields. Similarly, transplants of cell suspensions from all three donor regions (E14 or E18 hippocampal or neocortical donor tissue, or E14 superior collicular tissue) produced indistinguishable patterns of projection in the adult host corpus callosum and cingulum. Clearly the environment of the adult host tracts provides sufficient

cues to induce axon formation from neurons which do not normally project through those specific tracts.

3.4.9.3 Donor cell differentiation

My tissue samples would have contained neuroblasts as well as different types of neurons, and I do not know which of the donor cells gave rise to the interfascicular axons. It is possible that the experimental situation selects for special categories of cells (e.g. those belonging to more diffuse or 'global' systems, rather than the topographically precise 'point-to-point' systems; (Sotelo and Alvarado-Mallart, 1987). Alternatively, as has been shown in cortical transplantation experiments (Barbe and Levitt, 1991; O'Leary and Koester, 1993), the host tissue environment may alter the differentiation and neural connections of the transplanted developing donor cells.

Multipotential stem cells

There has been much recent interest in the possibility that the central nervous system may contain multipotential stem cells whose fate is determined by their environment. Nestin is the major intermediate filament protein of embryonic central nervous system progenitor cells (Lendahl *et al.,* 1990). Small numbers of these nestin positive progenitor cells remain in the adult nervous system and they can be induced to proliferate and differentiate in to either neurons or glia in culture by treatment with different growth factors (Cattaneo and McKay, 1990; Reynolds and Weiss, 1992). It has been shown that oncogene-mediated immortalisation of early neuroepithelial cells can produce cell lines which have

the potential to differentiate into different neuronal cell types characteristic of specific host regions into which they are transplanted (Renfranz *et al.,* 1991; Snyder *et al.,* 1992).

3.4.9.4 Specificity of axon growth

In contrast to the present results showing 'mismatched' axon growth from embryonic neurons transplanted into adult tracts, there are a number of experimental situations in which it has been demonstrated that the formation of terminal field projections from neuronal transplants placed in direct contact with specifically denervated adult host neuropil maintains appropriate tissue-type specificity (Zhou *et al.*, 1985, 1989) with only occasional abnormalities (e.g. Raisman and Ebner, 1983).

Wictorin *et al.*, (1991) demonstrated clear tissue-type specificity in the formation of interfascicular projection patterns from suspensions of different types of foetal mouse tissue transplanted into the ibotenate-lesioned adult rat striatum. Using M6 as an axonal marker, they showed that correctly matched striatal transplants grew axons through the internal capsule but in the caudal direction only, to selectively innervate the host globus pallidus. Control grafts of foetal neocortex transplanted to the lesioned striatum also projected axons through the internal capsule (as they do during development), however these axons did not innervate the globus pallidus but took a course through the corpus callosum and into the overlying cortex. Grafted foetal cerebellum however failed to grow

axons over any significant distance. Given a choice of two terminal fields both denervated by the striatal ibotenate acid lesions, axons from donor striatal and neocortical tissue selectively grew to the correct terminal fields, suggesting that tract degeneration was not determining the patterns of axon growth but possibly factors released from the target adult neuropil.

Non specific axon growth

Fujii, (1991) reported long interfascicular growth of axons from mismatched (olfactory bulb) tissue transplanted into the rostrum of the corpus callosum, and Li and Raisman, (1993) have shown that embryonic E15 mouse hippocampal neurons microtransplanted into the adult cortico-spinal tract will similarly grow long axons. Zwimpfer *et al.*, (1992) have demonstrated that adult retinal ganglion cell axons regenerating through a piece of peripheral nerve can be induced to invade an incorrect terminal field and even form inappropriate synapses in the adult cerebellum.

In the case of the present specificity study, microtransplants were placed directly into and enclosed within tracts that their axons would also never normally grow through in development, and all three mismatched donor tissue types were induced to grow long axons. However, in the absence of any possible axon guidance cues presented by their correct terminal fields, the patterns of axon growth and terminal field invasion were determined by the local tract structure (see below).

3.4.9.5 Are the newly formed mismatched axons maintained?

In their studies of fibres in the internal capsule, Wictorin and colleagues showed that in situations where the correct type of donor axons grew through the correct tract, and formed synapses in the appropriately matched denervated host target territory, both PHAL (Wictorin *et al.,* 1990b) and human neurofilament labelling (Wictorin *et al.,* 1990a) demonstrated that axons were still present at survival times after those where M6 staining has disappeared (Wictorin *et al.,* 1991). The disappearance of M6 staining in my material (after 7 weeks in the hippocampal and neocortical transplants, and 3 weeks in the E14 superior collicular transplants) could be due to a number of factors associated with axonal maturation. The molecule that bears the M6 epitope may be simply downregulated or ensheathment of the donor axons could be preventing access of the antibody (Wictorin *et al.,* 1991) as seen for the developing mouse optic nerve where loss of M6 immunoreactivity correlates with the onset of myelination (Lund *et al.,* 1986). It could also be due to retraction of the donor axons, possibly because they did not have access to denervated terminal target structures able to provide growth factors needed for their survival.

The 'non-specific' growth may therefore represent an early stage of neuronal differentiation, in which 'exuberant' axons grow out provisionally, but require to be 'validated' by contact with appropriate terminal fields before they are stabilised for permanent existence (Elberger, 1994; O'Leary *et al.,* 1990;

O'Leary and Terashima, 1988; Simon and O'Leary, 1992). This could provide a mechanism for adding a subsequent element of specificity to the initially non-specific, bi-directional growth I have observed.

Relationship of donor axons to tract structure

3.4.10.1 Adult host fibre tracts present a structured environment for donor axon growth

The structure of adult tracts is built around a longitudinal axis which is defined by the orientation of the axons, the interfascicular rows of glial cell nuclei, and the longitudinal processes of astrocytes (Suzuki and Raisman, 1992; Cf Fig. 1d in Bovolenta *et al.,* 1984). In complex tracts such as the fimbria and corpus callosum, the different fibre contingents interweave as they pass through the tract structure. The microtransplantation technique used in these studies leaves the internal organisation of the host fibre tracts largely undisturbed. Together with the use of small transplants which occupy only restricted parts of the overall host tract, this approach has made it possible to demonstrate that the routes taken by growing axons are strictly constrained by the local structure of the host fibre tracts.

3.4.10.2 Tract boundaries

Where different tracts lie immediately adjacent to each other (such as the fimbria and stria terminalis, or the corpus callosum and cingulum) the glia form a boundary which axons do not cross. The existence of such boundaries in development, and their possible chemical constituents (e.g. Brittis *et al.,* 1992; Faissner and Kruse, 1990; Silver *et al.,* 1993; Snow *et al.,* 1990) have recently been reviewed (Faissner and Steindler, 1995). In serial sections of my transplanted material I was able to see that transplants which spanned the

boundaries of two tracts gave rise to projections into both tracts (e.g. Fig. 39). However, when the transplants were confined to one side of the boundary, the donor axonal projections remained confined to the tract on that side - i.e. despite immediate proximity, donor fibres do not cross adult inter-tract boundaries. Possibly boundary guidance molecules expressed during development are still participating in the active guidance of new axon growth in adult tracts

3.4.10.3 Relationship of tract glia to long interfascicular axon growth

The finding that the donor axons grow in parallel to the longitudinal astrocytic processes of the host fibre tracts, suggests that the astrocytic processes could be the substrate directing the orientation of the growing donor axons. But although this could be true for the embryo-to-adult transplant situation, it must be borne in mind that at the time in normal brain development when the fimbrial and callosal axons are growing, the configuration of the glia is different, and longitudinal astrocytic processes are absent. However, despite the fact that the adult tract glial skeleton is quite different from that through which the embryonic axons grew, the adult structure still retains cues sufficient to direct rapid and efficient axon growth from embryonic transplants. Therefore, while the long interfascicular axon growth bears some resemblances to normal axon development, it is not a recapitulation, but a new phenomenon.

3.4.10.4 Phenotype of intermediate glial filaments (vimentin and GFAP)

The analysis of the glial framework of CNS tracts was greatly facilitated by the finding that vimentin selectively stained tract (as opposed to neuropil) astrocytes.

Figure 39

A, Palmgren stained horizontal section through the rostral part of the corpus callosum to show the longitudinally arranged fibres of the cingulum (cg) lying adjacent to the medial edge of the mass of transversely orientated fibres of the corpus callosum (CC). CGyr, cortex of the cingulate gyrus; CR, corona radiata; H, hippocampus; M, midline. **B,C,D**, Enlarged views of the boxed area in A, with a schematic representation of the different types of projections (arrows) according to the exact location of the transplants at the callosal/cingulum interface. The donor axonal projections from transplants in *B,C,* are restricted to the corpus callosum (large arrows) or the cingulum (smaller arrows), respectively, and do not cross the inter-tract boundary. **D**, Axons from transplants straddling the boundary project into both tracts. Scale bar, 500 μm.

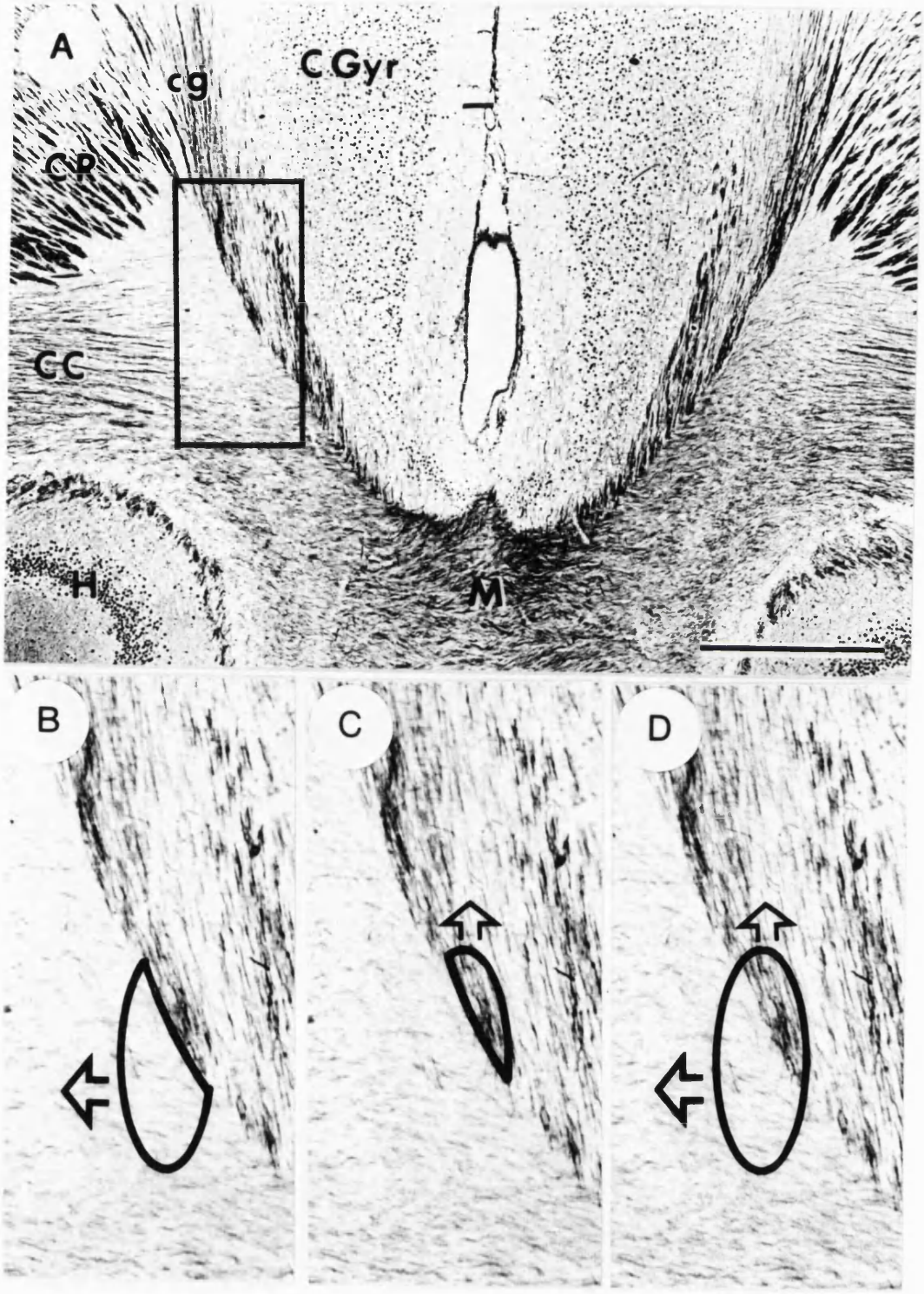
A
cg
CGyr
Cp
CC
H
M
B
C
D

Conversely, in aldehyde fixed material, GFAP favours neuropil astrocytes, which express little vimentin (Bovolenta *et al.,* 1984; Voigt, 1989).

The transplanted tissue itself forms a neuropil (as described for hippocampal transplants above) and here too, in contrast to the adjacent tract astrocytes, the astrocytes are GFAP-positive, and vimentin-negative. Within the transplants, the orientation of the axons and the GFAP staining of the astrocytic processes (Fig. 36A,B) show that the internal structure of the transplants is aligned with that of the host tract, suggesting that the development of this transplant neuropil alignment from the initially randomly mixed cell suspension is responding to local orientational cues in the host tract.

(A) ***Astrocytic alignment at interface***

There was sufficient overlap of the vimentin and GFAP staining patterns to show that the longitudinal astrocytic processes of the host fibre tract continue uninterrupted through the interface and into the transplant neuropil. These processes would thus be in a position to provide a continuous substrate for the donor axons as they emerge from the transplant and enter the host tract.

(B) ***Astroglia phenotypic changes***

During normal development the switch from astrocytic vimentin to GFAP has been correlated with the time of cessation of long axon growth (e.g. Bovolenta *et al.,* 1984). In my transplanted material there are indications that vimentin is upregulated (suggesting a reversion to a more immature phenotype) in the

astrocytes of those areas of the host tract through which the newly growing donor axons pass, and intense, sharply localised vimentin expression is induced in the M6-positive column of the otherwise vimentin negative grey matter of the cingulate cortex. I have not made a systematic investigation of further possible phenotypic changes in the glia associated with the newly growing axons (e.g. Schachner, 1991). I was unable to detect any upregulation of laminin associated with the donor axon growth (Cf Liesi, 1985; Liesi and Silver, 1988: the effects of laminin on axon growth are discusssed in *Chapter IV*).

3.4.10.5 Possibilities that glia may guide transplant axon growth

Is the observed correlation between the orientation of donor axons and that of the host tract astrocytic longitudinal processes merely circumstantial, or does it indicate that these astroglial processes are necessary for induction or maintenance of long interfascicular axon growth?

There is considerable evidence for a functional effect of glia on neuronal migration and neurite growth. Tissue culture observations indicate that astrocytes play a role in neuronal survival and the formation of neurites (e.g. Lindsay, 1979). Astrocytes from different areas may encode specific information determining the region-specific patterns of axon and dendrite formation (e.g. Rousselet *et al.,* 1988). As shown by the pioneering studies of Rakic (Nowakowski and Rakic, 1979; Rakic, 1971, 1972), developing dentate, neocortical, and cerebellar granule cells migrate to their definitive locations along radial processes (see also Hatten and Mason, 1986; Rickmann *et al.,*

1987), and the intracortical growth of developing callosal axons is similarly linked to radial glia (Norris and Kalil, 1991) . In the developing ferret optic nerve, the axon order changes in relation to a specific change from radial to 'interfascicular' glia (Guillery and Walsh, 1987), although growth cones do not preferentially associate with glial structures in the developing monkey optic nerve (Williams *et al.,* 1991). However, of the few transplantation studies which have described the host glial arrangement, Silverman *et al.*, (1991) showed that the axons from embryonic transplants did follow host tanycyte processes during their course through the grey matter of the mediobasal hypothalamus to the median eminence in adult hosts.

3.4.10.6 Relationship of host tract axons to long interfascicular growth of transplant axons

Whilst a causal correlation of donor axon growth with host glial processes is an attractive hypothesis, I cannot exclude the possibility that the growth and orientation of the donor axons is determined by the host axons. Moreover, degeneration of damaged host axons (as previously discussed above) - and/or the associated glial responses - may also play a part in promoting donor axon growth. Degeneration of axons causes responses in tract oligodendrocytes (Ludwin, 1992; Xie *et al.,* 1995) and microglia (Koshinaga and Whittemore, 1995; Milligan *et al.,* 1991; Schnitzer and Scherer, 1990) as well as astrocytes (Bignami and Dahl, 1976), but my present material does not enable me to say whether glial changes, such as re-expression of astrocytic vimentin (e.g. Takamiya *et al.,* 1988), are caused by degeneration of host axons, or whether they are themselves a response to the growth of the donor axons.

CONCLUSION

Adult myelinated central nervous system tracts present a highly permissive, indeed perhaps stimulatory environment for the growth of embryonic axons. Axon growth is not confined to a correct matching of donor neuron type to adult tract. However the patterns of axon growth and terminal field invasion are determined by the point of axon entry into the highly regular adult tract cytoarchitecture and subsequent strict alignment with adult axons, interfascicular glial rows and astrocytic longitudinal processes. It is possible that the astrocytic longitudinal processes, which are unique to adult CNS tracts, are providing guidance cues to the growing axons. The relatively atraumatic nature of the microtransplantation proceedure prevents glial scarring and promotes the establishment of an aligned astroglial interface with the host tract, no doubt contributing to the rapid outgrowth of the embryonic axons.

CHAPTER IV

Host innervation of microtransplants

INTRODUCTION

Adult axons will readily sprout and grow new synaptic connections in partially denervated central neuropil (for a review see Cotman *et al.,* 1981) as first demonstrated by Raisman, (1969) in the septum.

That adult axons are also capable of innervating transplants of embryonic nervous tissue placed adjacent to or directly into adult neuropil has been clearly demonstrated by a number of research groups. Kromer *et al.*, (1981a,1981b) showed innervation of embryonic hippocampal implants by regenerating axons of cholinergic septal neurons; host hippocampal mossy fibres will innervate transplants of late embryonic or early postnatal hippocampus embedded in the mossy fibre pathway (Field *et al.,* 1991; Raisman and Ebner, 1983); foetal caudate putamen transplanted into the ibotenic acid lesioned striatum of adult rats is innervated by the adjacent striatum and axons of the host substantia nigra (Campbell *et al.,* 1993; Clarke *et al.,* 1988a; Labandeira-Garcia *et al.,* 1991; Pritzel *et al.,* 1987; Wictorin *et al.,* 1989a) and embryonic neocortical tissue grafted to the adult neocortex is innervated by basal forebrain cholinergic fibres (Clinton and Ebner, 1988). A more recent study conducted in the adult cerebellum shows that cut olivocerebellar axons will regenerate into solid grafts of early embryonic cerebellum placed at the lesion site (Rossi *et al.,* 1995).

However, there have been few studies describing adult axon growth from white matter tracts directly into embryonic neuronal transplants. Reier and co-workers

(Jakeman and Reier, 1991; Reier *et al.*, 1983a) transplanted E14 foetal rat spinal cord into 2-4mm long intraspinal cavities formed by partial spinal cord lesions of adult rats. They noted 'substantial gliosis' and disruption at the graft interface with the adult white matter. WGA-HRP (Wheat germ agglutinin-HRP), Fluorogold or *Phaseolus vulgaris* leucoagglutinnin (PHA-L) axonal tracing and 5-HT staining for adult axons in the grafts revealed relatively few axons penetrating from the degenerating host white matter, with the majority of labelled axons originating in the adjacent grey matter.

Hausmann *et al.,* (1989) transplanted grafts of E16 thalamic and tectal tissue to the proximal stump of completely transected adult optic nerve and traced small numbers of rhodamine isothiocyanate (RITC) labelled retinal ganglion cell axons regenerating into the foetal grafts. Graft intergration with the proximal stump of the optic nerve was relatively poor probably due to inadequate vascularisation of the foetal tissue. Availability of the host vasculature to the transplant within the first 24 hours post operation is vital for graft survival and integration (Lawrence *et al.,* 1984; Lindsay and Raisman, 1984; Raisman *et al.,* 1985). Adult CNS fibre tracts generally only have about one-fifth the capillary density of neuropil (Lierse, 1964) and this, together with the damage to the tract structure caused by the solid transplantation method, have generated tissue necrosis and scarring at the graft/tract interface giving regenerating axons relatively poor access to the transplants.

In *Chapter III,* I described a method of 'microtransplanting' suspensions of embryonic neurons and glia directly into adult CNS white matter tracts. The transplants proved to be highly angiogenic and were quickly vascularized by the surrounding host tissue. GFAP and vimentin immunostaining showed no evidence of astroglial scarring and an open glial framework was promptly established at the host/graft interface, aligned with that of the surrounding adult tract. Overall, the microtransplantation proceedure caused minimal damage to the host tract structure and gave superior graft integration compared to that previously described for the solid transplantation method.

In the present study, I have investigated the ability of adult tract axons to innervate intra-tract microtransplants of embryonic hippocampal suspensions which are completely enclosed within the fimbria of adult rat hosts. Biotin-dextran tracer was microinjected into the fimbria to anterogradely label adult axon growth into the transplants. In order to prove that adult axons can also form synapses within intra-tract microtransplants, a contingent of axons originating in the contralateral hemisphere were transected in a further series of transplanted animals. The electron microscope was used to identify the electron dense degeneration of any synapses previously formed by the adult axons with the donor neurons.

4.2.1 Preparation of cell suspensions

Mouse E15 mixed neuron and glial hippocampal cell suspensions were prepared as previously described in *Chapter III*, with a cell density of approximately 20 x 10^6 cells/ml in defined medium (Bottenstein and Sato, 1979).

4.2.2 Surgery

All surgical proceedures were carried out under tribromoethanol anaesthesia (20 mg/100 g body weight, ip). Graft rejection was suppressed by maintaining the animals from the time of transplantion on cyclosporin A (Sandimmun, Sandoz; 10 mg/100 ml in the drinking water).

4.2.2.1 *Transplantation and tracer injection*

A 500nl microtransplant was stereotaxically injected into the medial fimbria of the left hemispheres of 12 adult female AS rats of body weight 180-200 g. At a survival time of 8 weeks post- transplantation, 8 of these animals received a 250nl injection of a 10% solution of 3000mw biotin dextran tracer (lysine fixable, Molecular Probes, Oregon, USA) in sterile saline to the left hemisphere lateral fimbria, using the air pressure pulse micro-injection proceedure (Fig. 1) and a standard graduated micro-pipette of 50 µm internal diameter and bevelled tip. After each injection the micropipette was kept in position for 1 min before being

withdrawn. Biotin-dextran amine is a sensitive anterograde tracer readily taken up and transported by axons en passant over long distances. It gives fine structural details of axon terminal morphology and is only weakly retrogradely transported as demonstrated by Brandt and Apkarian, (1992) in tracer studies in the rat and monkey.

The stereotaxic coordinates measured from the bregma with the head held in the flat skull position were; for transplants; caudal 1.6mm, lateral 1.3mm and ventral 4.1mm and for tracer; caudal 2.7mm, lateral 3.2mm, and ventral 3.6mm.

4.2.2.2 *Contralateral Fimbria Lesions*

At a survival time of 8 weeks post-transplantation, the remaining 4 microtransplanted animals received a unilateral lesion transecting the fimbria of the right hemisphere ie. the fimbria contralateral to the microtransplants. Stereotaxic coordinates for fimbria lesions measured from the bregma were 2.4mm caudal, with a specially prepared razor blade (NIMR Engineering)) inserted to a depth of 5.5mm ventral at the midline and drawn laterally cutting the fimbria before exiting through the parietal cortex and out of the skull via a previously drilled channel (the parietal muscle having been blunt dissected and retracted).

4.2.3 Histology

4.2.3.1 *Tracer*

At 48 hours survival post biotin dextran tracer injection, animals were sacrificed under deep terminal pentobarbitone anaesthesia (Sagatal, RMB Dagenham, UK) by transcardiac perfusion of about 100ml of PBS followed by 500ml of 4% paraformaldehyde, 0.5% glutaraldehyde, 0.2% picric acid in 0.1M PBS. Brains were dissected out and fixed for a further 2 hours at room temperature in the same fixative and then sectioned at 100 µm intervals in the horizontal plane (see above) on a Vibratome (General Scientific, UK). For all subsequent proceedures before being mounted, sections were free floating in 5ml wells. Sections were washed in several changes of 0.1M PBS over 30 mins and then incubated with ABC Vectastain (Vector), 0.1% Triton X100 (Sigma), to aid ABC penetration, and 0.5% BSA in 0.1M PBS for 4 hours at room temperature. The sections were then washed in several changes of 0.1M PBS over 1 hour, incubated for 5 min in 1% nickel chloride, followed by DAB treatment. The sections were were then mounted onto gelatin coated glass slides, dried overnight, counter-stained with aqueous thionin, dehydrated through a series of alcohols, cleared with Histoclear (National Diagnostics, Aylesbury, UK) and coverslipped.

4.2.3.2 *Electron microscopy of degenerating synapses*

At 3 days post fimbria lesion, the remaining 4 animals were deeply anaesthetised and transcardially perfused with a mixture of 1% paraformaldehyde and 1% glutaraldehyde in 0.1M PB at pH7.3. The brains

were removed, blocks taken containing the microtransplants, postfixed for 1.5 hours in 2% aqueous osmium tetroxide, dehydrated from 30% to absolute alcohol over 3 hours, and embedded in Epon embedding resin (TAAB Laboratory Equipment Ltd, Reading, UK). Semithin sections were stained with methylene blue and Azur II, and ultrathin sections with uranyl acetate and lead citrate. Degenerating synapses in the microtransplants were scanned for at 20,000x magnification on a Phillips transmission electron microscope.

RESULTS

4.3.1 Transplant location and morphology

All 12 transplants were located in the medial fimbria about 1mm from the midline and the septal nuclei and just rostral to field CA3 of the adjacent hippocampal neuropil (Fig. 40A, Cf Fig. 2, *Chapter III*) Transplant morphology was identical to that of the hippocampal intra-fimbrial grafts previously described in *Chapter III*, with light microscopy of 1-2µm semithin sections showing a homogeneous mixture of donor neurons and glia completely enclosed within the surrounding myelinated fibres of the host fimbria (Fig 5, *Chapter* III). A small proportion of the host tract fibres were degenerating but little more than previously observed for hippocampal microtransplants without a contralateral fibria lesion. With thionin staining of the Vibratome sections, the transplant neuropil could be easily distinguished from the surrounding highly regular tract glial framework as an ovoid mass about 1mm in length and 0.5 mm width elongated along the axonal axis of the tract (Fig. 40). As in the case of previous neuronal microtransplants, there were no signs of immune rejection.

4.3.2 Light microscopy of host to transplant axonal projection

Biotin dextran labelling of ipsilateral host fimbrial axons, showed that a number of these axons had crossed the transplant interface and penetrated the embryonic microtransplants by as much as 250 µm or more (Figs. 40 and 41). It was not possible to detemine beyond reasonable doubt which of the labelled axons were regenerating cut axons or collateral branches stimulated to grow

from the adjacent uncut tract axons which completely enclosed the transplants. Many axons had given rise to a terminal plexus with multiple branches narrowing into fine terminal segments exhibiting *en passant* or terminal varicosities which may indicate the presence of synaptic boutons (Figs. 40 and 41). The axons generally exhibited a tortuous morphology compared to that of the adjacent tract axons, with recurved segments looping back and fasiculating with the main stem of the axon (arrow in Fig. 41).

4.3.3 Electron microscopy of transplant neuropil and degenerating synapses

Under the electron microscope, it could be seen that the neuropil of the microtransplants contained neurons (with round pale nuclei containing relatively little chromatin), glia and axons, some of which could be identified as lesioned degenerating host fibres. The cytoplasm of the donor neurons contained characteristic organelles such as Golgi apparatus, rough endoplasmic reticulum and mitochondria. Dendrites formed within the transplants could be clearly identified by their distinctive microtubules and were seen to give rise to dendritic spines. Presynaptic axon terminals containing synaptic vesicles were observed in contact with donor neuronal cell bodies, dendritic shafts and spines, and could be identified by the characteristic thickening of their post synaptic membranes (Fig. 42 A-D). There were on average about 80 synapses per grid square (each grid square having an area of about 1600 μm^2), Twice as many synapses were situated on dendritic spines as compared to dendritic shafts, with less than 1% of the synapses located on the cell bodies of the donor neurons. Transection of the contralateral hippocampal derived host fimbria

Figure 40

A. A microtransplant in the medial fimbria showing host biotin dextran labelled axons that have entered a microtransplant; asterisk, terminal plexus. 100µm vibratome section. E15 hippocampal microtransplant, 8 weeks survival. **B** Higher power of A. Scale bars, (A) 200µm; (B) 100µm.

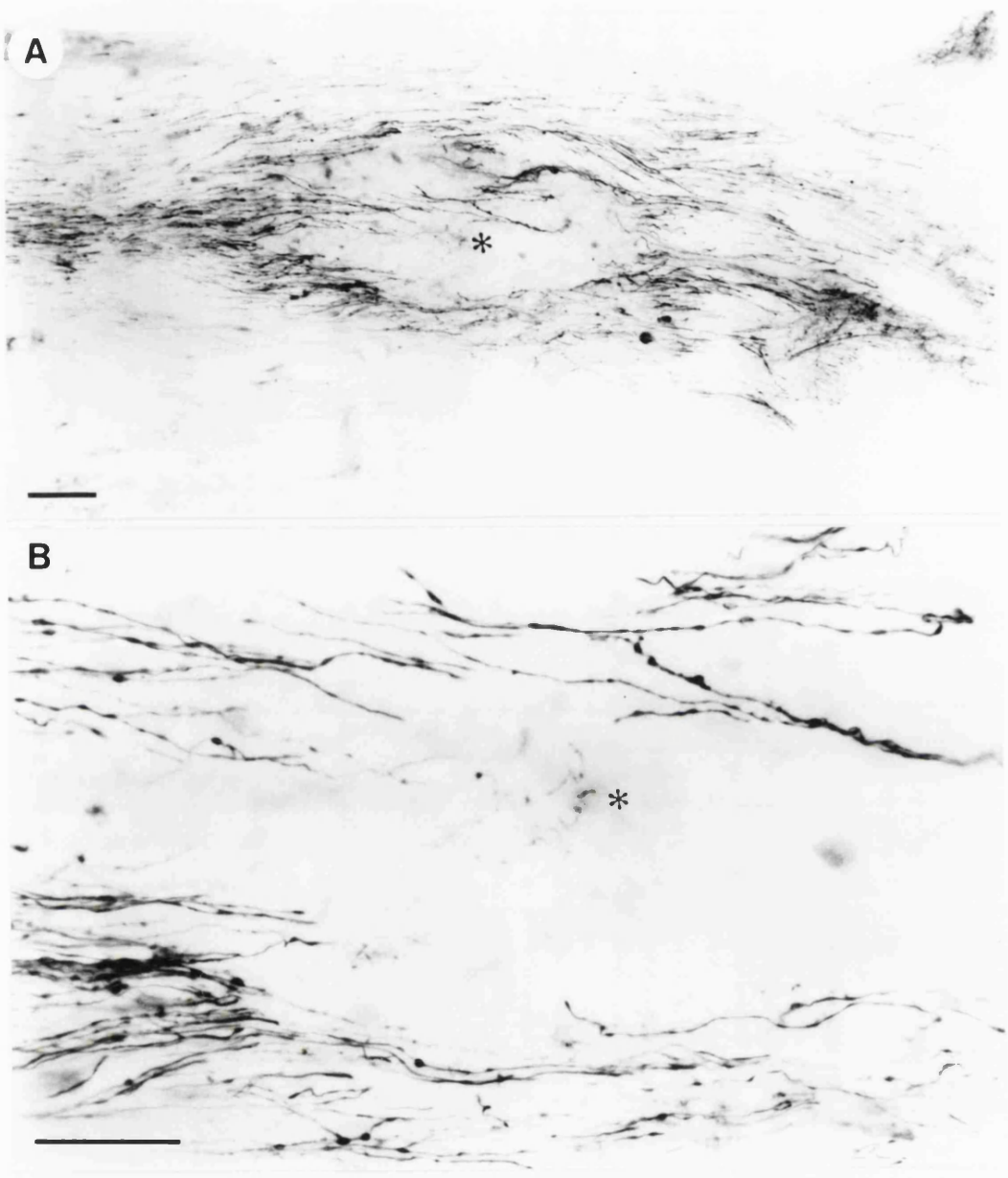
A
*
B
*

Figure 41

Camera lucida drawing of host biotin dextran labelled axons in photomicrographs *A* and *B* of *Fig 40*. Many of the host axons exhibit *en passant* or terminal varicosities which may indicate the presence of synaptic boutons. Host intratransplant axons have a generally tortuous morphology compared with that of the relatively straight tract axons (Rostral), some with recurved segments fasciculating with the main stem of the axon (arrow). Asterisk, terminal plexus. 100µm vibratome section. E15 hippocampal microtransplant, 8 weeks survival. Scale bar, 50µm.

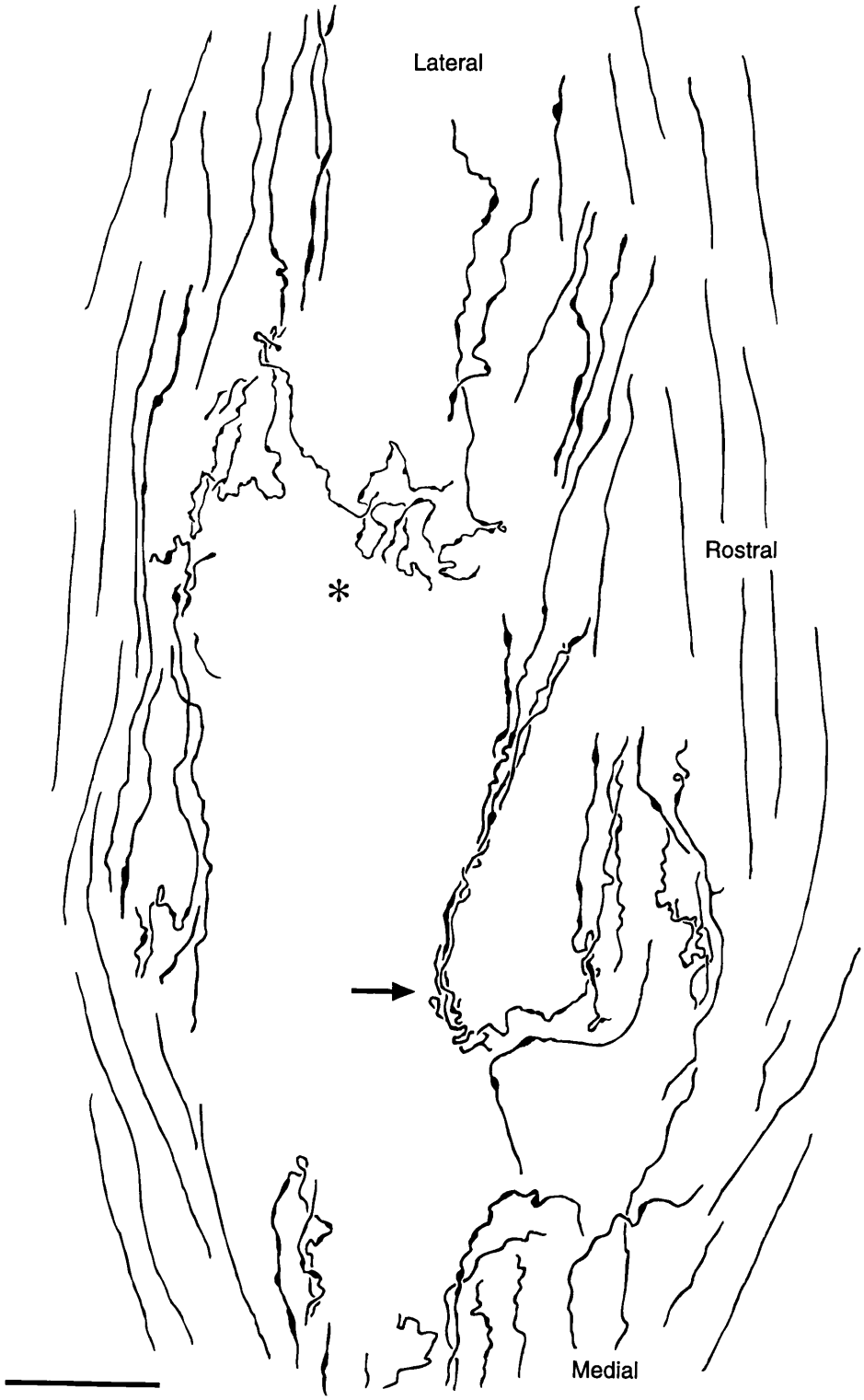
Lateral
Rostral
Medial

Figure 42

A-D Electron micrographs. Examples of degenerating axon terminals (D) making synaptic contact with dendritic spines (P) of neurons in the microtransplant. N, non-degenerating axon terminal. The electron density of the terminals indicates that they originated from host axons cut (in the contralateral fimbria) 3 days before sacrifice. E15 hippocampal microtransplant, 8 weeks survival. Scale bar, 1µm.

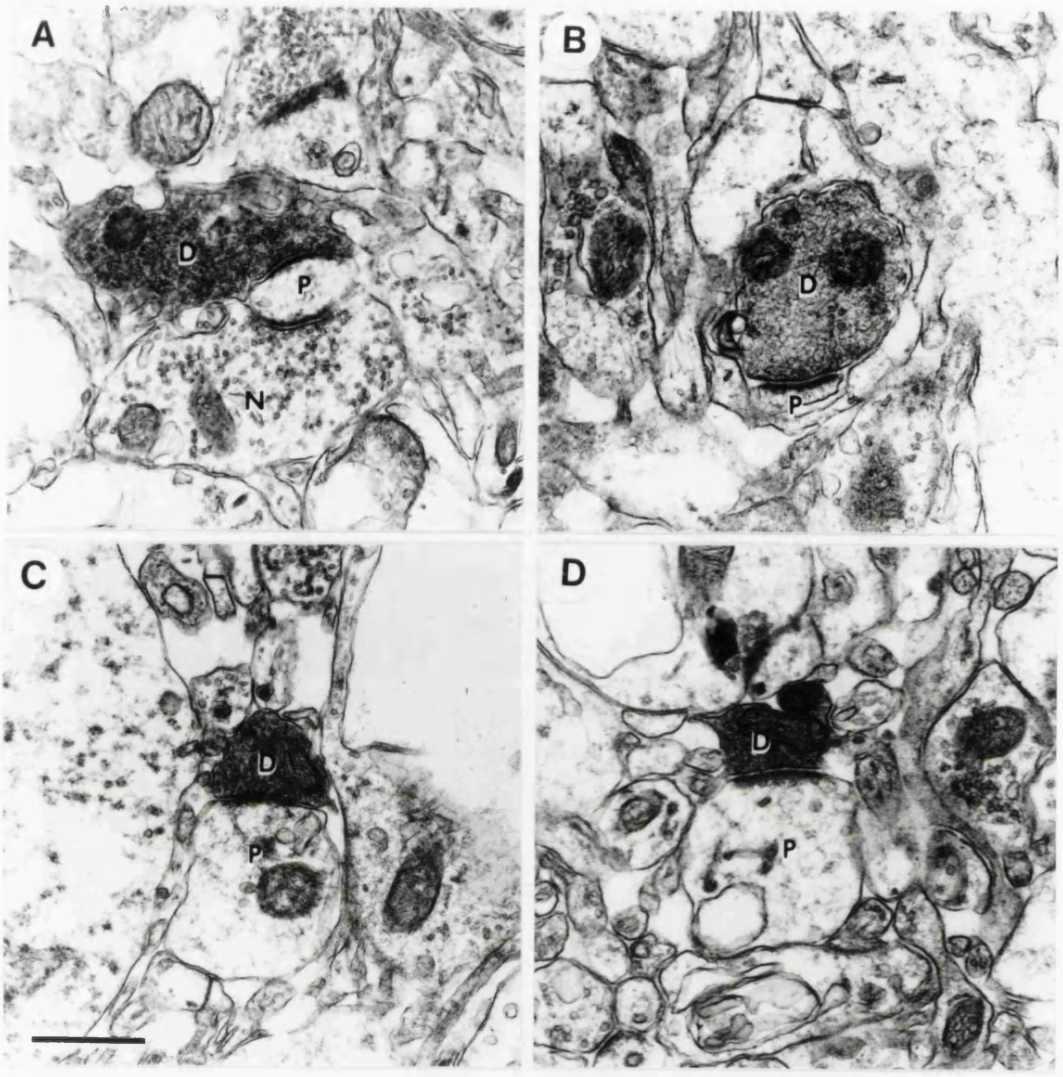
A
D
P
N
B
D
P
C
D
P
D
D
P

caused synapses which the axons had previously formed within the microtransplants, to degenerate and become electron dense when processed for electron microscopy (Fig. 42 A-D). The degenerating synapses were found exclusively on the dendritic spines of transplanted neurons.However, the degenerating synapses were relatively few in number, with only 1 or 2 found on average per grid square.

DISCUSSION

Light microscopic tracing with the orthograde axon tracer biotin dextran, showed that the host fimbrial axons readily crossed the interface from the host tract into the hippocampal microtransplants and formed complex arborisations. Electron microscopy after lesions of the commissural component of the host fimbria showed that some of these adult host fibres formed synapses, on dendritic spines of the transplanted embryonic neurons.

4,4,1 Origin of host fimbrial axons

The main projection fibres in the fimbria arise from the hippocampal pyramidal neurons of field CA3, the hilar pyramidal neurons of the dentate gyrus and neurons of the subiculum and septum (Swanson and Cowan, 1977; Swanson *et al.,* 1980, 1981). Wyss *et al.,* (1980) carried out a series of ^{3}H-amino acid injections into the different cytoarchitectonic fields of the hippocampus, subiculum and septum to determine the topographic localisation of their axons as they pass in the fimbria and ventral hippocampal commissure. Those fibres in the fimbria running dorsally, adjacent to pyramidal field CA3 were termed 'proximal' and those ventrally, towards the tip of the fimbria close to the *stria terminalis* termed 'distal'. The overall distibution is summarised in *Fig. 6* of their paper and shows that fibres in the fimbria and ventral hippocampal commissure are roughly topographically segregated. Axons from more rostral hippocampal and subicular areas (defined as closer to the septum) and those of the septum itself, are confined to the more proximal fimbria. Axons arising

from more caudal areas of the hippocampus and the subiculum are situated in the progressively more distal fimbria. This pattern of axon distribution is also true of axons coursing through the ventral hippocampal commissure. Therefore, from their localisation, it would be predicted that the hippocampal microtransplants grafted to the rostral/proximal region of the host fimbria would have been most likely to be innervated by CA3/CA4 pyramidal neuron axons from the rostal hippocampal and subicular areas and axons of septal origin. However it is also possible that the transplant may have stimulated the ingrowth of collaterals from axons situated in the more distal fimbria as not only cut, but also uncut axons could be seen to respond to the hippocampal microtransplants.

4.4.2 Axon growth stimuli and terminal field formation

The response of uncut axons indicates that the stimulus of axotomy is not essential for adult axon growth, but that the embryonic hippocampal tissue alone provided a sufficiently powerful growth stimulus to induce terminal formation even from uncut fimbrial axons. Thus adult hippocampal axons can not only innervate embryonic target tissue transplanted into host neuropil areas but are also able to initiate terminal sprouting from *en passant* axonal segments which are normally totally confined within the glial framework of central myelinated fibre tracts. What positive growth stimuli might the microtransplanted embryonic hippocampal neurons and glia be presenting to the adult tract axons to induce such ingrowth and terminal field formation?

4.4.2.1 *Chemotropic stimuli*

Cajal, (1893) was the first to propose that axonal growth cones might be guided by gradients of diffusible target derived attractants (chemotropism) and a century later there is evidence from *in vivo* and cell culture experiments that some growth cones can exhibit chemotropic behaviour (Heffner *et al.,* 1990; Lumsden and Davies, 1983, 1986; Sato *et al.,* 1994; Shirasaki *et al.,* 1995; Zheng *et al.,* 1995). In an elegant experiment, O' Leary *et al.*, (1990) disrupted the migration of basilar pontine neurons (the target cells for corticospinal axon collaterals) with X -ray irradiation of foetal rats. Basilar pontine neurons were subsequently ectopically positioned later in development but were still innervated by corticospinal axon collaterals which did not project to the normal position of the basilar pons . This result strongly suggests that the corticospinal axon collaterals are induced to innervate the basilar pons by some form of chemotropic stimulus, however the chemotropic factor released by the basilar pons has not as yet been identified.

The first molecule investigated for chemotropic effects on axon growth was nerve growth factor (NGF), the founder member of the neurotrophin family of molecules. Levi-Montalcini and colleagues showed that sympathetic axons grew abnormally into the CNS of the rat after intracerebral injection of nerve growth factor (Menesini-Chen *et al.,* 1978). Gunderson and Barrett, (1979) demonstrated with sequential photography in tissue culture, that regenerating E7-E12 chick spinal sensory axons were induced to turn in response to a steep gradient of NGF emanating from a micropipette. The axonal growth cones

were shown to follow the micropipette as it was repositioned in the culture medium. However the physiological significance of this result is unclear, as later studies have shown that NGF first appears in target tissues at the same time that growing axons arrive at the targets (Davies *et al.,* 1987).

Fibroblasts transfected with constructs directing high levels of secretion of NGF, promote adult axon sprouting and ingrowth when transplanted in the cerebral cortex (Kawaja and Gage, 1991) and spinal cord (Tuszynski *et al.,* 1994) of adult rats, and axon regeneration when inplanted into the lesioned septo-hippocampal system (Kawaja *et al.,* 1992). Hagg and Varon, (1993) infused NGF into the rostral lateral ventricle of adult rats and induced a positive chemotropic response from previously cut axons of the dorso-lateral septum.

Hippocampal neurons and astrocytes produce NGF (Mufson *et al.,* 1994; Yoshida and Gage, 1991) as well as a variety of other growth factors eg. Brain derived neurotrophic factor (BDNF, Zafra *et al.,* 1992), Neurotrophins 3 and 4/5 (NT3, NT4/5, Lindholm *et al.,* 1994), basic fibroblast growth factor (bFGF, Gomez-Pinilla *et al.*, 1992), ciliary neurotrophic factor (CNTF, Rudge *et al.,* 1994). It is therefore possible that the hippocampal microtransplants might have exerted an NGF mediated neurotropic effect on the host fimbrial axons, especially those originating in the septum.

That hippocampal pyramidal neurons have been induced to grow axons into the grafts is confirmed by the presence of their degenerating synapses found in the microtransplants after a contralateral fimbria lesion. However the possible chemotropic attraction of these axons by NGF or any of the other hippocampal derived growth factors remains to be investigated.

There is evidence that neurotransmitters such as acetylcholine can also act as growth cone chemoattractants in tissue culture (Zheng *et al.,* 1995) or conversely induce growth inhibition or retraction of neurites (Haydon *et al.,* 1984; Mattson *et al.,* 1988; Lipton *et al.,* 1988). However, chemotropism of adult fimbrial axons by neurotransmitters also remains to be investigated.

4.4.2.2 *Growth promoting substrate molecules*

Adult axon contact with growth promoting substrate molecules (Reichardt *et al.,* 1990) may also stimulate their growth from the tract environment into the intratract microtransplant neuropil.

(A) *Growth promotion by axon fasciculation*

Developmental studies have shown that axon fasciculation is associated with neurite extension (Dodd and Jessell, 1988; Jessell, 1988; Rutishauser and Jessell, 1988). In culture, video microscopic analysis showed an increase of axon growth from pontine explants when axons fasciculated with each other (Baird *et al.,* 1992). Embryonic axons are known to express several classes of growth promoting neural adhesion molecules, such as the N-CAM and L1

families of glycoproteins (Doherty and Walsh, 1992) and it is possible that the adult fimbrial axons have been stimulated to grow into the grafts by fasciculation with the hippocampal donor axons leaving the transplant.

(B) *Astrocytic growth promoting substrate molecules*

Immature astrocytes have been shown to support axon growth *in vivo*, (Kliot *et al.,* 1990; Smith *et al.,* 1986; Wunderlich *et al.,* 1994), and in tissue culture in contrast to more mature or reactive astrocytes (Fawcett *et al.,* 1989; Geisert and Stewart, 1991; Noble *et al.,* 1984; Rudge *et al.,* 1989; Smith *et al.,* 1990; Wang *et al.,* 1994). Immature astrocytes are known to express cell surface extracellular matrix and cell adhesion molecules such as laminin, fibronectin, heparin sulphate proteoglycan (HSPG), N-CAM and N-cadherin that promote neurite outgrowth from CNS neurons (Chiu *et al.,* 1986; Lander *et al.,* 1985; Letourneau *et al.,* 1994; Liesi *et al.,* 1983; Matthiessen *et al.,* 1989; Neugebauer *et al.,* 1988; Tomaselli and Reichardt, 1988; Tomaselli *et al.,* 1988). A number of recent papers have suggested that growth promoting substrate molecules direct axon growth via 'instructive influences' (Burden-Gulley *et al.,* 1995; Lemmon *et al.,* 1992) initiated via filopodial signalling (Gomez and Letourneau, 1994; Kuhn *et al.,* 1995) rather than by differential adhesion guidance of the growth cone (haptotaxis; Collins, 1978; Collins and Garrett, 1980; Letourneau, 1975)..

Smith *et al.*, (1990), showed that antibodies to NCAM, G4 / L1 and the integrin B1 receptor significantly reduced the axonal outgrowth of rat cortical and chick

retinal neurons on purified cultures of immature astrocytes and that the expression of many growth promoting cell surface extracellular matrix and cell adhesion molecules is downregulated as astrocytes mature (Smith *et al.,* 1993). However astrocyte promotion of neurite growth may not be related to expression of laminin or fibronectin. Blockade of the laminin/fibronectin receptors by monoclonal antibodies that inhibit neurite growth on laminin alone, does not diminish neurite growth on astrocytes (Tomaselli *et al.,* 1986)).

Furthermore, whilst astrocytes can clearly support the axonal growth of more mature CNS neurons, it has been suggested that laminin only promotes neurite growth from early embryonic and not late foetal or post-natal CNS neurons (Cohen *et al.,* 1986; Hall *et al.,* 1987). However integrin receptors for laminin have been shown to be reexpressed on regenerating adult retinal ganglion axons (Knoops *et al.*, 1993)

4.4.3 Elongative tract axon growth versus terminal field formation

A number of studies have suggested that the factors controlling rapid elongative tract growth of axons are different to those initiating entry into neuropil. In a recent developmental study of the corpus callosum, time lapse video microscopy was used to observe the dynamic behaviour of individual Di-I (1,1' dioctadecyl-3,3,3',3'-tetramethylindocarbocyanine perchlorate) labelled callosal growth cones extending in living brain slices from neonatal hamster sensorimotor cortex (Halloran and Kalil, 1994). On nearing target neuropil, the formerly rapidly growing callosal axons were seen to slow, pause and their growth cones display repeated cycles of collapse, withdrawal and resurgence.

Extension of axons into the overlying cortical targets occurred by collateral axon growth rather than by turning behaviour of the primary growth cones.

Integrin receptors have been shown to be downregulated on embryonic retinal ganglion cell axons when they reach the optic tectum (Cohen *et al.,* 1989) suggesting that different guidance cues are used for target recognition, compared to elongative tract growth, and receptors are switched accordingly. In tissue culture experiments, Baird *et al.,* (1992) have noted increased growth of axons from pontine explants grown in contact with cerebellar astroglial cells or other pontine axons but addition of cerebellar granule neurons (the axons normal target) arrested axon growth. Video microscopy showed that inhibition of pontine axon growth was mediated by contact with the cerebellar granule neurons. Baird and colleagues suggested that axoaxonal and axoglial contacts promoted elongative axon growth whilst contact with target neurons slows axon growth, as a possible prelude to synapse formation.

The embryonic hippocampal microtransplants of the present study not only presented axon growth promoting factors but also correctly matched target neurons, which might have exerted an inhibitory influence on growth of the adult fimbrial axons in order to initiate synapse formation. Although a number of adult axons in the present series of microtransplants were seen to run into the transplant neuropil and exit into the distal tract, I was not able to determine if these were truly newly growing axons, or simply undamaged host axons

engulfed by passive spread of the transplant suspension after microinjection (Olby *et al.,* 1995), and/or transplant growth.

4.4.4 Adult axons vary in their ability to regenerate

In the present series of intrafimbrial microtransplants, I have not carried out a systematic study to identify the types of adult axons responding to the grafts. However in a number of instances it has been demonstrated that axons of different adult neurons vary in their ability to respond to peripheral nerve grafts or transplanted embryonic nervous tissue (for review, see Fawcett, 1992). In a recent study by Rossi *et al.,* (1995) in the adult cerebellum, it was shown that cut Purkinje cell axons fail to regenerate into a solid graft of early embryonic cerebellum placed at the lesion site. This is in contrast to the similarly cut olivocerebellar axons which readily innervated the same transplant. In this case the presence of embryonic tissue alone seems to be an insufficient stimulus to promote Purkinje cell axon growth. Similarly, embryonic neocortical tissue grafted to the neocortex grey matter of adult rats is innervated by basal forebrain cholinergic fibres and not by local axons originating from ventrobasal thalamic neurons (Clinton and Ebner, 1988). However, the ventrobasal thalamic axons can be induced to grow into the neocortical tissue after lesions of the basal forebrain (Höhmann and Ebner, 1988), or lesions of the infraorbital nerve (Erzurumlu and Ebner, 1988). These experiments highlight the important fact that adult axons not only vary in their ability to respond to factors presented by embryonic tissue but that this ability can be modified by removing

competing/controlling fibre systems, or by inhibition of growth by presynaptic inputs.

4.4.5 Astroglial alignment

A number of groups have commented on a reduction of scar tissue formation after transplantion of solid pieces of embryonic tissue into lesions of white matter tracts, with some areas of the transplant/host interface having aligned astroglial processes (Hausmann *et al.,* 1989; Houle, 1992; Jakeman and Reier, 1991; Reier, 1986; Smith *et al.,* 1986). The hippocampal microtransplants used in the present study contained similar proportions of embryonic neurons and glia to the above solid transplants and therefore the apparent lack of any observable scar formation at the transplant/host interface (described in *Chapter III*) is undoubtedly due to the atruamatic nature of the transplantation method. It is possible that the aligned nature of the interface alone was sufficient to promote cut adult axon growth into the microtransplants. However it must be remembered that the interface presented by the microtransplants, is made up of not only adult tract glia but growth promoting donor embryonic astrocytes and precursors. The hypothesis that cut adult axon access to an aligned adult tract glial pathway may be sufficient to allow regeneration is tested in *Chapter V.*

CHAPTER V

Regeneration of cut adult axons is blocked even in the absence of glial scarring

INTRODUCTION

Although cut axons fail to regenerate in damaged fibre tracts in the adult CNS, they are able to grow for long distances if provided with a permissive environment, such as a graft of peripheral nerve (Richardson *et al.,* 1980; Vidal-Sanz *et al.,* 1987). This suggests that there is some inhibitory factor preventing their regeneration in damaged adult tracts. A rapidly expanding body of evidence shows that during development, axons are guided to their correct pathways by repulsive factors (Dodd and Schuchardt, 1995; Luo and Raper, 1994). This raises the possibility that comparable repulsive mechanisms may also be activated in the adult CNS after injury (Schwab *et al.,* 1993).

The current success in identifying the mechanisms of axon guidance in development rests on the basic anatomical groundwork put into identifying the cellular elements expressing the regulatory factors. What might be the comparable cellular elements giving rise to a repulsive influence in the much more complex environment of the damaged adult CNS? Surprisingly, there is little information about the arrangement of the glial elements that make up the environment of axons in adult central tracts (Suzuki and Raisman, 1992). Lesions of CNS tracts not only cut axons, but also cause a local area of glial cell death, resulting in major disruption of the overall glial framework, and triggering the formation of a glial scar, which has been proposed as a major impediment to axonal regeneration in the adult mammalian CNS (Berry *et al.,*

1983; Li and Raisman, 1995; Kruger *et al.,* 1986; Reier *et al.,* 1983a,b, 1986; Reier and Houle, 1988; Stensaas et al., 1987).

5.1.1 Microtransplants

In *Chapter III,* I used a microtransplantation technique to inject suspensions of embryonic neurons and glia into adult tracts (see also Davies *et al.,* 1993, 1994; Li and Raisman, 1993). Under these circumstances, the disturbance to the glial framework was minimal, there was no scarring, the glial processes of the graft and host became aligned across the interface, and the axons of the embryonic neurons extended rapidly for long distances along the host tract. In *Chapter IV*, I showed that the aligned astroglial interface also permitted the ingrowth of adult tract axons into the microtransplants. These observations raise the question of whether the sprouts formed by cut adult axons might also be able to extend along adult fibre tracts if it were possible to avoid inducing a glial scar, and thus provide the axons with physical access to a normally aligned glial framework.

5.1.2 Microlesions

To test this hypothesis, lesions of adult axons were performed using a microlesion approach designed to minimise disturbance to the tract vasculature and glia. The system of p75 positive fibres which project caudally through the cingulum (Peterson, 1994) was selected. This system has the advantage that the fibres all travel in one direction, and that although the microlesion technique only cuts a small proportion of the cingulate axons, the axotomy causes an

enhancement of p75 immunoreactivity making it possible to identify changes in the morphology of individual cut axons and their sprouts.

5.1.2.1 *p75 receptor*

The p75 receptor or low affinity NGF receptor (Chao *et al.,* 1986; Radeke *et al.,* 1987), herein known as the low affinity neurotrophin receptor (LANR), is a transmembrane receptor of 75 kD molecular weight with structural homology to the tumour necrosis factor (TNF) family receptors. p75 is expressed on a number of tissues during development and into adulthood (Bothwell, 1991), and immunohistochemistry for the receptor selectively stains a variety of CNS neurons and glia with marked expression in cholinergic neurons of the basal forebrain (Bothwell, 1991; Kiss *et al.,* 1988; Koh and Loy, 1989; Koh *et al.,* 1989; Pioro and Cuello, 1990a,b; Yan and Johnson, 1989; Woolf *et al.,* 1989). The p75 receptor which binds all the known neurotrophins such as NGF, BDNF, NT3 and NT4/5 (Rodriguez-Tebar *et al.,* 1990, 1992; Squinto *et al.,* 1991) is thought to act in conjunction with the Trk family of tyrosine kinase receptors, although the exact mode of this association remains unresolved (for a recent review see Chao and Hempstead, 1995).

5.1.2.2 *Tract structure analysis*

Electron microscopy and immunohistochemistry (for the complement 3 receptor and astroglial intermediate filaments GFAP and vimentin) were used to monitor the influx of macrophages, the concurrent changes in the tract microglial, and

the alignment of astrocytic processes making up the micro-environment of the cut axon tips at the lesion site.

5.2.1 Microlesions

Under tribromoethanol anaesthesia (20 mg/100 gm body weight, i.p.), in adult female rats (body weight 180-220 gm, of a locally maintained AS strain) a glass micropipette with a bevelled tip of external diameter about 70 µm, was stereotaxically inserted through a burr hole in the skull along a vertical track at 0.5 mm rostral and 0.6 mm lateral to the bregma (with the head held in the flat skull position) to a depth of 3.9 mm ventral to the bregma in the left hemisphere of the brain. The micropipette passed tangentially through the deeper layers of the cingulate cortex (at the rostro-caudal level of the septal nuclei), severing a narrow band of fibres in the cingulum, and penetrating a further 0.3 mm ventrally into the corpus callosum (Fig. 43). The micropipette was slowly withdrawn over a period of about 30 seconds. After post-operative survivals varying from 12 hours to 1 month (Table 3), 88 operated and 4 control unoperated animals were deeply anaesthetized (0.2 ml Expiral i.p.) and perfused transcardially with appropriate fixatives (see below).

5.2.2 Immunohistochemistry

5.2.2.1 *p75 (low affinity neurotrophin receptor)*

Animals were transcardially perfused with 100 ml 0.1 M PBS followed by 500 ml of 4% paraformaldehyde in 0.1 M PBS. The brains were dissected out, fixed for a further 6 hours in 4% paraformaldehyde in 0.1 M PBS, and sectioned at 100 µm intervals in the sagittal plane on a Vibratome (General Scientific, UK).

Figure 43

Schematic representation in sagittal (**A**) and coronal section (**B**) of the lesion track of the micropipette (P). The neurons of the cholinergic basal forebrain (CBF, lying lateral to this plane of section in the horizontal limb of the diagonal band (Peterson, 1994); give rise to the p75 positive axons (ax) passing over the rostrum (r) of the corpus callosum (CC), and back through the cingulum (Cg). (a) anterior commissure; (c) head of caudate nucleus; (ctx) cortex; (f) fimbria; (h) hippocampus; (s) septum;(t) thalamus; (v) lateral ventricle.

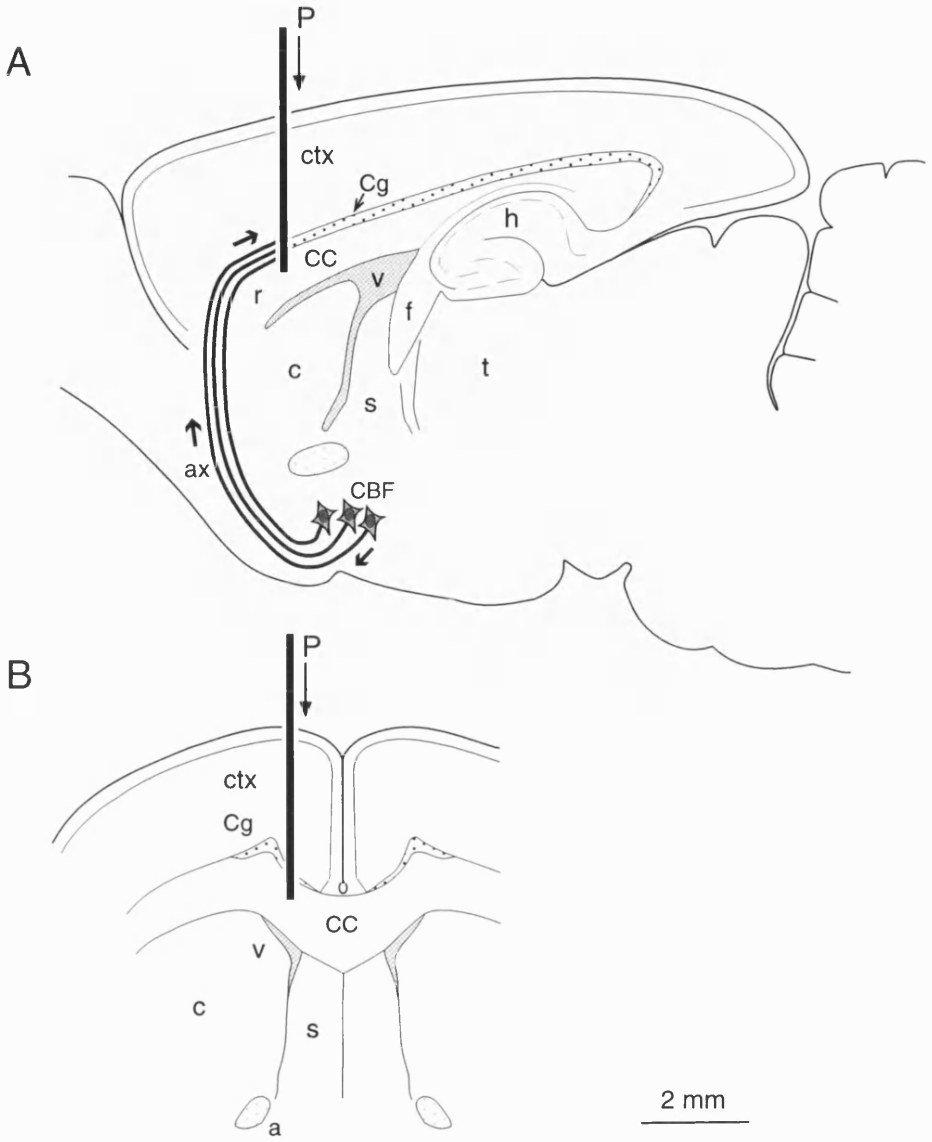
A
P
ctx
Cg
h
CC
v
r
f
c
t
s
ax
CBF
B
P
ctx
Cg
CC
v
c
s
a
2 mm

This thickness and plane of section have the effect of including the longest possible continuous length of cingulate axons in the sections.

Free floating sections were collected in 0.1 M PBS, incubated for 2 min in 96% ethanol (to aid antibody penetration), given several changes of PBS over 30 min, 30 min in a 10% solution of dried milk in PBS (as a source of non-specific protein), and then incubated overnight at 4°C in 1:100 monoclonal anti-p75 antibody (Boeringher-Mannheim) in 10% dried milk in PBS, followed over 3 h by several changes of PBS, 1 h in 1:300 biotinylated horse anti-mouse IgG (Vectastain, Vector) with 1% BSA (bovine serum albumin) in PBS at room temperature, several washes of PBS for 2 h, 1 h in ABC (Vectastain), several washes of PBS for 3 h, and the reaction product developed in 50 mg/100 ml diaminobenzidine (DAB) and 0.006% hydrogen peroxide in phosphate buffer with 10 mM imidazole at pH 5.8 for 3 min. The sections were mounted on gelatin coated slides, air dried, dehydrated, cleared with Histoclear (National Diagnostics, Aylesbury, UK), and mounted in a mixture of dibutyl phthalate, polystyrene and Histoclear. Camera lucida drawings were used to record the morphology of the cut axon tips.

5.2.2.2 *OX42 and GFAP and vimentin immunohistochemistry*

Animals were perfused with 200 ml 0.1 M PBS. The brains were removed and rapidly frozen in crushed dry ice. Cryostat sections were cut at 10 µm in the sagittal plane and collected on gelatin coated slides. Sections for OX42 immunohistochemistry were air dried for 1 h and lightly fixed for 5 min in 96%

ethanol. Adjacent sections for GFAP and vimentin immunohistochemistry were post-fixed for 30 min in 5% acetic acid in 96% ethanol. All sections were then washed for 30 min in several changes of 0.1 M PBS, blocked for 30 min in a 1% dried milk solution in 0.1 M PBS, and incubated overnight at 4°C in 1:200 OX42 (Serotec, Oxford), or 1:1000 monoclonal anti-GFAP antibody (Amersham, Bucks, UK), or 1:100 monoclonal anti-vimentin antibody (Amersham), with 1% dried milk solution in 0.1 M PBS, washed for 30 min in several changes of 0.1 M PBS, reacted for 30 min in 1:300 biotinylated horse anti-mouse secondary IgG with 1% BSA in PBS at room temperature, washed for 30 min in several changes of 0.1 M PBS, treated with ABC for 30 min, and washed for 30 min in several changes of 0.1 M PBS. The reaction product was developed for 5 min in 1% nickel chloride in distilled water, followed by DAB (as above), and the sections counter-stained with aqueous thionin, dehydrated, and cleared with Histoclear.

5.2.3 For staining all cingulate axons

10µm cryostat sections were cut in the sagittal plane so as to give the longest length of cingulum in each section from PBS perfused rapidly frozen brains. Sections were collected on to gelatin coated slides, dried, fixed by immersion in Carnoy's fluid, and stained with silver (Palmgren, 1948) see *Chapter II* for details.

5.3.4 For electron microscopy

Animals were perfused with 100ml PBS and then a mixture of 1% paraformaldehyde and 1% glutaraldehyde in 0.1 M PB at pH 7.3. The brains

were removed and sagittal 200 µm Vibratome sections taken through the lesion. Under a dissecting microscope, the lesion area was cut out, post-fixed for 1.5 h in 2% osmium tetroxide, dehydrated in graded alcohols over 3 h and flat embedded in Epon embedding resin (TAAB Laboratory Equipment Ltd, Reading, UK) on glass slides coated with a mould-releasing compound (Formen-Trenmittal Hobby Fluid, Hobby Wholesale, London SW27 0HH). Semithin sections were stained with methylene blue and Azur II, and ultrathin sections with uranyl acetate and lead citrate.

Table 3

Numbers of animals at the different survivals post microlesion.

Survival	*Number*
normal	4
12 hours	6
1 day	8
2 days	12
3 days	6
4 day	23
6 days	3
8 days	10
14 days	9
18 days	2
1 month	9
Total	92

RESULTS

5.3.1 Normal cingulum

5.3.1.1 *Axons*

Staining by reduced silver, methylene blue and electron microscopy show that, at the level where the lesions were made, the cingulum consists of a compact bundle of straight, parallel, axons of uniform, medium diameter. Only a small proportion of the cingulate axons were p75 immunoreactive. The entire course of these axons (Fig. 43A) could be traced from their p75 positive cells of origin in the horizontal limb of the diagonal band (Peterson, 1994), dorsally over the rostrum of the corpus callosum, and turning back caudally into the cingulum, with occasional collateral branches directed dorsally to the overlying cortex (Figs. 43, 44A).

5.3.1.2 *Glia*

The regular arrangement of the astrocytic, oligodendrocytic, and microglial cell bodies, and their processes, which has been described in the fimbria (Suzuki and Raisman, 1992) and tracts of the spinal cord (Li and Raisman, 1994), also occurs in the cingulum (*Chapter III*; Davies *et al.,* 1994). Thionin staining shows that the glial cell bodies are arranged in unicellular rows aligned along the longitudinal (axonal) axis of the tract and regularly spaced throughout its cross section. The astrocytes lie singly, separated by around ten contiguous oligodendrocytes, and all three types of glial cells generate an interwoven array of parallel processes along the longitudinal axis of the tract.

Figure 44

Normal structure of the cingulum bundle. **A**, p75 immunoreactive axons. **B**, GFAP immunoreactive astrocytes. **C**, OX42 immunoreactive microglia. The longitudinal alignment of the astrocytic processes and microglial cell bodies in the cingulum (Cg) contrast with the cingulate cortical neuropil lying dorsally (Ctx), and the corpus callosum ventrally (CC). Scale bars, 50 μm.

For this and subsequent figs: rostral to the left, caudal to the right.

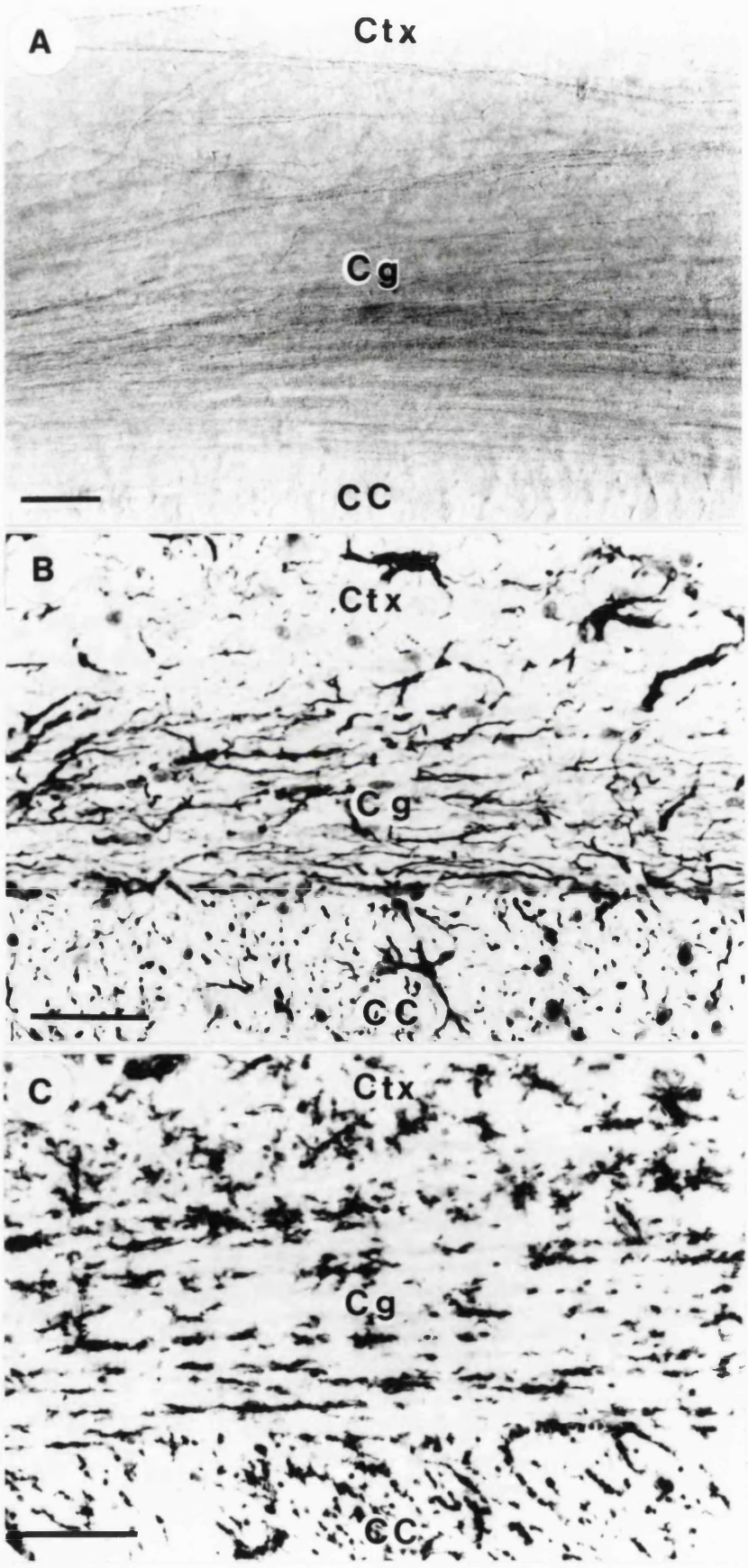
A
Ctx
Cg
CC
B
Ctx
Cg
CC
C
Ctx
Cg
CC

In the acid-alcohol fixed material the cell bodies and processes of the astrocytes in the normal, unoperated tract show moderate immunoreactivity to the monoclonal anti-GFAP antibody (Fig. 44B), but there is little detectable vimentin immunoreactivity. OX42 immunohistochemistry, shows that the microglia are interspersed regularly throughout the tract (Fig. 44C) and, like astrocytes, they also lie singly and generate arrays of longitudinal processes (Fig.47A; see also Perry *et al.,* 1985).

5.3.2 Microlesions

The microlesions did not give rise to any appreciable areas of necrotic material, and there was no cavitation. In a few cases there was an occasional row of extravasated red blood cells tracking along the perivascular extracellular space, suggesting that there had been a brief localised break in the wall of a micro-vessel.

5.3.2.1 *1-2 day survival*

(A) *Axons*

The cut p75-positive axons were readily identified by a marked increase in p75 immunoreactivity which extended retrogradely (i.e. in a rostral direction), for 200 - 500 µm from the level of the lesion. The cut axons formed a parallel array (Fig. 45B) occupying a narrow sheet of tissue confined to the 70 µm medio-lateral area directly damaged by the micropipette penetration. The cut ends were irregularly expanded to around 2 µm diameter, with single or multiple terminal or preterminal varicosities of up to 7 - 10 µm. While the p75 positive

axons are only a minor component of the cingulum, electron microscopy of ultrathin sections showed that at the lesion site virtually all the cingulate axons had developed comparable varicosities (Fig. 45A).

(B) *Glia*

Both thionin and OX42 staining showed a mass of densely packed, rounded, 'amoeboid' cells about 10 μm in diameter, occupying and confined to the line of insertion of the micropipette (Fig. 45C). These cells were of a type not found in the normal cingulum. They had a characteristic thick superficial rim of intensely OX42-positive material, surrounding an OX42-negative cytoplasm and a large nucleus. Electron microscopy (Fig. 45D) showed medium dark, finely granular cytoplasm, with the mitochondria packed close to the nucleus, and the cell surfaces extended into short, blunt interdigitating villous processes which presumably account for the thick superficial rims of OX42-immunoreactive material seen in the light microscope. These cells had few of the electron dense or electron lucent cytoplasmic bodies typically found in macrophages in lesions where (unlike the present material), the degree of tissue damage and necrosis leads to considerable amounts of dead material needing to be phagocytosed and digested.

OX42 positive ramified microglia were difficult to distinguish in the dense mass of OX42 positive amoeboid cells in the lesion track, but at the edges of the lesion track, especially caudally, OX42 immunoreactivity showed that the tract microglia were becoming hypertrophic.

Figure 45

Changes at 2 days after operation. **A**, Electron micrograph showing that virtually all myelinated and unmyelinated cingulate axons at the lesion site form varicosities packed with organelles (mitochondria, dense bodies, synaptic vesicles, microtubules and bundles of neurofilaments). **B**, camera lucida drawing of the expanded cut ends of the p75-positive cingulate axons immediately rostral to the lesion track (hatched). **C**, Massed OX42-positive, rounded, 'amoeboid' cells filling the lesion track through the cingulum (Cg) and corpus callosum (CC). **D**, Electron micrograph of an amoeboid cell in the lesion track; characteristically, the mitochondria are packed into a perinuclear zone, and the remaining, moderately electron dense, finely granular cytoplasm is extended into short, blunt, interdigitating villous processes (e.g. asterisks). **E**, Electron micrograph showing massive, watery-pale cytoplasmic swelling of an astrocyte (a) adjacent to a blood vessel (bv); (n) nucleus; (p) electron dense perivascular cell. Scale bars, 5 μm (A,D,E), 50 μm (B,C).

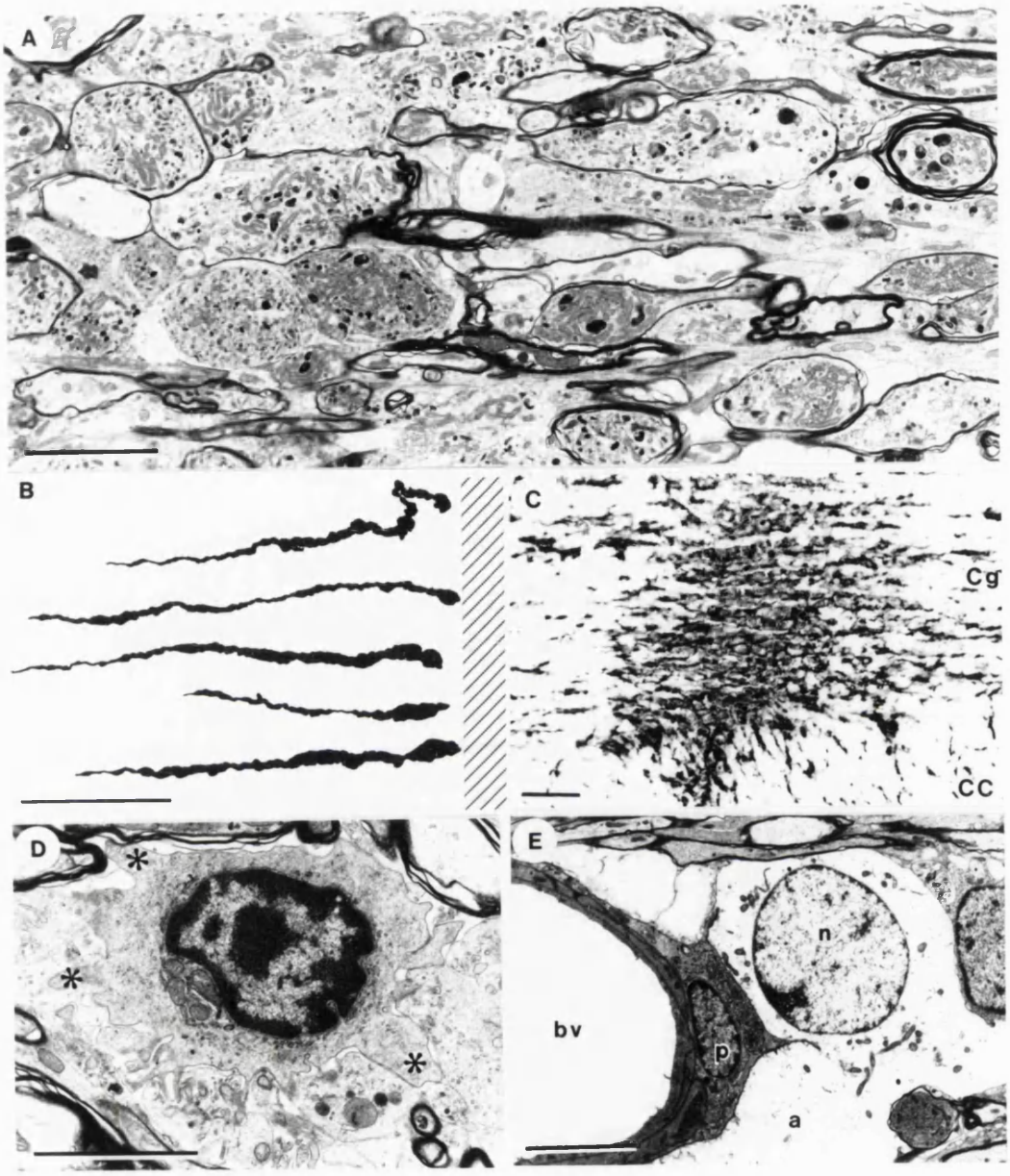
A
B
C
Cg
CC
D
E
n
bv
p
a

There was a consistent decrease in GFAP immunoreactivity of the astrocytes in the lesioned tract area, but as yet no detectable vimentin immunoreactivity. Semi- and ultra-thin sections, however, showed that the astrocytes had already reacted, with marked cytoplasmic swelling, especially in the perivascular regions (Fig. 45E).

5.3.2.2 *4 day survival*

(A) *Axons*

p75 immunostaining showed that the cut axons had now developed short sprouts for up to 500 µm proximal to the cut. The greatly expanded cut ends of the axons (Fig. 46A,B) were still largely aligned with the micropipette track, but some had already started to make hook-like turns.

(B) *Glia*

Compared with 2 days survival time, thionin staining (Fig. 46C) showed a marked reduction in hypercellularity in the cingulum. This was due to the disappearance of the rounded, amoeboid cells from the pipette track. The tract showed a normal, longitudinal unicellular alignment of the rows of tract glial cell bodies, although the cells tended to be more densely packed in the region of the lesion.

OX42 immunohistochemistry confirmed that the rounded OX42-positive amoeboid cells had disappeared from the cingulum. The hypertrophy and increased OX42 immunoreactivity of the resident tract microglia had reached it's peak at this time.

Figure 46

Changes at 4 days after operation. **A**, Photomicrograph, and **B**, camera lucida drawing to show the morphology of the expanded cut ends of the p75 positive cingulate axons at the lesion site (hatched in B). **C**, the rows of cingulate tract glial cell bodies are more densely packed along the line of the lesion (arrowheads), but the previous dense mass of amoeboid cells in the lesion track through the cingulum has disappeared, although remaining in the overlying cortical neuropil; thionin stain. **D**, A flare of enhanced OX42 immunoreactivity in the population of resident cingulate ramified microglial cells extending from the lesion track (arrowheads) in a caudal direction (arrows) along the beam of orthograde degenerating axons. **E**, **F**, responses in astrocytes showing enhanced immunoreactivity for vimentin (**E**), and GFAP (**F**). (CC) corpus callosum; (Cg) cingulum; (Ctx) cortex. Scale bars, 50 μm.

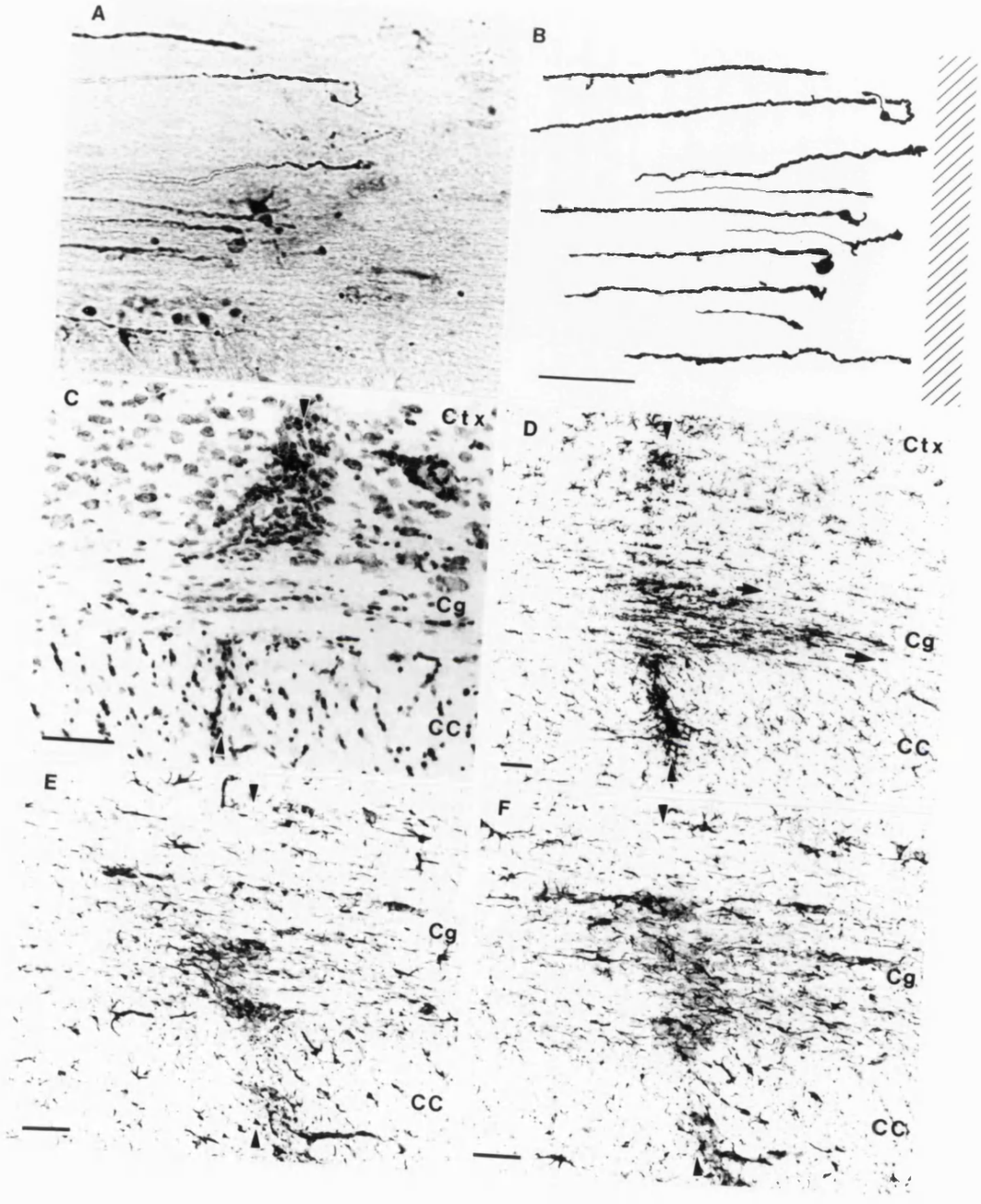
A
B
C
Ctx
Cg
CC
D
Ctx
Cg
CC
E
Cg
CC
F
Cg
CC

Even though greatly thickened, the microglial processes maintained a parallel longitudinal orientation in the cingulum (Fig. 47B), and individual processes could be traced for considerable distances from the cell body. This hypertrophic response extended caudally for 500 - 700 µm from the lesion - i.e. along the beam of orthograde degenerating axons (Fig. 46D).

At the 4 day survival time, the astrocytes at the lesion site also reached a peak of hypertrophy and enhancement of both vimentin and GFAP immunoreactivity (Fig. 46E,F).

5.3.2.3 *8 day survival*

(A) *Axons*

p75 immunostaining of the cut axons (Figs. 48, 49A) showed that the side branches tended to be longer, and the large terminal expansions of the cut main stems had become more complex, with recurved segments, some of which now gave rise to short sprouts extending back through the tract. As at earlier survival times, neither the sprouts nor the main stems of the axons had advanced across the lesion site, nor was there any appreciable retraction from it.

(B) *Glia*

The glial cell bodies remained in normally spaced longitudinal rows, and their numbers now seemed little different from normal (Fig. 49B). Compared with earlier times, there was a marked reduction in OX42 immunoreactivity in the tract (Fig. 49C). The microglial longitudinal processes were normally aligned.

Figure 47

OX42 immunostaining to show a normal resident cingulate ramified microglial cell from an unoperated animal (**A**), contrasted with (**B**) a group of hypertrophic ramified tract microglia (such as shown in *Fig. 46D*) at the lesion site after 4 days. Scale bar, 20 μm.

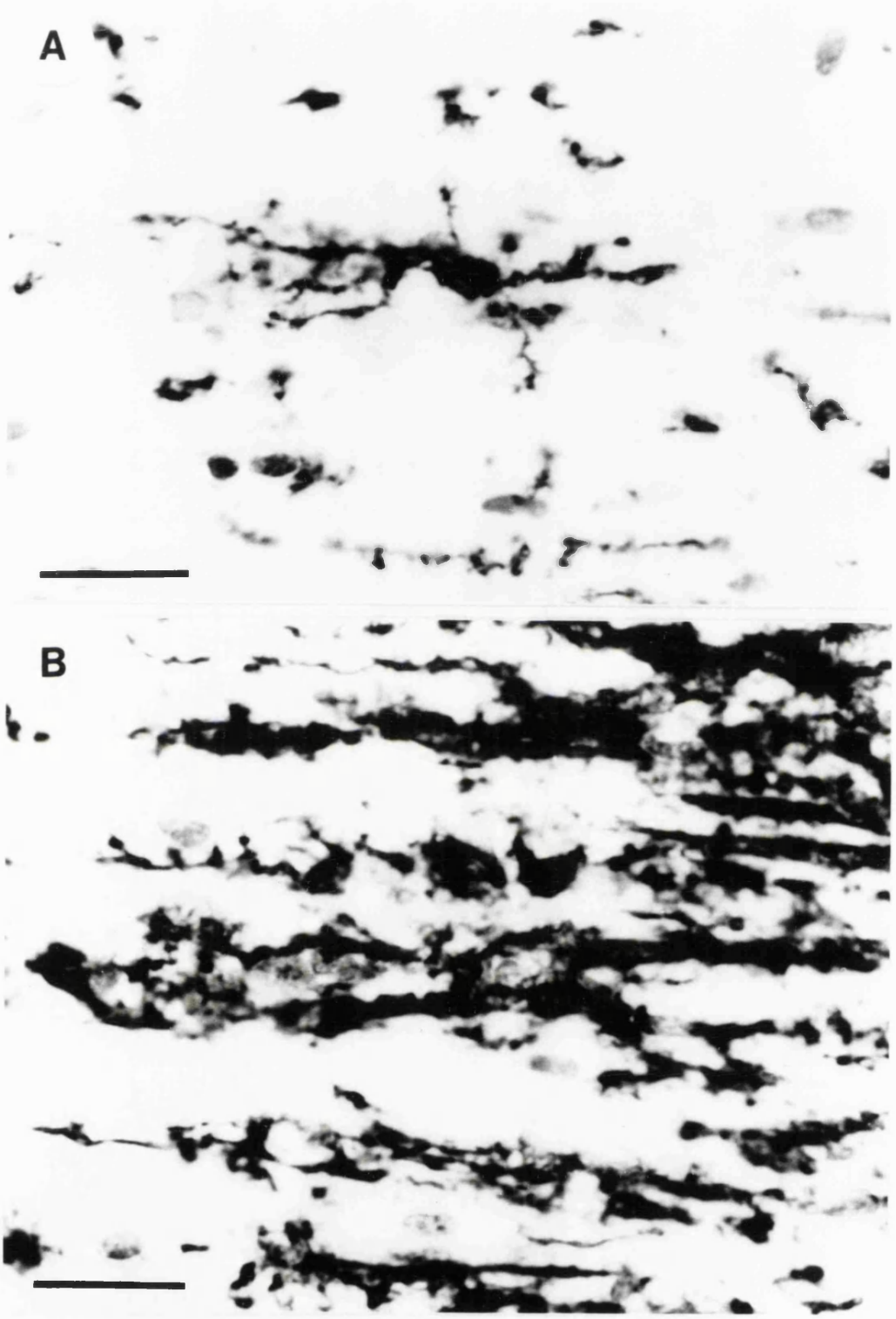
A
B

Figure 48

Camera lucida drawing (from *Fig. 49A*) to show the morphology of the terminal expansions and side branches of the cut p75 positive cingulate axons at 8 days after operation. Hatched area, lesion. Scale bar, 50 µm.

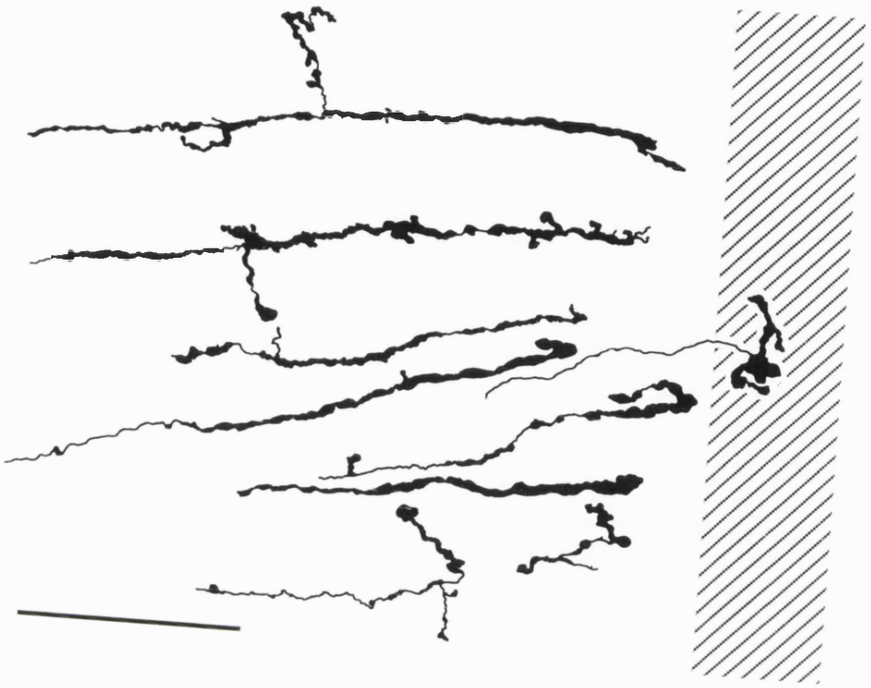

Figure 49

Changes at 8 days after operation. The cingulum (Cg) runs longitudinally through the middle third of the micrographs. **A**, Terminal expansions and side branches of the cut p75 positive cingulate axons (see camera lucida drawing in *Fig. 48*). **B**, Thionin stain, **C**, OX42 immunostain, and **D**, GFAP immunostain show that the arrangement of the cingulate glia is by now little different from the normal, unoperated tract illustrated in *Fig. 44.* Along the former pipette track (arrowheads) through the cortical neuropil dorsal to the cingulum, and to a lesser extent in the corpus callosum, ventral to the cingulum, the OX42 immunostain shows that there is still appreciable hypertrophy of microglia. Scale bar, 50 μm.

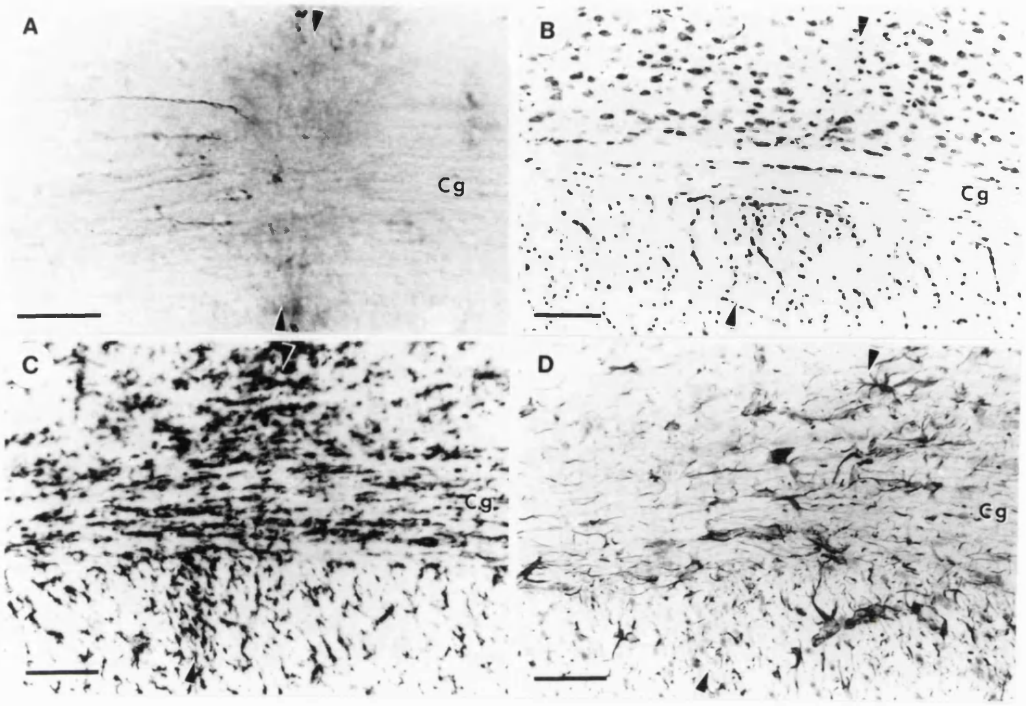
A
Cg
B
Cg
C
Cg
D
Cg

The vimentin immunoreactivity had subsided, and GFAP immunoreactivity was also greatly reduced, but still to a level slightly above normal (Fig. 49D). The astrocytic longitudinal processes were slightly hypertrophic, but normally aligned.

5.3.2.4 *14 and 30 days survival*

(A) *Axons*

At no time did I find cut axons which had been able to cross the lesion site. By 14 days, a number of axons which turned backward into the tract had reached lengths of extension which, in the forward direction, would have been sufficient to carry them across the lesion site. Occasional axons had retracted for up to 100 µm from the lesion site, or formed large terminal expansions. The arrows in Fig. 50 indicate an example of an axon which has retracted, turned back and extended for around 100 µm in a retrograde direction along the tract. Beyond 14 days down-regulation of p75 immunoreactivity precluded further analysis of the changes in the cut axons.

(B) *Glia*

By 14 days, the increased microglial OX42 immunoreactivity had subsided, and the microglial arrangement in the tract lesion site resembled that of an undamaged tract. By 1 month, the upregulation of astrocytic GFAP had disappeared, and the arrangement and alignment of the tract glial cells was indistinguishable from normal.

Figure 50

Camera lucida drawings with some corresponding photomicrographs to show terminal axonal expansions at 14 days after operation. Arrows indicate an axon which has retracted from the lesion site, turned, and extended in the reverse direction in the tract. Scale bar, 50 μm.

DISCUSSION

5.4.1 Adult axons can grow

Cut adult central axons will not regenerate along their normal fibre tracts. That they do retain the power of growth under appropriate circumstances is indicated by a number of observations: (1) they will readily grow new synaptic connections in denervated central neuropil (Raisman, 1969), (2) they will regenerate into transplants of embryonic neural tissue (Field *et al.,* 1991; Wictorin *et al.,* 1989b; *Chapter IV*), (3) they will extend for long distances along peripheral nerve grafts (Richardson *et al.,* 1980; Vidal-Sanz *et al.,* 1987), (4) they will sprout in response to transplanted Schwann cells (Brook *et al.,* 1994; Li and Raisman, 1994; Montero-Menei *et al.,* 1992; Neuberger *et al.,* 1992; Paíno and Bunge, 1991), and (5) - in the present observations - they will produce sprouts capable of elongation backward along the tract from the lesion site. This suggests that the failure of axon regeneration after lesions is due to some non-permissive property peculiar to damaged adult tracts. This could be the presence of inhibitory molecules (Schwab *et al.,* 1993) and/or an inadequate supply of growth stimuli (Berry, 1985; Hagg *et al.,* 1991; Kawaja and Gage, 1991; Lindsay *et al.,* 1982; Tuszynski *et al.,* 1994) or the lack of appropriate surface molecules (Kuhn *et al.,* 1995; Liesi, 1985).

5.4.2 Lesions of white matter tracts

In the general introduction I have described the orderly glial arrangement present in normal adult central tracts (Davies *et al.,* 1994; Li and Raisman,

1994; Suzuki and Raisman, 1992) ie. the presence of three types of glial cell bodies, each with its own characteristic spacing, and each of which generates an array of longitudinal processes (Fig. 51A). Under most circumstances, when a traumatic lesion is made in an adult tract, the glial cells react by forming a "scar" proposed to inhibit regeneration (Berry *et al.,* 1983; Li and Raisman, 1995; Kruger *et al.,* 1986; Reier *et al.,* 1983a,b, 1986; Reier and Houle, 1988; Stensaas et al., 1987). There is an early invasion of macrophages (Li and Raisman, 1995; Stichel and Müller, 1994) which persist for many months (Dusart and Schwab, 1994; Li and Raisman, 1995; Stichel and Muller, 1994), astrocytic proliferation (Latov *et al.,* 1979; Skoff, 1975), invasion of fibroblasts from the meninges and deposition of intraparenchymal basal lamina at the lesion site. In lesions of the spinal cord, Schwann cells have also been observed to migrate via blood vessels into the damaged cortico-spinal and sensory column tracts (Li and Raisman, 1995). Not only does the lesion site have a very different cellular composition compared to that observed in normal tract but the longitudinal array of glial processes is also lost (Li and Raisman, 1995).

5.4.3 Microlesions

The microlesion experiment described in this chapter was designed to test whether access to a normally aligned glial framework would provide a sufficient condition to allow axon regeneration. For this purpose, I designed the present microlesion approach, which cut a beam of cingulate axons, but caused minimal damage to the tract glial framework, and consequently allowed a seemingly normal arrangement of the tract glial cells to be rapidly reestablished.

Figure 51

Schematic representation to show: **A**, the normal arrangement of astrocytes (a), microglia (m), and axons (x) in the cingulum. **B**, Transient influx of amoeboid macrophage/microglia (p) into the lesion track at 1-2 days; x, terminal expansions formed by the cut p75 positive axons (solid black); orthograde degenerating distal axon segments represented by trails of dots. **C**, Reactive hypertrophy of astrocytes (a) and resident tract microglia (m) along the course of the orthograde degeneration at 4 days. **D**, Subsidence of reactive glial changes and persistence of blocked axons at 8 days.

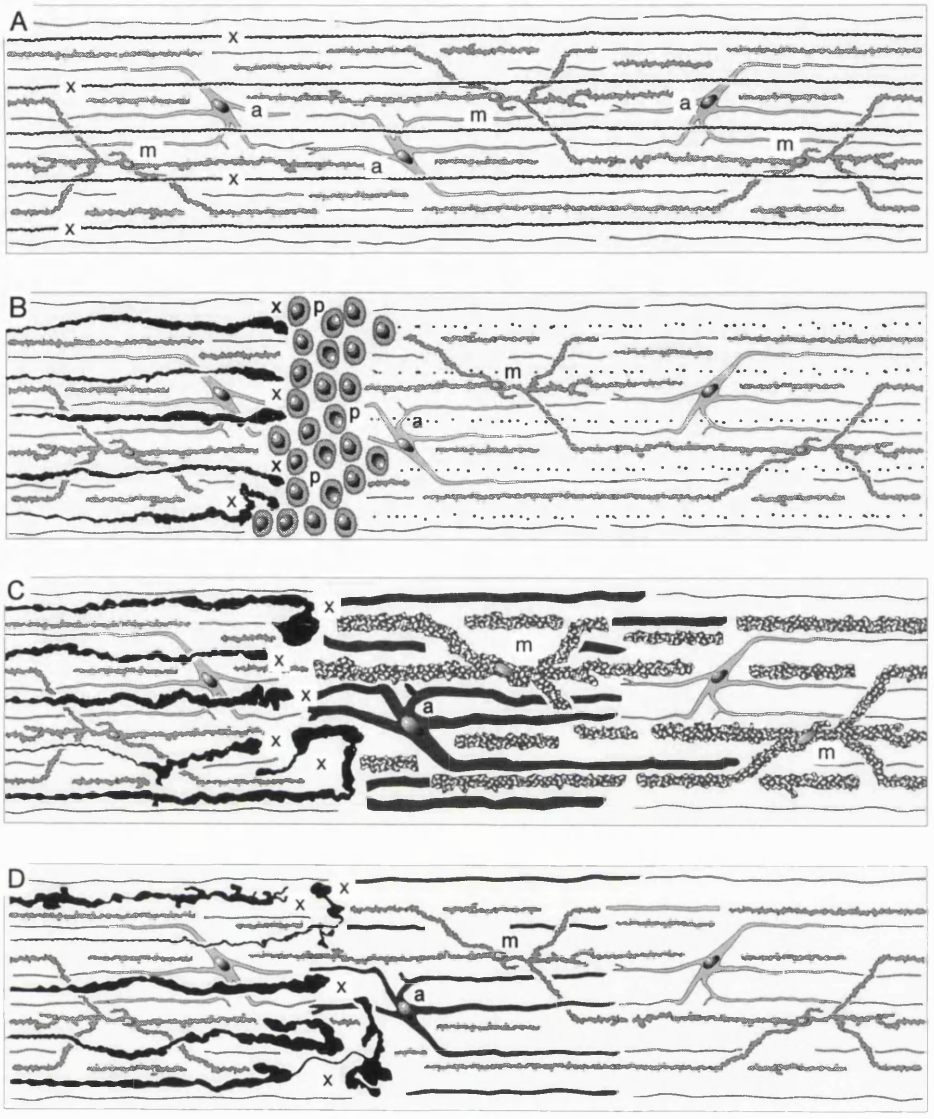
A
x
x
a
m
a
m
m
a
x
x
x
B
x
p
x
p
x
p
x
m
a
C
x
x
x
x
x
m
a
m
D
x
x
x
m
x
a
x

It should, however, be remembered that it cannot be excluded that other staining methods might show anatomical changes in the tract glia after microlesions. Intracellular filling of astrocytes, for example, reveals far more of the cell processes than GFAP immunostaining (Butt and Ransom, 1989: Suzuki and Raisman, 1992), and could provide a more sensitive indicator of responses to microlesions.

With the stains used in the present analysis, however, it can be said that what appears to be an 'open' tract glial framework Is non-permissive for axon growth. A comparable situation may be presented by the centrally directed branches of crushed dorsal roots which regenerate towards the spinal cord, but fail to cross, and often turn back at the dorsal root entry zone, even though this region has not been subjected to direct trauma (Bignami *et al.,* 1984; Cajal, 1928; Carlstedt, 1988; Liuzzi and Lasek, 1987; Perkins *et al.,* 1980; Pindzola *et al.,* 1993; Stensaas *et al.,* 1979, 1987). It has been suggested this effect is associated with absence of growth enhancing molecules (Bignami *et al.,* 1984) or expression of inhibitory molecules (Pindzola *et al.,* 1993).

The finding that such an apparently "open" tract glial framework is non-permissive for axon growth indicates that neither astrocytic scarring nor the continued presence of macrophages (as seen in larger lesions; see below) are causes of the failure of axon regeneration in this material.

5.4.4 Effects of microlesions on axons

Although the use of such microlesions allows a very clear picture of glial changes, it raises the problem of how to identify the small number of cut axons among the remaining large numbers of undamaged tract axons. The marked enhancement of p75 immunoreactivity for the first 2 weeks post lesion, provides an excellent specific marker for a contingent of cut axons in the cingulum. Comparable enhancement of p75 in adult axons has been demonstrated in a number of central and peripheral sites after axotomy, such as the fimbria/fornix and sciatic nerve, (Johnson *et al.,* 1987) and lesions of a subset of Purkinje cell axons in the cerebellum (Dusart *et al.,* 1994; Martínez-Murillo *et al.,* 1993).

Upregulation of p75 expression has been shown to be maintained in a number of situations where adult axons regenerate. In the peripheral nervous system, Rende *et al.,* (1992, 1993) using ligation and crushing lesions of the sciatic nerve which allow axonal regeneration, have noted intense p75 immunoreactivity in regenerating spinal cord motor neuron axons. Rende and collaborators came to the conclusion that p75 upregulation is not just a generic signal of cellular damage but expressed by motor neurons actively growing axons. Similarly, it has been reported (Redd and Byers, 1994) that there is a marked increase of p75 in cut tooth sensory nerve axons when they regenerate back to the dental junctional epithelium. Kawaja and Gage, (1991), using intracerebral transplants of primary fibroblasts genetically engineered to secrete nerve growth factor, demonstrated a maintained increase of p75 expression in cut cholinergic CNS axons growing within their grafts. The strongly p75

immunoreactive fibres were seen entering the transplants from as early as 1 week, and continued up to 8 weeks post transplantation. These results suggest that the down-regulation of p75 receptor immunoreactivity in the present material may be associated with the failure of the cut cingulate axons to regenerate, as at no time up to 30 days post lesion were any p75 positive axons seen to cross the lesion site.

The present failure of cut cholinergic axons to regenerate in tracts is in contrast to a number of published studies demonstrating reappearance of cholinergic markers in neuropil after axotomy. This can occur as a result of 'bridging' procedures which enable cut axons to reach denervated neuropil (Björklund *et al.,* 1979; Kawaja *et al.,* 1992; Kromer *et al.,* 1981a; Hagg *et al.,* 1990; Neuberger *et al.,* 1992; Tuszynski *et al.,* 1990), or by 'collateral' sprouting from uncut axons in adjacent areas (Gage *et al.,* 1984), also demonstrated by Farris *et al.,* (1995) with lesions of the cingulate cortex. The ability of uncut axons to fill in a denervated terminal field has also frequently been demonstrated for non-cholinergic axons (e.g. Cotman *et al.,* 1981; Raisman, 1969), and this indicates that the failure of regeneration is not necessarily a property of the axon itself but arises from some combination of features specific to the structure of central fibre tracts.

5.4.5 Effects of microlesions on glia

It is the highly regular arrangement of glial cells and their processes in central fibre tracts (Fig. 51A; Davies *et al.,* 1994; Li, Raisman, 1994; Suzuki, Raisman,

1992) which makes it possible to analyze the effects of cingulate microlesions on the glial population. The cellular responses to the microlesions consist of two phases: (1) an early, transient invasion of amoeboid macrophage/microglia along the micropipette track at 1-2 days (Fig. 51B), followed by (2) hypertrophy of the resident tract ramified microglia and astrocytes along the path of the degenerating axon fragments, reaching a peak at 4 days (Fig. 51C), and leading to the progressive restoration of a normally aligned glial framework by 8 days (Fig. 51D).

5.4.5.1 *Amoeboid cells*

The appearance of rounded, 'amoeboid' OX42 immunoreactive cells within the tract glial framework at 1 day after lesion is remarkable for its early onset, its strict localisation to the micropipette track, and its equally rapid disappearance. These characteristic, rounded cells with dense OX42-immunoreactive rims are readily identified in electron micrographs. Their morphology resembles that taken up by a variety of cells of the blood monocyte/macrophage/microglial family when cultured on fibroblasts, but which convert to a ramified microglial morphology in the presence of astrocytes (e.g. Fig. 8 in Sievers *et al.,* 1994). While the amoeboid cells are only a transient element in the microlesions, the fact that the environment of the cut axon tips is infiltrated during the first two postoperative days by a dense mass of macrophage/microglial cells capable of secreting powerful cytokines (Gehrmann *et al.,* 1995; Giulian *et al.,* 1994) may induce later changes which prevent axon regeneration.

5.4.5.2 *Resident Ramified Tract Microglia*

The general morphology of microglia in adult fibre tracts has been recorded by Gehrmann *et al.,* (1995) and Perry *et al.,* (1985). The present material shows the regular, solitary spacing and alignment present in normal tracts (Fig. 51A). In contrast to the earlier restricted localisation of the OX42 immunoreactive amoeboid cells to the micropipette track, the later activation of resident ramified tract microglia extends caudally among the degenerating distal fragments of the cut axons. Within the corpus callosum, however, it extends symmetrically away from the lesion on both sides. These two patterns correspond to the respective distribution of degeneration of the distal fragments of the cut cingulate and callosal axons. Both microglia and astrocytes have been shown to be involved in phagocytosis of these fragments and their associated myelin sheaths (Stichel and Müller, 1994; Stichel *et al.,* 1995).

5.4.5.3 *Astrocytes*

The rather minor, and reversible structural changes in cingulate astrocytes after a microlesion contrast with the progressive development of dense astroglial scars seen after larger lesions (Reier, 1986). A recent study of corticospinal tract lesions (Li and Raisman, 1995) shows that the slow but inexorable development of an astrocytic scar is associated with the continued presence of a cavity filled with necrotic material and débris-laden phagocytic amoeboid macrophages which are still present at 13 weeks after the lesion. It seems likely that the persistence of necrotic material maintains a stimulus for the macrophages.

Figure 52

A, Microlesions, which cut axons (ax), lead to a transient influx of amoeboid macrophage/microglia (mp) which, not being retained by the presence of necrotic material, rapidly leave the lesion site, after only a transient stimulation of resident tract ramified microglia (mgl) and astrocytes (astro). **B**, After larger lesions, leading to necrosis, bleeding and exudation, the amoeboid macrophage/microglia remain in an activated state, phagocytosing necrotic material and débris, and persist in the lesion site (phago), where they act as a continuous stimulus sufficient to trigger the positive feed-back cascade (GM-CSF, IL-1, TGFß1 etc) of mutual activation of the tract astrocytes and tract ramified microglia, thus leading to the progressive formation of a re-duplicated astroglial scar.

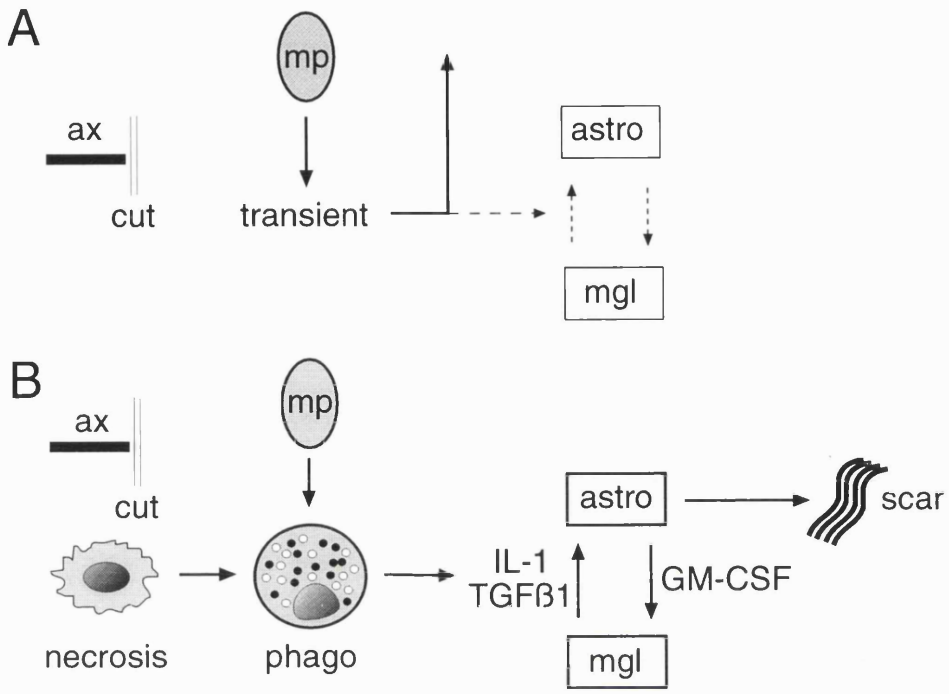
A
mp
ax
cut
transient
astro
mgl
B
mp
ax
cut
astro
scar
IL-1
TGFß1
GM-CSF
necrosis
phago
mgl

This may present continuous activational signals (such as the cytokines IL-1 and TGFß1) to the astrocytes (Gehrmann *et al.,* 1995; Giulian *et al.,* 1994), which in turn would release factors, such as GM-CSF (Lee *et al.,* 1994; Thery and Mallat, 1993), maintaining the activated state of the microglia (Fig. 52B). This positive feedback loop would lead to the build up of an astroglial scar (Logan *et al.,* 1994; Gagelin *et al.,* 1995). The absence of necrosis in microlesions is associated with only a transient macrophage invasion, insufficient to trigger off this cascade of activational feed-back signals between the tract microglia and astrocytes, and therefore followed by only a slight and reversible astrocytic hypertrophy and no scar (Fig. 52A).

5.4.6 Comparison with chemorepulsion of developing axons

The in vitro work on the secreted protein collapsin/semaphorin III (Luo *et al.,* 1993, 1995) indicates that the events guiding axon growth are registered at the growth cone, whose subsequent reorganisation determines whether the axon will stop, advance or turn (Fan *et al.,* 1993; Fan and Raper, 1995). In vivo studies of the developing visual system show that growth cones undergo marked morphological changes when they slow down at decision points, such as the optic chiasma (Godement *et al.,* 1990, 1994; Sretavan and Reichardt, 1993). In the present material the large expanded cut ends of the cingulate axons resemble the growth-arrested chiasmal axons. The 180° turns and backward extension (Fig. 46B, arrows in Fig. 50) are characteristic features of cultured axons exposed to collapsing factors (e.g. Fig. 1 in Fan and Raper, 1995). This suggests that comparable repulsive mechanisms associated with

the lesion site may be responsible for the axonal behaviour seen in the cut adult cingulum.

5.4.7 Possible sources of repulsive cues

In development, specialised midline non-neuronal cells such as the floorplate (Colamarino and Tessier-Lavigne, 1995a, 1995b; Guthrie and Pini, 1995; Messersmith *et al.,* 1995; Tamada *et al.,* 1995), roofplate (Snow *et al.,* 1990) and possibly the midline cells of the optic chiasm (Marcus *et al.,* 1995) generate axon-repulsive factors. In adult CNS lesions, cells which have been implicated as possible sources of factors inhibiting axon growth include:

5.4.7.1 *Oligodendrocytes*

Schwab and colleagues have proposed that two molecules, NI-35 and NI-250 associated with mature myelinating adult oligodendrocytes (Caroni and Schwab, 1988), could have a general growth inhibitory effect on adult axons. This is a particularly attractive suggestion, firstly, because unlike the specific action of molecules such as the netrins and semaphorins on defined types of axon, the inhibitory effect is general, and could therefore explain the general failure of regeneration observed for adult central axons. Secondly, since mature, myelinating oligodendrocytes only appear late in development and are concentrated in adult fibre tracts, the expression of these molecules correlates with the time and place where axon growth fails (Caroni and Schwab, 1989). The axon growth inhibitory effects of NI-35/250 can be prevented by addition of a blocking monoclonal antibody, Mab IN-1 in tissue culture (Bandtlow *et al.,*

1990). Tumour cells which secrete Mab IN-1, transplanted adjacent to lesions of the corticospinal tract in postnatal and young adult rats, have been shown to promote axonal sprouting around the lesion site (Schnell and Schwab, 1990). The regenerative effects of the antibody could be further enhanced by infusion of NT3 into the lesion area (Schnell *et al.,* 1994). Immunostaining for NI-35/250 after transection of the adult fornix has shown that although these molecules are not present at the lesion site, they are found in the degenerating tract distal to the lesion and can remain for several months (Stichel *et al.,* 1995).

However as discussed in *Chapter III*, there are a number of in vitro experimental results (Ard *et al.,* 1991; Fawcett *et al.,* 1992; Kobayashi *et al.,* 1995) which are at odds with the theory of general myelin induced inhibition of axon growth. Similarly in vivo, when retinal ganglion cell axons (RGC) are cut in adult Browman-Wyse mutant rats in which both oligodendrocytes and CNS myelin are absent from the proximal (retinal) end of the optic nerve, Berry *et al.,* (1992) have shown that the RGC axons fail to regenerate in the exclusively astrocytic environment. Berry and collaborators suggested therefore that central myelin is not an absolute requirement for regenerative failure and that inhibition by astrocytes or absence of trophic factors may be important contributing factors.

5.4.7.2 *Astrocytes*

Whereas embryonic astrocytes are permissive for axon growth, they lose this property when they mature (Fawcett *et al.,* 1989; Rudge and Silver, 1990; Smith

et al., 1986; Smith-Thomas *et al.,* 1994, 1995; Wang *et al.,* 1994). Mansour *et al.,* (1990) have proposed that glial hyaluronate-binding protein (an ECM structural glycoprotein of white matter tracts), inhibits axon regeneration and is found in association with astrocytes in the degenerating tract distal to a lesion. Bovolenta *et al.,* (1993) isolated a 160-220 kD molecule from myelin free membranes taken from injured rat brain which in tissue culture prevented initiation of neurite formation when presented as a substrate bound molecule and growth cone retraction when added in soluble form. McKeon *et al.,* (1991) have shown that reactive adult axons secrete cytotactin/tenascin (CT) and chondroitin-6-sulphate containing proteoglycan (C-6-PG) extracellular matrix molecules which inhibit neurite outgrowth in culture. Smith-Thomas *et al.,* (1995) have noted a significant increase in DRG axon growth on primary astrocyte cultures treated with inhibitors of proteoglycan synthesis (beta-D-xylosides and sodium chlorate). Pindzola *et al.,* (1993) demonstrated that the expression of these molecules correlates with the critical period in development beyond which axons will not regenerate across the dorsal root entry zone and suggested that their upregulation and preferential association with adult white matter astrocytes after root lesions may inhibit adult axon regeneration.

5.4.8 Lack of growth stimuli

Kawaja and Gage, (1991), demonstrated cholinergic axon sprouting into transplants of fibroblasts engineered to secrete NGF placed in the cerebral cortex of adult host rats, and showed that reactive grey matter astrocytes were permissive for growth of adult axons given high levels of NGF. While my

observation that some axon sprouts turn back and elongate in the reverse direction in the proximal part of the tract favours the view that there is an inhibitory influence at the lesion site, a significant contributory factor could be the absence of adequate levels of growth stimulating factors in damaged adult tracts.

CONCLUSION

There seems little doubt that the necrotic tissue filled cavity and subsequent glial scar formed in major spinal injuries, acts as a considerable physical barrier to axon regeneration. However, the microlesion procedure provides a model system which still demonstrates total blockade of forward white matter axon growth even though débris and glial scarring are virtually eliminated. The minimal damage to glia and vasculature at the lesion site, affords a clear view of the changes in axon behaviour and morphology when presented with a viable tissue environment of normally aligned but reactive glial. The formation of expanded stationary growth cones or the 180° turning response of others axons from an apparently "open" tract, are comparable to those induced by chemorepulsion in development. In future experiments, I hope to identify if any of the known molecules which inhibit axon growth in tissue culture are expressed within a tract microlesion, and if so, which elements of the lesion site are presenting them.

CHAPTER VI

General Discussion

GENERAL DISCUSSION

The glial scar and necrotic tissue filled cavity so often formed in adult tract lesions present a considerable physical barrier for regenerating tract axons, and therefore developing means of preventing their formation or bridging this environment with an axon growth promoting substrate would be advantageous for regeneration of adult axons.

Clearly some cut adult CNS axons have the ability to regenerate through peripheral nerve grafts, avoiding the lesion site and distal tract, and can be induced to elongate and reinnervate neuropil placed directly in contact with the end of the graft (Benfey and Aguayo, 1982; Berry *et al.,* 1988a, 1988b; Campbell *et al.,* 1991, 1992; David and Aguayo,1981,1995; Richardson *et al.,* 1980; Vidal-Sanz *et al.,* 1987). However, in the case of a complex system of fibre tracts, such as the spinal cord, any attempts at trying to regenerate and redistribute the many different constituents of cut spinal axons directly into their appropriate neuropil with a series of peripheral nerve grafts, would be practically impossible. Therefore it is vitally important in considering future strategies for CNS repair, to attempt to re-introduce regenerating cut axons back into their original tracts distal to the lesion, and hopefully utilize these existing pathways to redistribute regenerating axons back to their correct destinations. However, so far, attempts to reintroduce regenerating axons into the distal portion of a lesioned CNS tract (in contrast to neuropil) from Schwann cell grafts (Xu *et al.,* 1995), have met with limited success. Possibly these grafts of peripheral nerve

tissue develop an inhibitory interface with the distal host tract, or the adult tract environment is in some way non-permissive to new adult axon growth.

6.1 Microtransplants

Adult white matter tracts do, however, present a highly permissive environment for the growth of embryonic axons. Indeed, adult tracts can induce embryonic axons to extend for distances many times longer than those they would traverse during normal development. The atraumatic nature of the microtransplantation technique described in *Chapters II and III*, prevented scar formation and gave the embryonic axons immediate access to an "open" transplant/tract interface aligned with the complex glial architecture of the adult tract. The small size of the microtransplants permitted their accurate placement within different areas of a particular adult fibre tract and demonstrated that the patterns of axon growth from "mismatched" grafts were determined by the adult tract structure not the donor neuron type. The new axon growth respected intertract boundaries and grew in strict alignment with the adult axons and the astrocytic longitudinal processes, which are characteristic of central tracts. Studying the projections formed by transplanted embryonic neurons provides a method for exploring the ability of adult fibre tracts to sustain directed axon growth, an understanding of which is essential if we hope to regrow adult axons through adult tracts.

The microtransplant experiments described in *Chapter IV* showed that the lack of astroglial scar formation at the "open" aligned transplant interface also permitted the ingrowth of adult tract axons into the grafts. However, the

tract/transplant interface was not only composed of adult tract derived glia but also of embryonic neurons and astrocytes, which may have presented axon growth promoting chemoattractants and extracellular matrix molecules to the adult tract axons. The hypothesis that access to an aligned pathway of adult tract glia might be sufficient to promote regeneration of cut adult axons was tested in *Chapter V* with the microlesion approach.

6.2 Microlesions

The microlesion technique provides an in vivo model system which virtually eliminates tissue necrosis and glial scarring but still demonstrates total blockade of forward white matter adult axon growth. The minimal damage to glia and vasculature at the lesion site, affords a clear view of the changes in axon behaviour and morphology when presented with a viable tissue environment of normally aligned but reactive glia. The formation of expanded stationary growth cones, or the 180^0 turning response of other axons from an apparently "open" tract, suggests a molecular inhibition of axon growth comparable to those induced by chemorepulsion in development.

Understanding the molecular basis of the failure of central axon regeneration holds out the future possibility of devising methods for repair of brain and spinal cord injuries. Those genes and molecules which have so far been identified as regulators of axon growth have been largely characterised by the use of developing or *in vitro* systems which are anatomically simple, enabling single interactions to be pinpointed and tested (Colamarino and Tessier-Lavigne,

1995b; Dodd and Schuchardt, 1995; Luo *et al.,* 1995; Matthes *et al.,* 1995). Extending this approach to the adult CNS will necessitate a comprehensive knowledge of the behaviour of the cellular elements that make up the complex and structured environment of the cut axons. In devising a microlesion procedure which largely eliminates débris, disorganisation and scarring, I have described a system which reduces some of the extraneous factors, so that the causes of the failure of axon growth can be studied against the background of a normally arranged glial framework, and future molecular investigations and interventions can be more accurately targeted to specific cell elements.

REFERENCES

Ard, M. D., Bunge, M. B., Wood, P. M., Schachner, M. and Bunge, R. P. (1991) Retinal neurite growth on astrocytes is not modified by extracellular matrix, anti-L1 antibody, or oligodendrocytes. *Glia*, **4**, 70-82.

Baird, D. H., Hatten, M. E. and Mason, C. A. (1992) Cerebellar target neurons provide a stop signal for afferent neurite extension in vitro. *J. Neurosci.*, **12**, 619-634.

Bandtlow, C., Zachleder, T. and Schwab, M. E. (1990) Oligodendrocytes arrest neurite growth by contact inhibition. *J. Neurosci.*, **10**, 3837-3848.

Barbe, M. F. and Levitt, P. (1991) The early commitment of fetal neurons to the limbic cortex. *J. Neurosci.*, **11**, 519-533.

Barclay, A. N., Letarte-Muirhead, M. and Williams, A. F. (1976) Chemical characterisation of the Thy-1 glycoproteins from the membranes of rat thymocytes and brain. *Nature*, **263**, 563-567.

Bates, C. A. and Stelzner, D. J. (1993) Extension and regeneration of corticospinal axons after early spinal injury and the maintenance of corticospinal topography. *Exp. Neurol.*, **123**, 106-117.

Benfey, M. and Aguayo, A. J. (1982) Extensive elongation of axons from rat brain into peripheral nerve grafts. *Nature*, **296**, 150-151.

Berry, M., Maxwell, W. L., Logan, A., Mathewson, A., McConnel, P., Ashhurst, D. E. and Thomas, G. H. (1983) Deposition of scar tissue in the central nervous system. *Acta Neurochir. [suppl]*, **32**, 31-53.

Berry, M. (1985) Regeneration and plasticity in the CNS. Swash, M. and Kennard, C. (eds), *Scientific Basis of Clinical Neurology*. Churchill Livingstone, London, pp. 658-679.

Berry, M., Hall, S. F., Rees, L., Gregson, N. and Sievers, J. (1988a) Response of axons and glia at the site of anastomosis between the optic nerve and cellular or acellular sciatic nerve grafts. *J. Neurocytol.*, **17**, 727-744.

Berry, M., Rees, L., Hall, S., Yiu, P. and Sievers, J. (1988b) Optic axons regenerate into sciatic nerve isografts only in the presence of Schwann cells. *Brain Res. Bull.*, **20**, 223-231.

Berry, M., Hall, S., Rees, L., Carlile, J. and Wyse, J. P. H. (1992) Regeneration of axons in the optic nerve of the adult Browman-Wyse (bw) mutant rat. *J. Neurocytol.*, **21**, 426-448.

Bignami, A., Chi, N. H. and Dahl, D. (1984) Regenerating dorsal roots and the nerve entry zone: an immunofluorescence study with neurofilament and laminin antisera. *Exp. Neurol.*, **85**, 426-436.

Bignami, A. and Dahl, D. (1976) The astroglial response to stabbing. Immunofluorescence studies with antibodies to astrocyte-specific protein (GFA) in mammalian and submammalian vertebrates. *Neuropathol. appl. Neurobiol.*, **2**, 99-110.

Björklund, A., Kromer, L. F. and Stenevi, U. (1979) Cholinergic reinnervation of the rat hippocampus by septal implants is stimulated by perforant path lesion. *Brain Res.*, **173**, 57-64.

Björklund, A. and Stenevi, U. (1984) Intracerebral neural implants: neuronal replacement and reconstruction of damaged circuitries. *Annu. Rev. Neurosci.*, **7**, 279-308.

Bothwell, M. (1991) Tissue localization of nerve growth factor and nreve growth factor receptors. *Curr. Top. Microbiol. Immunol.*, **165**, 55-70.

Bottenstein, J. and Sato, G. H. (1979) Growth of a rat neuroblastoma cell line in serum-free supplemented medium. *Proc. Natl. Acad. Sci. USA*, **76**, 514-517.

Bovolenta, P., Liem, R. K. H. and Mason, C. A. (1984) Development of cerebellar astroglia: transitions in form and cytoskeletal content. *Dev. Biol.*, **102**, 248-259.

Bovolenta, P., Wandosell, F. and Nieto-Sampedro, M. (1991) Neurite outgrowth over resting and reactive astrocytes. *Restor. Neurol. Neurosci.*, **2**, 221-228.

Bovolenta, P., Wandosell, F. and Nieto Sampedro, M. (1993) Characterization of a neurite outgrowth inhibitor expressed after CNS injury. *Eur. J. Neurosci.*, **5**, 454-465.

Brandt, H. M. and Apkarian, A. V. (1992) Biotin-dextran: A sensitive anterograde tracer for neuroanatomic studies in rat and monkey. *J. Neurosci. Methods*, **45**, 35-40.

Brittis, P. A., Canning, D. R. and Silver, J. (1992) Chondroitin sulfate as a regulator of neuronal patterning in the retina. *Science*, **255**, 733-736.

Brook, G. A., Lawrence, J. M., Shah, B. and Raisman, G. (1994) Extrusion transplantation of Schwann cells into the adult rat thalamus induces directional host axon growth. *Exp. Neurol.*, **126**, 31-43.

Burden-Gulley, S. M., Payne, H. R. and Lemmon, V. (1995) Growth cones are actively influenced by substrate-bound adhesion molecules. *J. Neurosci.*, **15**, 4370-4381.

Butt, A. M. and Ransom, B. R. (1989) Visualization of oligodendrocytes and astrocytes in the intact rat optic nerve by intracellular injection of Lucifer Yellow and horseradish peroxidase. *Glia*, **2**, 470-475.

Cajal, S. R. (1893) La retine des vertebres. *La Cellule*, **9**, 119-158.

Cajal, S. R. (1928) *Degeneration and Regeneration of the Nervous System*. Hafner, New York.

Campbell, G., Anderson, P. N., Turmaine, M. and Lieberman, A. R. (1991) GAP-43 in the axons of mammalian CNS neurons regenerating into peripheral nerve grafts. *Exp. Brain Res.*, **87**, 67-74.

Campbell, G., Lieberman, A. R., Anderson, P. N. and Turmaine, M. (1992) Regeneration of adult rat CNS axons into peripheral nerve autografts: Ultrastructural studies of the early stages of axonal sprouting and regenerative axonal growth. *J. Neurocytol.*, **21**, 755-787.

Campbell, K., Kalen, P., Wictorin, K., Lundberg, C., Mandel, R. J. and Bjorklund, A. (1993) Characterization of GABA release from intrastriatal striatal transplants: dependence on host-derived afferents. *Neuroscience*, **53**, 403-415.

Carlstedt, T., Dalsgaard, C. J. and Molander, C. (1987) Regrowth of lesioned dorsal root nerve fibers into the spinal cord of neonatal rats. *Neurosci. Lett.*, **74**, 14-18.

Carlstedt, T. (1988) Reinnervation of the mammalian spinal cord after neonatal dorsal root crush. *J. Neurocytol.*, **17**, 335-350.

Caroni, P. and Schwab, M. E. (1988) Two membrane protein fractions from rat central myelin with inhibitory properties for neurite growth and fibroblast spreading. *J. Cell Biol.* **106**, 1281-1288.

Caroni, P. and Schwab, M. E. (1989) Co-distribution of neurite growth inhibitors and oligodendrocytes in rat CNS: appearance follows nerve fiber growth and precedes myelination. *Dev. Biol.*, **136**, 287-296.

Cattaneo, E. and McKay, R. (1990) Proliferation and differentiation of neuronal stem cells regulated by nerve growth factor. *Nature*, **347**, 762-765.

Chao, M. V., Bothwell, M. A., Ross, A. H., Koprowski, H., Lanahan, A. A., Buck, C. R. and Sehgal, A. (1986) Gene transfer and molecular cloning of the human NGF receptor. *Science*, **232**, 518-521.

Chao, M. V. and Hempstead, B. L. (1995) p75 and Trk: a two receptor system. *Trends Neurosci.*, **18(7)**, 321-326.

Chen, D. F., Jhaveri, S. and Schneider, G. E. (1995) Intrinsic changes in developing retinal neurons result in regenerative failure of their axons. *Proc. Natl. Acad. Sci. USA*, **92**, 7287-7291.

Chiu, A. Y., Matthew, W. D. and Patterson, P. H. (1986) A monoclonal antibody that blocks the activity of a neurite regeneration-promoting factor: Studies on the binding site and its localization in vivo. *J. Cell Biol.*, **103**, 1838-1398.

Cho, E. Y. P. and So, K. F. (1987) Rate of regrowth of damaged retinal ganglion cell axons regenerating in a peripheral nerve graft in adult hamsters. *Brain Res.*, **419**, 369-374.

Clarke, D. J., Brundin, P., Strecker, R. E., Nilsson, O. G., Björklund, A. and Lindvall, O. (1988a) Human fetal dopamine neurons grafted in a rat model of Parkinson's disease - ultrastructural evidence for synapse formation using tyrosine hydroxylase immunocytochemistry. *Exp. Brain Res.*, **73**, 115-126.

Clarke, D. J., Dunnett, S. B., Isacson, O., Sirinathsinghji, D. J. S. and Björklund, A. (1988b) Striatal grafts in rats with unilateral neostriatal lesions - I. Ultrastructural evidence of afferent synaptic inputs from the host nigrostriatal pathway. *Neuroscience*, **24**, 791-802.

Clinton, R. J. and Ebner, F. F. (1988) Time Course of Neocortical Graft Innervation AChE-Positive Fibers. *J. comp. Neurol.*, **277**, 557-577.

Cohen, J., Burne, J. F., Winter, J. and Bartlett, P. (1986) Retinal ganglion cells lose response to laminin with maturation. *Nature*, **322**, 465-467.

Cohen, J., Nurcombe, V., Jeffrey, P. and Edgar, D. (1989) Developmental loss of functional laminin receptors on retinal ganglion cells is regulated by their target tissue, the optic tectum. *Development*, **107**, 381-387.

Colamarino, S. A. and Tessier-Lavigne, M. (1995a) The axonal chemoattractant netrin-1 is also a chemorepellent for trochlear motor axons. *Cell*, **81**, 621-629.

Colamarino, S. A. and Tessier-Lavigne, M. (1995b) The role of the floor plate in axon guidance. *Annu. Rev. Neurosci.*, **18**, 497-529.

Collins, F. (1978) Induction of neurite outgrowth by a conditioned-medium factor bound to the culture substratum. *Proc. Natl. Acad. Sci. USA*, **75**, 5210-5213.

Collins, F. and Garrett, J. E. (1980) Elongating nerve fibers are guided by a pathway of material released from embryonic nonneuronal cells. *Proc. Natl. Acad. Sci. USA*, **77**, 6226-6228.

Cotman, C. W., Nieto-Sampedro, M. and Harris, E. W. (1981) Synapse replacement in the nervous system of adult vertebrates. *Physiol. Rev.*, **61**, 684-784.

David, S. and Aguayo, A. J. (1981) Axonal elongation into peripheral nervous system "bridges" after central nervous system injury in adult rats. *Science*, **214**, 931-933.

David, S. and Aguayo, A. J. (1985) Axonal regeneration after crush injury of rat central nervous system fibres innervating peripheral nerve grafts. *J. Neurocytol.*, **14**, 1-12.

Davies, A. M., Bandtlow, C., Heumann, R., Korsching, S., Rohrer, H. and Thoenen, H. (1987) Timing and site of nerve growth factor synthesis in developing skin in relation to innervation and expression of the receptor. *Nature*, **326**, 353-358.

Davies, S. J. A., Field, P. M. and Raisman, G. (1993) Long fibre growth by axons of embryonic mouse hippocampal neurons micro-transplanted into the adult rat fimbria. *Eur. J. Neurosci.*, **5**, 95-106.

Davies, S. J. A., Field, P. M. and Raisman, G. (1994) Long interfascicular axon growth from embryonic neurons transplanted into adult myelinated tracts. *J. Neurosci.*, **14**, 1596-1612.

Deacon, T. W., Pakzaban, P., Burns, L. H., Dinsmore, J. and Isacson, O. (1994) Cytoarchitectonic development, axon-glia relationships, and long distance axon growth of porcine striatal xenografts in rats. *Exp. Neurol.*, **130**, 151-167.

Dodd, J. and Jessell, T. M. (1988) Axon guidance and the patterning of neuronal projections in vertebrates. *Science*, **242**, 692-699.

Dodd, J. and Schuchardt, A. (1995) Axon guidance: A compelling case for repelling growth cones. *Cell*, **81**, 471-474.

Doherty, P. and Walsh, F. S. (1992) Cell adhesion molecules, second messengers and axonal growth. *Curr. Opin. Neurobiol.*, **2**, 595-601.

Dusart, I., Morel, M. P. and Sotelo, C. (1994) Parasagittal compartmentation of adult rat Purkinje cells expressing the low-affinity nerve growth factor receptor: changes of pattern expression after a traumatic lesion. *Neuroscience*, **63**, 351-356.

Dusart, I. and Schwab, M. E. (1994) Secondary cell death and the inflammatory reaction after dorsal hemisection of the rat spinal cord. *Eur. J. Neurosci.*, **6**, 712-724.

Elberger, A. J. (1994) The corpus callosum provides a massive transitory input to the visual cortex of cat and rat during early postnatal development. *Behav. Brain Res.*, **64**, 15-23.

Emmett, C. J., Jaques-Berg, W. and Seeley, P. J. (1989) Microtransplantation of neural cells into adult rat brain. *Neuroscience*, **38**, 213-222.

Emmett, C. J., Lawrence, J. M., Raisman, G. and Seeley, P. J. (1991) Cultured epithelioid astrocytes migrate after transplantation into the adult rat brain. *J. comp. Neurol.*, **310**, 330-341.

Erzurumlu, R. S. and Ebner, F. F. (1988) Peripheral nerve transection induces innervation of embryonic neocortical transplants by specific thalamic fibers in adult mice. *J. comp. Neurol.*, **272**, 536-544.

Faissner, A. and Kruse, J. (1990) J1/tenascin is a repulsive substrate for central nervous system neurons. *Neuron*, **5**, 627-637.

Faissner, A. and Steindler, D. (1995) Boundaries and inhibitory molecules in developing neural tissues. *Glia*, **13**, 233-254.

Fan, J., Mansfield, S. G., Redmont, T., Gordon-Weeks, P. R. and Raper, J. (1993) The organization of f-actin and microtubules in growth cones exposed to a brain-derived collapsing factor. *J. Cell Biol.*, **121**, 867-878.

Fan, J. and Raper, J. A. (1995) Localized collapsing cues can steer growth cones without inducing their full collapse. *Neuron*, **14**, 263-274.

Farris, T. W., Butcher, L. L., Oh, J. D. and Woolf, N. J. (1995) Trophic-factor modulation of cortical acetylcholinesterase reappearance following transection of the medial cholinergic pathway in the adult rat. *Exp. Neurol.*, **131**, 180-192.

Fawcett, J. W., Housden, E., Smith-Thomas, L. and Meyer, R. L. (1989) The growth of axons in three-dimensional astrocyte cultures. *Dev. Biol.*, **135**, 449-458.

Fawcett, J. W. (1992) Intrinsic neuronal determinants of regeneration. *Trends Neurosci.*, **15**, 5-8.

Fawcett, J. W., Fersht, N., Housden, L., Schachner, M. and Pesheva, P. (1992) Axonal growth on astrocytes is not inhibited by oligodendrocytes. *J. Cell Sci.*, **103**, 571-579.

Field, P. M., Seeley, P. J., Frotscher, M. and Raisman, G. (1991) Selective innervation of embryonic hippocampal transplants by adult host dentate granule cell axons. *Neuroscience*, **41**, 713-727.

Fujii, M. (1989) Long-distance fiber outgrowth from the heterotopically transplanted olfactory bulb in the rat. *Neurosci. Res.*, **7**, 208-218.

Fujii, M. (1991) Non-specific characteristics of intracerebral elongation from the olfactory bulb transplanted into the young adult host neocortex or hippocampal formation, demonstrated immunohistochemically by the mouse Thy-1 allelic system. *Neurosci. Res.*, **9**, 285-291.

Gage, F. H., Björklund, A. and Stenevi, U. (1984) Cells of origin of the ventral cholinergic septohippocampal pathway undergoing compensatory collateral sprouting following fimbria-fornix transection. *Neurosci. Lett.*, **44**, 211-216.

Gagelin, C., Pierre, M., Gavaret, J. -M. and Toru-Delbauffe, D. (1995) Rapid TGFβ1 effects on actin cytoskeleton of astrocytes: comparison with other factors and implications for cell motility. *Glia*, **13**, 283-293.

Gehrmann, J., Matsumoto, Y. and Kreutzberg, G. W. (1995) Microglia: intrinsic immunoeffector cell of the brain. *Brain Res. Rev.*, **20**, 269-287.

Geisert, E. E. and Stewart, A. M. (1991) Changing interactions between astrocytes and neurons during CNS maturation. *Dev. Biol.*, **143**, 335-345.

Giulian, D., Li, J., Li, X., George, J. and Rutecki, P. A. (1994) The impact of microglia-derived cytokines upon gliosis in the CNS. *Dev. Neurosci.*, **16**, 128-136.

Godement, P., Salaün, J. and Mason, C. A. (1990) Retinal axon pathfinding in the optic chiasm: divergence of crossed and uncrossed fibers. *Neuron*, **5**, 173-186.

Godement, P., Wang, L. C. and Mason, C. A. (1994) Retinal axon divergence at the optic chiasm: dynamics of growth cone behavior at the midline. *J. Neurosci.*, **14**, 7024-7039.

Gomez, T. M. and Letourneau, P. C. (1994) Filopodia initiate choices made by sensory neuron growth cones at laminin/fibronectin borders *in vitro*. *J. Neurosci.*, **14**, 5959-5972.

Gomez-Pinilla, F., Cotman, C. W. and Nieto-Sampedro, M. (1988) NGF receptor immunoreactivity in rat brain: topographic distribution and response to entorhinal ablation. *Neurosci. Lett.*, **82**, 260-266.

Gomez-Pinilla, F., Lee, J. W. , Cotman, C. W. (1992) Basic FGF in adult rat brain; cellular distribution and response to entorhinal lesion and fimbria-fornix transection. *J. Neurosci.* **12**, 345-355.

Guillery, R. W. and Walsh, C. (1987) Changing glial organization relates to changing fiber order in the optic nerve of ferrets. *J. comp. Neurol.*, **265**, 203-217.

Gunderson, R. W. and Barrett, J. N. (1979) Neuronal chemotaxis: chick dorsal root axons turn toward high concentrations of nerve growth factor. *Science*, **206**, 1079-1080.

Guth, L. (1956) Regeneration in the mammalian peripheral nervous system. *Physiol. Rev.*, **36**, 441-478.

Guthrie, S. and Pini, A. (1995) Chemorepulsion of developing motor axons by the floor plate. *Neuron*, **14**, 1117-1130.

Hagg, T., Vahlsing, H. L., Manthorpe, M. and Varon, S. (1990) Nerve growth factor infusion into the denervated adult rat hippocampal formation promotes its cholinergic reinnervation. *J. Neurosci.*, **10**, 3087-3092.

Hagg, T., Gulati, A. K., Behzadian, M. A., Vahlsing, H. L., Varon, S. and Manthorpe, M. (1991) Nerve growth factor promotes CNS cholinergic axonal regeneration into acellular peripheral nerve grafts. *Exp. Neurol.*, **112**, 79-88.

Hagg, T. and Varon, S. (1993) Neurotropism of nerve growth factor for adult rat septal cholinergic axons *in vivo*. *Exp. Neurol.*, **119**, 37-45.

Hall, D. E., Neugebauer, K. M. and Reichardt, L. F. (1987) Embryonic neural retinal cell response to extracellular matrix proteins: Developmental changes and effects of CSAT antibody. *J. Cell Biol.*, **104**, 623-634.

Halloran, M. C. and Kalil, K. (1994) Dynamic behaviors of growth cones extending in the corpus callosum of living cortical brain slices observed with video microscopy. *J. Neurosci.*, **14**, 2161-2177.

Hatten, M. E. and Mason, C. A. (1986) Neuron-astroglia interactions *in vitro* and *in vivo*. *Trends Neurosci.*, **9**, 168-174.

Hausmann, B., Sievers, J., Hermanns, J. and Berry, M. (1989) Regeneration of axons from the adult rat optic nerve: influence of fetal brain grafts, laminin, and artificial basement membrane. *J. comp. Neurol.*, **281**, 447-466.

Haydon, P. G., McCobb, D. P. and Kater, S. B. (1984) Serotonin selectively inhibits growth cone motility and synaptogenesis of specific identified neurons. *Science*, **226**, 561-564.

Heffner, C. D., Lumsden, A. G. S. and O'Leary, D. D. M. (1990) Target control of collateral extension and directional axon growth in the mammalian brain. *Science*, **247**, 217-220.

Houle, J. (1992) The structural integrity of glial scar tissue associated with a chronic spinal cord lesion can be altered by transplanted fetal spinal cord tissue. *J. Neurosci. Res.*, **31**, 120-130.

Höhmann, C. F. and Ebner, F. F. (1988) Basal forebrain lesions facilitate adult host fiber ingrowth into neocortical transplants. *Brain Res.*, **448**, 53-66.

Jakeman, L. B. and Reier, P. J. (1991) Axonal projections between fetal spinal cord transplants and the adult rat spinal cord: a neuroanatomical tracing study of local interactions. *J. comp. Neurol.*, **307**, 311-334.

Jessell, T. M. (1988) Adhesion molecules and the hierarchy of neural development. *Neuron*, **1**, 3-13.

Johnson, E. M.,Jr., Taniuchi, M., Brent Clark, H., Springer, J. E., Koh, S., Tayrien, M. W. and Loy, R. (1987) Demonstration of the retrograde transport of nerve growth factor receptor in the peripheral and central nervous system. *J. Neurosci.*, **7**, 923-929.

Kakulas, B. A. (1985) Pathology of spinal injuries. *CNS Trauma*, **1**, 117-129.

Kalil, K. and Reh, T. (1979) Regrowth of severed axons in the neonatal central nervous system: Establishment of normal connections. *Science*, **205**, 1158-1161.

Kalil, K. and Reh, T. (1982) A light and electron microscopic study of regrowing pyramidal tract fibers. *J. comp. Neurol.*, **211**, 265-275.

Kawaja, M. D., Rosenberg, M. B., Yoshida, K. and Gage, F. H. (1992) Somatic gene transfer of nerve growth factor promotes the survival of axotomized septal neurons and the regeneration of their axons in adult rats. *J. Neurosci.*, **12**, 2849-2864.

Kawaja, M. D. and Gage, F. H. (1991) Reactive astrocytes are substrates for the growth of adult CNS axons in the presence of elevated levels of nerve growth factor. *Neuron*, **7**, 1019-1030.

Kiss, J., McGovern, J. and Patel, A. J. (1988) Immunohistochemical localization of cells containing nerve growth factor receptors in the different regions of the adult rat forebrain. *Neuroscience*, **27**, 731-748.

Kliot, M., Smith, G. M., Siegal, J. D. and Silver, J. (1990) Astrocyte-polymer implants promote regeneration of dorsal root fibers into the adult mammalian spinal cord. *Exp. Neurol.*, **109**, 57-69.

Kobayashi, H., Watanabe, E. and Murakami, F. (1995) Growth cones of dorsal root ganglion but not retina collapse and avoid oligodendrocytes in culture. *Dev. Biol.*, **168**, 383-394.

Koester, S. E. and O'Leary, D. D. (1993) Connectional distinction between callosal and subcortically projecting cortical neurons is determined prior to axon extension. *Dev. Biol.*, **160**, 1-14.

Koh, S., Oyler, G. A. and Higgins, G. A. (1989) Localization of nerve growth factor receptor messenger RNA and protein in the adult rat brain. *Exp. Neurol.*, **106**, 209-221.

Koh, S. and Loy, R. (1989) Localization and development of nerve growth factor-sensitive rat basal forebrain neurons and their afferent projections to hippocampus and neocortex. *J. Neurosci.*, **9**, 2999-3018.

Konigsmark, B. (1970) Methods for the counting of neurons. Nauta, W. J. H. and Ebbesson, S. O. E. (eds), *Contemporary Research Methods in Neuroanatomy*. Springer-Verlag, Berlin, pp. 315-340.

Koshinaga, M. and Whittemore, S. R. (1995) The temporal and spatial activation of microglia in fiber tracts undergoing anterograde and retrograde degeneration following spinal cord lesion. *J. Neurotrauma*, **12**, 209-222.

Kromer, L. F., Björklund, A. and Stenevi, U. (1981a) Regeneration of the septohippocampal pathways in adult rats is promoted by utilizing embryonic hippocampal implants as bridges. *Brain Res.*, **210**, 173-200.

Kromer, L. F., Björklund, A. and Stenevi, U. (1981b) Innervation of embryonic hippocampal implants by regenerating axons of cholinergic septal neurons in the adult rat. *Brain Res.*, **210**, 153-171.

Kruger, S. J., Sievers, C., Hansen, M., Sadler, M. and Berry, M. (1986) Three morphologically distinct types of interface develop between adult host and fetal brain transplants: Implications for scar formation in the adult central nervous system. *J. comp. Neurol.*, **249**, 103-116.

Kuhn, T. B., Schmidt, M. F. and Kater, S. B. (1995) Laminin and fibronectin guideposts signal sustained but opposite effects to passing growth cones. *Neuron*, **14**, 275-285.

Labandeira-Garcia, J. L., Wictorin, K., Cunningham, E. T. J. and Björklund, A. (1991) Development of intrastriatal grafts and their afferent innervation from the host. *Neuroscience*, **42**, 407-426.

Lagenaur, C., Kunemund, V., Fischer, G., Fushiki, S. and Schachner, M. (1992) Monoclonal M6 antibody interferes with neurite extension of cultured neurons. *J. Neurobiol.*, **23**, 71-88.

Lander, A. D., Fujii, D. K. and Reichardt, L. F. (1985) Laminin is associated with the "neurite outgrowth-promoting factors" found in conditioned media. *Proc. Natl. Acad. Sci. USA*, **82**, 2183-2187.

Latov, N., Nilaver, G., Zimmerman, E. A., Johnson, W. G., Silverman, A. J., Defendini, R. and Cote, L. (1979) Fibrillary astrocytes proliferate in response to brain injury. *Dev. Biol.*, **72**, 381-384.

Lawrence, J. M., Huang, S. K. and Raisman, G. (1984) Vascular and astrocytic reactions during establishment of hippocampal transplants in adult host brain. *Neuroscience*, **12**, 745-760.

Lawrence, J. M., Morris, R. J., Wilson, D. J. and Raisman, G. (1990) Mechanisms of allograft rejection in the rat brain. *Neuroscience*, **37**, 431-462.

Lee, S. C., Liu, W., Brosnan, C. F. and Dickson, D. W. (1994) GM-CSF promotes proliferation of human fetal and adult microglia in primary cultures. *Glia*, **12**, 309-318.

Lemmon, V., Burden, S. M., Payne, H. R., Elmslie, G. J. and Hlavin, M. L. (1992) Neurite growth on different substrates: permissive versus instructive influences and the role of adhesive strength. *J. Neurosci.*, **12**, 818-826.

Lendahl, U., Zimmerman, L. B. and McKay, R. D. (1990) CNS stem cells express a new class of intermediate filament protein. *Cell*, **60**, 585-595.

Letourneau, P. C. (1975) Cell-to-substratum adhesion and guidance of axonal elongation. *Dev. Biol.*, **44**, 92-101.

Letourneau, P. C., Condic, M. L. and Snow, D. M. (1994) Interactions of developing neurons with the extracellular matrix. *J. Neurosci.*, **14**, 915-928.

Li, D., Field, P. M. and Raisman, G. (1995) Failure of axon regeneration in postnatal rat entorhino-hippocamp al slice co-culture is due to the age of the axon, not that of the pathway or target. *Eur. J. Neurosci.*, **7**, 1164-1171.

Li, Y. and Raisman, G. (1993) Long axon growth from embryonic neurons transplanted into myelinated tracts of the adult rat spinal cord. *Brain Res.*, **629**, 115-127.

Li, Y. and Raisman, G. (1994) Schwann cells induce sprouting in motor and sensory axons in the adult rat spinal cord. *J. Neurosci.*, **14**, 4050-4063.

Li, Y. and Raisman, G. (1995) Sprouts from cut corticospinal axons persist in the presence of astrocytic scarring in long-term lesions of the adult rat spinal cord. *Exp. Neurol.*, **134**, 102-111.

Lierse, W. (1964) Die Kapillardichte im Wirbelteirhirn. *Acta Anat. (Basel)*, **54**, 1-54.

Liesi, P., Dahl, D. and Vaheri, A. (1983) Laminin is produced by early rat astrocytes in primary culture. *J. Cell Biol.*, **96**, 920-924.

Liesi, P. (1985) Laminin-immunoreactive glia distinguish regenerative adult CNS systems from non-regenerative ones. *EMBO J.*, **4**, 2505-2512.

Liesi, P. and Silver, J. (1988) Is astrocyte laminin involved in axon guidance in the mammalian CNS? *Dev. Biol.*, **130**, 774-785.

Lindholm, D., Castrén, E., Berzaghi, M., Blöchl, A. and Thoenen, H. (1994) Activity-dependent and hormonal regulation of neurotrophin mRNA levels in the brain--Implications for neuronal plasticity. *J. Neurobiol.*, **25**, 1362-1372.

Lindsay, R. M. (1979) Adult rat brain astrocytes support survival of both NGF-dependent and NGF-insensitive neurons. *Nature*, **282**, 80-82.

Lindsay, R. M., Barber, P. C., Sherwood, M. R. C., Zimmer, J. and Raisman, G. (1982) Astrocyte cultures from adult rat brain. Derivation, characterization and neurotrophic properties of pure astroglial cells from corpus callosum. *Brain Res.*, **243**, 329-343.

Lindsay, R. M. and Raisman, G. (1984) An autoradiographic study of neuronal development, vascularization and glial cell migration from hippocampal transplants labelled in intermediate explant culture. *Neuroscience*, **12**, 513-530.

Lipton, S. A., Forsch, M. P., Pillips, M. D., Tauck, D. L. and Aizenmann, E. (1988) Nicotinic antagonists enhance process outgrowth by rat retinal ganglion cells in culture. *Science*, **239**, 1293-1296.

Liuzzi, F. J. and Lasek, R. J. (1987) Astrocytes block axonal regeneration in mammals by activating the physiological stop pathway. *Science*, **237**, 642-644.

Logan, A., Berry, M., Gonzalez, A. M., Frautschy, S. A., Sporn, M. B. and Baird, A. (1994) Effects of transforming growth factor β_1 on scar production in the injured central nervous system of the rat. *Eur. J. Neurosci.*, **6**, 355-363.

Ludwin, S. K. (1992) Oligodendrocytes from optic nerves subjected to long term Wallerian degeneration retain the capacity to myelinate. *Acta Neuropathol. (Berl.)*, **84**, 530-537.

Lumsden, A. G. S. and Davies, A. M. (1983) Earliest sensory nerve fibres are guided to peripheral targets by attractants other than nerve growth factor. *Nature*, **306**, 786-787.

Lumsden, A. G. S. and Davies, A. M. (1986) Chemotropic effect of specific target epithelium in the developing mammalian nervous system. *Nature*, **323**, 538-539.

Lund, R. D., Chang, F. L. F., Hankin, M. H. and Lagenaur, C. F. (1985) Use of a species-specific antibody for demonstrating mouse neurons transplanted to rat brains. *Neurosci. Lett.*, **61**, 221-226.

Lund, R. D., Perry, V. H. and Lagenaur, C. F. (1986) Cell surface changes in the developing optic nerve of mice. *J. comp. Neurol.*, **247**, 439-446.

Luo, Y., Raible, D. and Raper, J. A. (1993) Collapsin: A protein in brain that induces the collapse and paralysis of neuronal growth cones. *Cell*, **75**, 217-227.

Luo, Y., Shepherd, I., Li, J., Renzi, J., Chang, S. and Raper, J. A. (1995) A family of molecules related to collapsin in the embryonic chick nervous system. *Neuron*, **14**, 1131-1140.

Luo, Y. and Raper, J. A. (1994) Inhibitory factors controlling growth cone motility and guidance. *Curr. Opin. Neurobiol.*, **4**, 648-654.

MacClaren, R. E. and Taylor, J. S. H. (1995) A critical period for axon regrowth through a lesion in the developing mammalian retina. *Eur. J. Neurosci.*, **7**, 2111-2118.

Mansour, H., Asher, R., Dahl, D., Labkovsky, B., Perides, G. and Bignami, A. (1990) Permissive and non-permissive reactive astrocytes: immunofluorescence study with antibodies to the glial hyaluronidate-binding protein. *J. Neurosci. Res.*, **25**, 300-311.

Marcus, R. C., Blazeski, R., Godement, P. and Mason, C. A. (1995) Retinal axon divergence in the optic chiasm: Uncrossed axons diverge from crossed axons within a midline glial specialization. *J. Neurosci.*, **15**, 3716-3729.

Martínez-Murillo, R., Caro, L. and Nieto-Sampedro, M. (1993) Lesion-induced expression of low-affinity nerve growth factor receptor-immunoreactive protein in Purkinje cells of the adult rat. *Neuroscience*, **52**, 587-593.

Matthes, D. J., Sink, H., Kolodkin, A. L. and Goodman, C. S. (1995) Semaphorin II can function as a selective inhibitor of specific synaptic arborizations. *Cell*, **81**, 631-639.

Matthiessen, H. P., Schmalenbach, C. and Muller, H. W. (1989) Astroglia-released neurite growth-inducing activity for embryonic hippocampal

neurons is associated with laminin bound in a sulfated complex and free fibronectin. *Glia*, **2**, 177-188.

Mattson, M. P., Dou, P. and Kater, S. B. (1988) Outgrowth regulating actions of glutamate in isolated hippocampal pyramidal neurons. *J. Neurosci.*, **8**, 2087-2100.

McKeon, R. J., Schreiber, R. C., Rudge, J. S. and Silver, J. (1991) Reduction of neurite outgrowth in a model of glial scarring following CNS injury is correlated with the expression of inhibitory molecules on reactive astrocytes. *J. Neurosci.*, **11**, 3398-3411.

Menesini-Chen, M. G., Chen, J. S. and Levi-Montalcini, R. (1978) Sympathetic nerve fiber ingrowth in the central nervous system of neonatal rodents upon intracerebral NGF injections. *Arch. Ital. Biol.*, **116**, 53-84.

Messersmith, E. K., Leonardo, E. D., Shatz, C. J., Tessier-Lavigne, M., Goodman, C. S. and Kolodkin, A. L. (1995) Semaphorin III can function as a selective chemorepellent to pattern sensory projections in the spinal cord. *Neuron*, **14**, 949-959.

Milligan, C. E., Levitt, P. and Cunningham, T. J. (1991) Brain macrophages and microglia respond differently to lesions of the developing and adult visual system. *J. comp. Neurol.*, **314**, 136-146.

Montero-Menei, C. N., Pouplard-Barthelaix, A., Gumpel, M. and Baron-Van Evercooren, A. (1992) Pure Schwann cell suspension grafts promote regeneration of the lesioned septo-hippocampal cholinergic pathway. *Brain Res.*, **570**, 198-208.

Mufson, E. J., Conner, J. M., Varon, S. and Kordower, J. H. (1994) Nerve growth factor-like immunoreactive profiles in the primate basal forebrain and hippocampal formation. *J. comp. Neurol.*, **341**, 507-519.

Neuberger, T. J., Cornbrooks, C. J. and Kromer, L. F. (1992) Effects of delayed transplantation of cultured Schwann cells on axonal regeneration from central nervous system cholinergic neurons. *J. comp. Neurol.*, **315**, 16-33.

Neugebauer, K. M., Tomaselli, K. J., Lilien, J. and ReichardtLFX, (1988) N-cadherin, NCAM, and integrins promote retinal neurite outgrowth on astrocytes in vitro. *J. Cell Biol.*, **107**, 1177-1187.

Noble, M., Fok-Seang, J. and Cohen, J. (1984) Glia are a unique substrate for the in vitro growth of central nervous system neurons. *J. Neurosci.*, **4**, 1892-1903.

Norris, C. R. and Kalil, K. (1991) Guidance of callosal axons by radial glia in the developing cerebral cortex. *J. Neurosci.*, **11**, 3481-3492.

Nowakowski, R. S. and Rakic, P. (1979) The mode of migration of neurons to the hippocampus: A Golgi and electron microscopic analysis in fetal rhesus monkey. *J. Neurocytol.*, **8**, 697-718.

O'Leary, D. D. M., Bicknese, A. R., De Carlos, J. A., Heffner, C. D., Koester, S. I., Kutka, L. J. and Terashima, T. (1990) Target selection by cortical axons: alternative mechanisms to establish axonal connections in the developing brain. *Cold Spring Harbor Symp. Quant. Biol.*, **55**, 453-468.

O'Leary, D. D. M. and Terashima, T. (1988) Cortical axons branch to multiple subcortical targets by interstitial axon budding: implications for target recognition and "waiting periods". *Neuron*, **1**, 901-910.

Olby, N. J., O'Leary, M. T., Targett, M. P. and Blakemore, W. F. (1995) The effect of injection technique on the passive spread of astrocytes following transplantation into rat spinal cord white matter. *Restor. Neurol. Neurosci.*, **7**, 171-174.

Paíno, C. L. and Bunge, M. B. (1991) Induction of axon growth into Schwann cell implants into lesioned adult rat spinal cord. *Exp. Neurol.*, **114**, 254-257.

Palmgren, A. (1948) A rapid method for selective silver staining of nerve fibres and nerve endings in mounted paraffin sections. *Acta Zool.*, **29**, 377-392.

Perkins, S., Carlstedt, T., Mizuno, K. and Aguayo, A. J. (1980) Failure of regenerating dorsal root axons to regrow into the spinal cord. *Can. J. Neurol. Sci.*, **7**, 323.

Perry, V. H., Hume, D. A. and Gordon, S. (1985) Immunohistochemical localization of macrophages and microglia in the adult and developing mouse brain. *Neuroscience*, **15**, 313-326.

Peterson, G. M. (1994) Differential projections to the hippocampus by neurons of the medial septum and vertical limb of the diagonal band. *Brain Res.*, **646**, 129-134.

Pindzola, R. R., Doller, C. and Silver, J. (1993) Putative inhibitory extracellular matrix molecules at the dorsal root entry zone of the spinal cord during development and after root and sciatic nerve lesions. *Dev. Biol.*, **156**, 34-48.

Pioro, E. P. and Cuello, A. C. (1990a) Distribution of nerve growth factor receptor-like immunoreactivity in the adult rat central nervous system. Effect of colchicine and correlation with the cholinergic system-II. Brainstem, cerebellum, and spinal cord. *Neuroscience*, **34**, 89-110.

Pioro, E. P. and Cuello, A. C. (1990b) Distribution of nerve growth factor receptor-like immunoreactivity in the adult rat central nervous system. Effect of

colchicine and correlation with the cholinergic system-I. Forebrain. *Neuroscience*, **34**, 57-87.

Pritzel, M., Isacson, O., Brundin, P., Wiklund, L. and Björklund, A. (1987) Afferent and efferent connections of striatal grafts implanted into the ibotenic acid lesioned neostriatum in adult rats. *Exp. Brain Res.*, **65**, 112-126.

Radeke, M. J., Misko, T. P., Hsu, C., Herzenberg, L. A. and Shooter, E. M. (1987) Gene transfer and molecular cloning of the rat nerve growth factor receptor. *Nature*, **325**, 593-597.

Raisman, G. (1969) Neuronal plasticity in the septal nuclei of the adult rat. *Brain Res.*, **14**, 25-48.

Raisman, G., Lawrence, J. M., Zhou, C. -F. and Lindsay, R. M. (1985) Some neuronal, glial and vascular interactions which occur when developing hippocampal primordia are incorporated into adult host hippocampi. Björklund, A. and Stenevi, U. (eds), *Neural Grafting in the Mammalian CNS.* Elsevier, Amsterdam, pp. 125-150.

Raisman, G. and Ebner, F. F. (1983) Mossy fibre projections into and out of hippocampal transplants. *Neuroscience*, **9**, 783-801.

Rakic, P. (1971) Neuron-glia relationship during granule cell migration in developing cerebellar cortex. A Golgi and electron microscopic study in *Macacus rhesus*. *J. comp. Neurol.*, **141**, 283-312.

Rakic, P. (1972) Mode of cell migration to the superficial layers of fetal monkey neocortex. *J. comp. Neurol.*, **145**, 61-84.

Redd, P. E. and Byers, M. R. (1994) Regeneration of junctional epithelium and its innervation in adult rats: a study using immunocytochemistry for p75 nerve growth factor receptor and calcitonin gene-related peptide. *J. Period. Res.*, **29**, 214-224.

Reichardt, L. F., Bossy, B., Carbonetto, S., DeCurtis, I., Emmett, C., Hall, D. E. and Ignatius, M. J. (1990) Neuronal receptors that regulate axon growth. *Cold Spring Harbor Symp. Quant. Biol.*, **55**, 341-350.

Reier, P. J., Perlow, M. J. and Guth, L. (1983a) Development of embryonic spinal cord transplants in the rat. *Dev. Brain Res.*, **10**, 201-219.

Reier, P. J., Stensaas, L. J. and Guth, L. (1983b) The astrocytic scar as an impediment to regeneration in the central nervous system. Kao, C. C., Bunge, R. P. and Reier, P. J. (eds), *Spinal Cord Reconstruction*. Raven Press, New York, pp. 163-195.

Reier, P. J. (1986) Gliosis following CNS injury: The anatomy of astrocytic scars and their influences on axonal elongation. Fedoroff, S. and Vernadakis, A. (eds), *Astrocytes, Vol. 3.* Raven Press, New York, pp. 163-196.

Reier, P. J. and Houle, J. D. (1988) The glial scar: It's bearing on axonal elongation and transplantation approaches to CNS repair. *Adv. Neurol.*, **47**, 87-138.

Rende, M., Hagg, T., Manthorpe, M. and Varon, S. (1992) Nerve growth factor receptor immunoreactivity in neurons of the normal adult rat spinal cord and its modulation after peripheral nerve lesions. *J. comp. Neurol.*, **319**, 285-298.

Rende, M., Provenzano, C. and Tonali, P. (1993) Modulation of low-affinity nerve growth factor receptor in injured adult rat spinal cord motoneurons. *J. comp. Neurol.*, **338**, 560-574.

Renfranz, P. J., Cunningham, M. G. and McKay, R. D. G. (1991) Region-specific differentiation of the hippocampal stem cell line HiB5 upon implantation into the developing mammalian brain. *Cell*, **66**, 713-729.

Reynolds, B. A. and Weiss, S. (1992) Generation of neurons and astrocytes from isolated cells of the adult mammalian central nervous system. *Science*, **255**, 1707-1710.

Richardson, P. M., McGuinness, U. M. and Aguayo, A. J. (1980) Axons from the CNS neurones regenerate into PNS grafts. *Nature*, **284**, 264-265.

Rickmann, M., Amaral, D. G. and Cowan, W. M. (1987) Organization of radial glial cells during the development of the rat dentate gyrus. *J. comp. Neurol.*, **264**, 449-479.

Rodriguez-Tebar, A., Dechant, G. and Barde, Y. A. (1990) Binding of a brain derived neurotrophin factor to the nerve growth factor receptor. *Neuron*, **4**, 487-492.

Rodriguez-Tebar, A., Dechant, G., Gotz, R. and Barde, Y. A. (1992) Binding of neurotrophin-3 to its neuronal receptors and interactions with nerve growth factor and brain-derived neurotrophic factor. *EMBO J.*, **11**, 917-922.

Rossi, F., Jankovski, A. and Sotelo, C. (1995) Differential regenerative response of Purkinje cell and inferior olivary axons confronted with embryonic grafts: environmental cues versus intrinsic neuronal determinants. *J. comp. Neurol.*, **359**, 663-677.

Rousselet, A., Fetler, L., Chamak, B. and Prochiantz, A. (1988) Rat mesencephalic neurons in culture exhibit different morphological traits in the presence of media conditioned on mesencephalic or striatal astroglia. *Dev. Biol.*, **129**, 495-504.

Rudge, J. A., Smith, G. M. and Silver, J. (1989) An in vitro model of wound healing in the CNS: analysis of cell reaction and interaction at different ages. *Exp. Neurol.*, **103**, 1-16.

Rudge, J. S., Li, Y., Pasnikowski, E. M., Mattsson, K., Pan, L., Yancopoulos, G. D., Wiegand, S. J., Lindsay, R. M. and Ip, N. Y. (1994) Neurotrophic factor receptors and their signal transduction capabilities in rat astrocytes. *Eur. J. Neurosci.*, **6**, 693-705.

Rudge, J. S. and Silver, J. (1990) Inhibition of neurite outgrowth on astroglial scars *in vitro*. *J. Neurosci.*, **10**, 3594-3603.

Rutishauser, U. and Jessell, T. M. (1988) Cell adhesion molecules in vertebrate neural development. *Physiol. Rev.*, **68**, 819-857.

Sato, M., Lopez-Mascaraque, L., Heffner, C. D. and O'Leary, D. D. M. (1994) Action of a diffusible target-derived chemoattractant on cortical axon branch induction and directed growth. *Neuron*, **13**, 791-803.

Schachner, M. (1991) Cell surface recognition and neuron-glia interactions. *Ann. NY Acad. Sci.*, **633**, 105-112.

Schlessinger, A. R., Cowan, W. M. and Swanson, L. W. (1978) The time of origin of neurons in Ammon's horn and the associated retrohippocampal fields. *Anat. Embryol.*, **154**, 153-173.

Schmidt, R. H., Kasik, S. A. and Bhatnagar, R. K. (1980) Regenerative critical periods for locus coeruleus in postnatal rat pups following intracisternal 6-hydroxydopamine: A model of noradrenergic development. *Brain Res.*, **191**, 173-190.

Schmidt, R. H. and Bhatnagar, R. K. (1979) Critical periods for noradrenergic regeneration in rat brain regions following neonatal subcutaneous 6-hydroxydopamine. *Life Sci.*, **25**, 1641-1650.

Schnell, L., Schneider, R., Kolbeck, R., Barde, Y. -A. and Schwab, M. E. (1994) Neurotrophin-3 enhances sprouting of corticospinal tract during development and after adult spinal cord lesion. *Nature*, **367**, 170-173.

Schnell, L. and Schwab, M. E. (1990) Axonal regeneration in the rat spinal cord produced by an antibody against myelin-associated neurite growth inhibitors. *Nature*, **343**, 269-272.

Schnitzer, J. and Scherer, J. (1990) Microglial cell responses in the rabbit retina following transection of the optic nerve. *J. comp. Neurol.*, **302**, 779-791.

Schwab, M. E. (1990) Myelin-associated inhibitors of neurite growth. *Exp. Neurol.*, **109**, 2-5.

Schwab, M. E., Kapfhammer, J. P. and Bandtlow, C. E. (1993) Inhibitors of neurite growth. *Annu. Rev. Neurosci.*, **16**, 565-595.

Shewan, D., Berry, M. and Cohen, J. (1995) Extensive regeneration *in vitro* by early embryonic neurons on immature and adult CNS tissue. *J. Neurosci.*, **15**, 2057-2062.

Shirasaki, R., Tamada, A., Katsumata, R. and Murakami, F. (1995) Guidance of cerebellofugal axons in the rat embryo: Directed growth toward the floor plate and subsequent elongation along the longitudinal axis. *Neuron*, **14**, 961-972.

Siegal, J. D., Kliot, M., Smith, G. M. and Silver, J. (1990) A comparison of the regeneration potential of dorsal root fibers into gray or white matter of the adult rat spinal cord. *Exp. Neurol.*, **109**, 90-97.

Sievers, J., Parwaresch, R. and Wittge, H. -U. (1994) Blood monocytes and spleen macrophages differentiate into microglia-like cells on monolayers of astrocytes: morphology. *Glia*, **12**, 245-258.

Simon, D. K. and O'Leary, D. D. M. (1992) development of topographic order in the mammalian retinocollicular projection. *J.Neurosci.*, **12**, 1212-1232.

Silver, J., Edwards, M. A. and Levitt, P. (1993) Immunocytochemical demonstration of early appearing astroglial structures that form boundaries and pathways along axon tracts in the fetal brain. *J. comp. Neurol.*, **328**, 415-436.

Silverman, R. C., Gibson, M. J. and Silverman, A. J. (1991) Relationship of glia to GnRH axonal outgrowth from third ventricular grafts in hpg hosts. *Exp. Neurol.*, **114**, 259-274.

Smith, G. M., Miller, R. H. and Silver, J. (1986) Changing role of forebrain astrocytes during development, regenerative failure, and induced regeneration upon transplantation. *J. comp. Neurol.*, **251**, 23-43.

Smith, G. M., Rutishauser, U., Silver, J. and Miller, R. H. (1990) Maturation of astrocytes in vitro alters the extent and molecular basis of neurite outgrowth. *Dev. Biol.*, **138**, 377-390.

Smith, G. M., Jacobberger, J. W. and Miller, R. H. (1993) Modulation of adhesion molecule expression on rat cortical astrocytes during maturation. *J. Neurochem.*, **60**, 1453-1466.

Smith-Thomas, L. C., Fok-Seang, J., Stevens, J., Du, J. -S., Muir, E., Faissner, A., Geller, H. M., Rogers, J. H. and Fawcett, J. W. (1994) An inhibitor of neurite outgrowth produced by astrocytes. *J. Cell Sci.*, **107**, 1687-1695.

Smith-Thomas, L. C., Stevens, J., Fok-Seang, J., Faissner, A., Rogers, J. H. and Fawcett, J. W. (1995) Increased axon regeneration in astrocytes grown in the presence of proteoglycan synthesis inhibitors. *J. Cell Sci.*, **108**, 1307-1315.

Snow, D. M., Lemmon, V., Carrino, D. A., Caplan, A. I. and Silver, J. (1990) Sulfated proteoglycans in astroglial barriers inhibit neurite outgrowth in vitro. *Exp. Neurol.*, **109**, 111-130.

Snyder, E. Y., Deitcher, D. L., Walsh, C., Arnold Aldea, S., Hartwieg, E. A. and Cepko, C. L. (1992) Multipotent neural cell lines can engraft and participate in development of mouse cerebellum. *Cell*, **68**, 33-51.

Sotelo, C. and Alvarado-Mallart, R. M. (1987) Reconstruction of the defective cerebellar circuitry in adult Purkinje cell degeneration mutant mice by Purkinje cell replacement through transplantation of solid embryonic implants. *Neuroscience*, **20**, 1-22.

Squinto, S. P., Stitt, T. N., Aldrich, T. H., Davis, S., Bianco, S. M., Radziejewski, C., Glass, D., Masiakowski, P., Furth, M. E., Valenzuela, D. M., DiStefano, P. S. and Yancopoulos, G. D. (1991) trkB encodes a functional receptor for brain-derived neurotrophic factor and neurotrophin-3 but not nerve growth factor. *Cell*, **65**, 885-893.

Sretavan, D. W. and Reichardt, L. F. (1993) Time-lapse video analysis of retinal ganglion cell axon pathfinding at the mammalian optic chiasm: growth cone guidance using intrinsic chiasm clues. *Neuron*, **10**, 761-777.

Stensaas, L. J., Burgess, P. R. and Horch, K. W. (1979) Regenerating dorsal root axons are blocked by spinal cord astrocytes. *Soc. Neurosci. Abstr.*, **5**, 684.

Stensaas, L. J., Partlow, L. M., Burgess, P. R. and Horch, K. W. (1987) Inhibition of regeneration: The ultrastructure of reactive astrocytes and abortive axon terminals in the transition zone of the dorsal root. *Prog. Brain Res.*, **71**, 457-468.

Stichel, C. C., Wunderlich, G., Schwab, M. E. and Müller, H. W. (1995) Clearance of myelin constituents and axonal sprouting in the transected postcommissural fornix of the adult rat. *Eur. J. Neurosci.*, **7**, 401-411.

Stichel, C. C. and Müller, H. W. (1994) Extensive and long-lasting changes of glial cells following transection of the postcommissural fornix in the adult rat. *Glia*, **10**, 89-100.

Streit, W. J. (1990) An improved staining method for rat microglial cells using the lectin from Griffonia simplicifolia (GSA I-B4). *J. Histochem. Cytochem.*, **38**, 1683-1687.

Strömberg, I., Bygdeman, M. and Almqvist, P. (1992) Target-specific outgrowth from human mesencephalic tissue grafted to cortex or ventricle of immunosuppressed rats. *J. comp. Neurol.*, **315**, 445-456.

Suzuki, M., Jaques-Berg, W., Emmett, C. J., Lawrence, J. M., Field, P. M., Seeley, P. J. and Raisman, G. (1989) A technique for microtransplantation of embryonic hippocampal neurons into adult rat fimbria. *Neurosci. Lett. Suppl.*, **36**, s93.

Suzuki, M. and Raisman, G. (1992) The glial framework of central white matter tracts: Segmented rows of contiguous interfascicular oligodendrocytes and solitary astrocytes give rise to a continuous meshwork of transverse and longitudinal processes in the adult rat fimbria. *Glia*, **6**, 222-235.

Suzuki, M. and Raisman, G. (1994) Multifocal pattern of postnatal development of the macroglial framework of the rat fimbria. *Glia*, **12**, 294-308.

Swanson, L. W., Sawchenko, P. E. and Cowan, W. M. (1980) Evidence that the commissural, associational and septal projections of the regio inferior of the hippocampus arise from the same neurons. *Brain Res.*, **197**, 207-212.

Swanson, L. W., Sawchenko, P. E. and Cowan, W. M. (1981) Evidence for collateral projections by neurons in ammon's horn, the dentate gyrus, and the

subiculum: a multiple retrograde labeling study in the rat. *J. Neurosci.*, **1**, 548-559.

Swanson, L. W. and Cowan, W. M. (1977) An autoradiographic study of the organization of the efferent connections of the hippocampal formation in the rat. *J. comp. Neurol.*, **172**, 49-84.

Takahashi, T., Misson, J. P. and Caviness, V. S. (1990) Glial process elongation and branching in the developing murine neocortex - a qualitative and quantitative immunohistochemical analysis. *J. comp. Neurol.*, **302**, 15-28.

Takamiya, Y., Kohsaka, S., Toya, S., Otani, M. and Tsukada, Y. (1988) Immunohistochemical studies on the proliferation of reactive astrocytes and the expression of cytoskeletal proteins following brain injury in rats. *Dev. Brain Res.*, **38**, 201-210.

Tamada, A., Shirasaki, R. and Murakami, F. (1995) Floor plate chemoattracts crossed axons and chemorepels uncrossed axons in the vertebrate brain. *Neuron*, **14**, 1083-1093.

Thery, C. and Mallat, M. (1993) Influence of interleukin-1 and tumor necrosis factor alpha on the growth of microglial cells in primary cultures of mouse cerebral cortex: involvement of colony-stimulating factor 1. *Neurosci. Lett.*, **150**, 195-199.

Tiveron, M. C., Barboni, E., Pliego Rivero, F. B., Gormley, A. M., Seeley, P. J., Grosveld, F. and Morris, R. (1992) Selective inhibition of neurite outgrowth on mature astrocytes by Thy-1 glycoprotein. *Nature*, **355**, 745-748.

Tomaselli, K. J., Reichardt, L. F. and Bixby, J. L. (1986) Distinct molecular interactions mediate neuronal process outgrowth on nonneuronal cell surfaces and extracellular matrices. *J. Cell Biol.*, **103**, 2659-2672.

Tomaselli, K. J., Neugebauer, K. M., Bixby, J. L., Lilien, J. and Reichardt, L. F. (1988) N-cadherin and integrins: two receptor systems that mediate neuronal process outgrowth on astrocyte surfaces. *Neuron*, **1**, 33-43.

Tomaselli, K. J. and Reichardt, L. F. (1988) Peripheral mononeuron interactions with laminin and Schwann cell-derived neurite-promoting molecules: developmental regulation of laminin receptor function. *J. Neurosci. Res.*, **21**, 275-285.

Tuszynski, M. H., Buzsaki, G. and Gage, F. H. (1990) Nerve growth factor infusions combined with fetal hippocampal grafts engance reconstruction of the lesioned septohippocampal projection. *Neuroscience*, **36**, 33-44.

Tuszynski, M. H., Peterson, D. A., Ray, J., Baird, A., Nakahara, Y. and Gage, F. H. (1994) Fibroblasts genetically modified to produce nerve growth factor

induce robust neuritic ingrowth after grafting to the spinal cord. *Exp. Neurol.*, **126**, 1-14.

Tønder, N., Sørensen, T. and Zimmer, J. (1989) Enhanced host perforant path innervation of neonatal dentate tissue after grafting to axon sparing, ibotenic acid lesions in adult rats. *Exp. Brain Res.*, **75**, 483-496.

Tønder, N., Sørensen, T. and Zimmer, J. (1990) Grafting of fetal CA3 neurons to excitotoxic axon-sparing lesions of the hippocampal CA3 area in adult rats. Storm-Mathisen, J., Zimmer, J. and Ottersen, O. P. (eds), *Understanding the Brain through the Hippocampus. The hippocampal region as a model for studying brain structure and function. Progress in Brain Research, Vol. 83.* Elsevier, Amsterdam, pp. 391-409.

Varga, Z. M., Bandtlow, C. -E., Erulkar, S. D., Schwab, M. E. and Nicholls, J. G. (1995) The critical period for repair of CNS of neonatal opossum (*Monodelphis domestica*) in culture: correlation with development of glial cells, myelin and growth-inibitory molecules. *Eur. J. Neurosci.*, **7**, 2119-2129.

Vidal-Sanz, M., Bray, G. M., Villegas-Pérez, M. P., Thanos, S. and Aguayo, A. J. (1987) Axonal regeneration and synapse formation in the superior colliculus by retinal ganglion cells in the adult rat. *J. Neurosci.*, **7**, 2894-2909.

Voigt, T. (1989) Development of glial cells in the cerebral wall of ferrets: direct tracing of their transformation from radial glia into astrocytes. *J. comp. Neurol.*, **289**, 74-88.

Wang, L. -C., Baird, D. H., Hatten, M. E. and Mason, C. A. (1994) Astroglial differentiation is required for support of neurite outgrowth. *J. Neurosci.*, **14**, 3195-3207.

Wictorin, K., Clarke, D. J., Bolam, J. P. and Björklund, A. (1989a) Host corticostriatal fibres establish synaptic connections with grafted striatal neurons in the ibotenic acid lesioned striatum. *Eur. J. Neurosci.*, **1**, 189-195.

Wictorin, K., Simerly, R. B., Isacson, O., Swanson, L. W. and Björklund, A. (1989b) Connectivity of striatal grafts implanted into the ibotenic acid-lesioned striatum - III. Efferent projecting graft neurons and their relation to host afferents within the grafts. *Neuroscience*, **30**, 313-330.

Wictorin, K., Brundin, P., Gustavii, B., Lindvall, O. and Björklund, A. (1990a) Reformation of long axon pathways in adult rat central nervous system by human forebrain neuroblasts. *Nature*, **347**, 556-558.

Wictorin, K., Clarke, D. J., Bolam, P. and Björklund, A. (1990b) Fetal striatal neurons grafted into the ibotenate lesioned adult striatum: efferent projections and synaptic contacts in the host globus pallidus. *Neuroscience*, **37**, 301-316.

Wictorin, K., Lagenaur, C. F., Lund, R. D. and Björklund, A. (1991) Efferent projections to the host brain from intrastriatal striatal mouse-to-rat grafts: time course and tissue-type specificity as revealed by a mouse specific neuronal marker. *Eur. J. Neurosci.*, **3**, 86-101.

Wictorin, K. and Björklund, A. (1989) Connectivity of striatal grafts implanted into the ibotenic acid-lesioned striatum - II. Cortical afferents. *Neuroscience*, **30**, 297-312.

Williams, A. F. (1985) Immunoglobulin-related domains for cell surface recognition. *Nature*, **314**, 579-580.

Williams, R. W., Borodkin, M. and Rakic, P. (1991) Growth cone distribution patterns in the optic nerve of fetal monkeys: implications for mechanisms of axon guidance. *J. Neurosci.*, **11**, 1081-1094.

Woodhams, P. L., Webb, M., Atkinson, D. J. and Seeley, P. J. (1989) A monoclonal antibody, Py, distinguishes different classes of hippocampal neurons. *J. Neurosci.*, **9**, 2170-2181.

Woolf, N. J., Gould, E. and Butcher, L. L. (1989) Nerve growth factor receptor is associated with cholinergic neurons of the basal forebrain but not the pontomesencephalon. *Neuroscience*, **30**, 143-152.

Wu, D. -Y., Jhaveri, S. and Schneider, G. E. (1995) Glial environment in the developing superior colliculus of hamsters in relation to the timing of retinal axon ingrowth. *J. comp. Neurol.*, **358**, 206-218.

Wunderlich, G., Stichel, C. C., Schroeder, W. O. and Müller, H. W. (1994) Transplants of immature astrocytes promote axonal regeneration in the adult rat brain. *Glia*, **10**, 49-58.

Wyss, J. M., Swanson, L. W. and Cowan, W. M. (1980) The organization of the fimbria, dorsal fornix and ventral hippocampal commissure in the rat. *Anat. Embryol.*, **158**, 303-316.

Xiao, X. M. and Martin, G. F. (1991) Evidence for new growth and regeneration of cut axons in developmental plasticity of the Rubrospinal Tract in the North American Opossum. *J. comp. Neurol.*, **313**, 103-112.

Xie, D., Schultz, R. L. and Whitter, E. F. (1995) The oligodendroglial reaction to brain stab wounds: An immunohistochemical study. *J. Neurocytol.*, **24**, 435-448.

Xu, X. M., Guénard, V., Kleitman, N. and Bunge, M. B. (1995) Axonal regeneration into Schwann cell-seeded guidance channels grafted into transected adult rat spinal cord. *J. comp. Neurol.*, **351**, 145-160.

Yan, Q. and Johnson, E. M. J (1989) Immunohistochemical localization and biochemical characterization of nerve growth factor receptor in adult rat brain. *J. comp. Neurol.*, **290**, 585-598.

Yoshida, K. and Gage, F. H. (1991) Fibroblast growth factors stimulate nerve growth factor synthesis and secretion by astrocytes. *Brain Res.*, **538**, 118-126.

Zafra, F., Lindholm, D., Castrén, E., Hartikka, J. and Thoenen, H. (1992) Regulation of brain-derived neurotrophic factor and nerve growth factor mRNA in primary cultures of hippocampal neurons and astrocytes. *J. Neurosci.*, **12**, 4793-4799.

Zheng, J. Q., Felder, M., Connor, J. A. and Poo, M. (1995) Turning of nerve growth cones induced by neurotransmiters. *Nature*, **368**, 140-144.

Zhou, C. F., Raisman, G. and Morris, R. J. (1985) Specific patterns of fibre outgrowth from transplants to host mice hippocampi, shown immunohistochemically by the use of allelic forms of Thy-1. *Neuroscience*, **16**, 819-833.

Zhou, C. F., Li, Y. and Raisman, G. (1989) Embryonic entorhinal transplants project selectively to the deafferented entorhinal zone of adult mouse hippocampi, as demonstrated by the use of Thy-1 allelic immunohistochemistry.

Effect of timing of transplantation in relation to deafferentation. *Neuroscience*, **32**, 349-362.

Zwimpfer, T. J., Aguayo, A. J. and Bray, G. M. (1992) Synapse formation and preferential distribution in the granule cell layer by regenerating retinal ganglion cell axons guided to the cerebellum of adult hamsters. *J. Neurosci.*, **12**, 1144-1159.

Additional references

Knoops, B., Carbonetto, S., Aguayo, A. J. (1993) β1 integrin subunit expression by central nervous system neurons is regulated following contact with the environment of the peripheral nervous system. Soc. Neurosci. Abstr. **19**, 679.

So, K. F. and Aguayo, A. J. (1985) Lengthy regrowth of cut axons from ganglion cells after peripheral nerve transplantation into the retina of adult rats. Brain Res. **328**, 349-354.

Snow, D. M., Steindler, D. A., Silver, J. (1990) Molecular and cellular characterization of the glial roof plate of the spinal cord and optic tectum: a possible role for a proteoglycan in the development of an axon barrier. Dev. Biol. **138**, 359-376.